See: NIST SP861, W. L. Grosshandler, et al., Editors

4. FLAME SUPPRESSION EFFECTIVENESS

Anthony Hamins, Grzegorz Gmurczyk, William Grosshandler,
R. Gregory Rehwoldt, Isaura Vazquez, and Thomas Cleary
Building and Fire Research Laboratory

Cary Presser
Chemical Sciences and Technology Laboratory

and Kalyanasundaram Seshadri
AMES Department, University of California at San Diego, La Jolla, CA

4.1 Overview

A flame will be extinguished when the time required for the chain reaction which sustains combustion exceeds the time it takes to replenish the necessary heat and reactants. A characteristic time for reaction, t_{chem}, can be estimated from the inverse of a global kinetic rate coefficient, k, expressed in Arrhenius form as

$$t_{chem} \sim k^{-1} = B^{-1} \exp(\frac{E_0}{RT}), \ (seconds) \tag{1}$$

where B is a molecular collision frequency factor, E_0 is a global activation energy, R is the ideal gas constant, and T is the gas temperature. Assuming reactant species and heat are transported at about the same rate (*i.e.*, unity Lewis number), a characteristic time, t_{flow}, for replenishing both can be estimated from a convective flow velocity, U, and a length scale, L, by

$$t_{flow} \sim \frac{L}{U} \ (seconds). \tag{2}$$

The Damköhler number is the ratio of the characteristic flow time to the characteristic chemical reaction time, *i.e.*, $D_n \equiv t_{flow}/t_{chem}$. Liñan (1974) showed that as the maximum flame temperature and the fuel burning rate decrease, a critical value Damköhler number is reached, D_n*, where the flame abruptly extinguishes. The Damköhler number criteria suggests a number of strategies for extinguishing fires that include increasing the strain rate or flame stretch (to decrease t_{flow}), or cooling, reactant removal, and chemical inhibition (to increase t_{chem}).

A large number of studies have been conducted on fire suppression. Williams (1980) summarizes the fundamental processes of flame extinction. The suppression effectiveness of a number of inert, halogenated, and metal agents been studied phenomenologically in counterflow flames (Milne *et al.*, 1970; Kent and Williams, 1974; Seshadri and Williams, 1975; Mitani, 1983) and in co-flowing cup burner flames (Simmons and Wolfhard, 1956; Creitz, 1961, 1972; Bajpai, 1974a; Hirst and Booth, 1977; Tucker *et al.*, 1981; and Sheinson *et al.*, 1989). A number of investigators have studied the structure of inhibited flames in order to learn about the mechanisms of flame inhibition. A global measure of the chemical effectiveness of an agent has been quantified through heat capacity considerations (Tucker *et al.*, 1981; Sheinson *et al.*, 1989). Pitts *et al.* (1990) outline current understanding

of fire suppression, incorporating a comprehensive review of the relevant literature, in addition to a discussion of agent effectiveness, test methods, and the role of different suppression mechanisms.

The objective of this part of the study was to rank experimentally the effectiveness of various chemicals for suppressing different laboratory-scale flames, and to project the relative effectiveness to the performance one would expect in the Wright Laboratory simulated full-scale fire suppression facilities.

4.1.1 Comparison of Experimental Configurations. Fundamental studies have shown that the character of the fluid mechanical flow field is a key parameter in controlling flame extinction. A discussion of the importance of the flow field strain rate or flame stretch is given by Williams (1980). As the strain rate increases, t_{flow} in Equation 2 decreases and a flame becomes weaker and easier to extinguish by agent addition. In order to understand the chemical effectiveness of an agent, other parameters such as fluid mechanics which influence flame extinction must be well-controlled. For the applications considered here, an engine nacelle and a dry bay, the fluid mechanics and thus the strain rate is not well defined due principally to variability in the flowfield geometry. Observation in the Wright Laboratory simulated fire suppression facilities, however, indicate that the fires of interest are turbulent and thereby characterized by a range of strain rates. The configurations listed in Table 1 were designed to improve our understanding of the suppression effectiveness of agents under a variety of possible combustion scenarios.

Four experimental configurations were used to rank the relative effectiveness of suppression agents. They are listed in Table 1 and include the laminar opposed flow diffusion flame burner (OFDF), the cup burner, the turbulent spray flame burner, and the deflagration tube. Table 1 also lists differences in the parameters which characterize combustion in each of the test configurations including the nature of the flow field and the pressure regime. In a typical fire the fuel and air are nonpremixed, as represented by the cup burner and the OFDF burner.

Opposed flow and coflow systems provide two fundamental approaches for studying diffusion flame extinction. Past experience has shown the OFDF configuration to be a convenient geometry for detailed fundamental studies of the structure and mechanisms of extinction of diffusion flames (Hamins, 1985; Hamins and Seshadri, 1984a, 1984b, 1986, 1987; Hamins *et al.*, 1985; Seshadri and Williams, 1975, 1978a). The critical conditions of flame extinction measured in the opposed flow configuration, can be readily interpreted using currently available asymptotic theories of flame extinction (Fendell, 1965; Peters, 1982, 1984; Williams, 1985), and the results can also be extended to turbulent nonpremixed combustion (Peters, 1982, 1984). Interpretation of experimental results of flame extinction using asymptotic theories requires knowledge of the characteristic flow time in the flame, t_{flow}. In the opposed flow configuration, the value of t_{flow} is related to the velocity of the reactant streams or the flow field strain rate (Seshadri and Williams, 1978b), which is an independently controlled experimental parameter.

This is not the case for a coflow system like the cup burner. In the coflowing configuration, the shape of the flame is approximately conical and the value of t_{flow} cannot be related easily to the flow velocities of the reactant streams. It has been recently shown that in the coflowing configuration the value of t_{flow} at the flame varies with height above the exit of the burner (Seshadri *et al.*, 1990). Therefore, interpretation of extinction data obtained in the coflowing configuration is not straightforward. Also, in the coflowing configuration premixing of the fuel and oxidizer can occur near the vicinity of the surface of the liquid fuel and the exit of the oxidizer duct where the fuel vapors and the oxidizer initially come into contact. This premixing can influence the mechanisms of flame extinction. However, in the opposed flow configuration, premixing, other than that resulting directly from diffusion of reactants through the flame, is eliminated completely. A significant advantage of the opposed flow configuration is that there are numerous computer programs available for predicting the

Table 1. Experimental Configurations

Configuration	Type of Combustion and Flow Field	Pressure	Agents	Fuels
Opposed Flow Diffusion Flame	laminar non-premixed	ambient	13 gaseous agents & $NaHCO_3$	heptane, JP-8
Cup Burner	quasi-laminar non-premixed	ambient	14 gaseous agents, $NaHCO_3$, & 18 additional agents	JP-5, JP-8, 5606, 83282, heptane, propane
Spray Burner	turbulent spray	ambient	14 gaseous agents & $NaHCO_3$	83282, JP-8
Deflagration Tube	turbulent premixed	variable	14 gaseous agents	ethene

structure and critical conditions of flame extinction (Bui and Seshadri, 1992; Chelliah, 1992; Smooke *et al.*, 1986). Although, such programs have also been developed for predicting the structure of flames stabilized in the coflowing configuration, these programs require considerably more computational time. Careful interpretation of the data, however, show that there exists a correspondence between the results obtained in the opposed flow and coflow configurations.

Consideration of in-flight fire scenarios in engine nacelles and dry bays prompted the development of two unique test configurations, the deflagration tube and the spray flame burner. Although it is not possible to estimate the value of t_{flow} for the spray burner or the deflagration tube, extinction experiments in these configurations are of interest because they mimic combustion behavior in engine nacelle and dry bay fires, where t_{flow} is also not well characterized.

In contrast to all of the other configurations listed in Table 1, combustion is premixed in the deflagration tube. In the spray burner, although the fuel and oxidizer are initially nonpremixed, combustion occurs in the form of a turbulent two-phase spray which is neither purely premixed nor nonpremixed, but can be thought of as an ensemble of partially premixed flames. Whereas the flames are laminar in the OFDF and are nearly laminar in the cup burner, they are highly turbulent in the other two configurations. Atmospheric combustion occurs in all of the configurations except the deflagration tube, where final pressures can be much larger than atmospheric.

The differences in the structure of the flames in each of the test configurations is likely to have a large impact on the relative suppression effectiveness of the agents. The introduction of an inert or chemical inhibitor to a flame impacts the stability of the flame by influencing the flame structure through changes in the temperature and species concentration fields. At the same time, the structures of premixed and nonpremixed flames are distinct. The mechanism for suppression may be distinct in detonations and diffusion flames because the chemistry may take place at different pressures, and chemical rate constants are pressure sensitive which could enhance or diminish the importance of particular chemical reactions. In non-premixed flames, combustion can be limited by the rate at which the reactants are brought together, whereas in premixed flames, combustion is limited by the chemical kinetics. Spray flames represent a complicated combustion situation where fuel droplets vaporize and react with the oxidizer, which can be composed of either pure air, air mixed with combustion products or air mixed with fuel vapor. Because of the inherent differences in the

structure of the combustion zone in each of the configurations, it would be very surprising if the agents displayed identical agent suppression effectiveness in the different test configurations.

4.1.2 Fuels and Agents Tested. In the four configurations, a number of different fuels were tested. Table 1 lists these fuels. They consisted of gaseous fuels (propane and ethene), multi-component liquid fuels (JP-5 and JP-8 jet fuels, and 5606 and 83282 hydraulic fluids) and a single component liquid fuel (heptane). The jet fuels and hydraulic fluids contain many components and can vary in composition from batch to batch. Thus, the heats of combustion (Gascoyne Laboratories, 1993) and elemental composition (Galbraith Laboratories, 1993) for the fuel batch used in the experiments reported here were determined as listed in Table 2.

4.1.3 Agents. Thirteen gaseous agents were tested in all configurations. The agents included nitrogen; four perfluorinated compounds, C_2F_6, C_3F_8, C_4F_{10}, and cyclo-C_4F_8; four hydrogen/fluorine compounds, CF_3HFCF_3, $CF_3H_2CF_3$, C_2HF_5, and CFH_2CF_3; the mixture 60% CH_2F_2/40% C_2HF_5; the chlorinated agents CHF_2Cl and $CHFClCF_3$; and CF_3Br. In addition, CF_3I and sodium bicarbonate powder ($NaHCO_3$) were tested in all configurations except the OFDF burner and the deflagration tube, respectively.

Eighteen additional agents were tested in the cup burner including inert gases, other halocarbons, a silicon compound, and a nitrogen compound. In addition, several liquid agents were tested. A detailed explanation for the selection of additional agents for cup burner testing is given in Section 5.

In addition to the gaseous and liquid agents described above, sodium bicarbonate, a solid powder, was also tested in the first three configurations listed in Table 1. The objective of these tests was to quantitatively compare the suppression effectiveness of sodium bicarbonate to CF_3Br and the other gaseous agents.

Sodium bicarbonate powder is currently a popular fire suppressant and its effectiveness is well known. Because of its zero ozone depletion potential, it deserves consideration for a wider range of applications. Few flame extinction measurements have been conducted with powders in test devices where the effectiveness of the powder could be directly compared with gaseous agents, and where flow field effects were minimized.

Some previous studies indicated that particle size is an important parameter in flame extinction using dry powders. Milne *et al.*, (1970) studied the extinction of methane/air opposed flow diffusion flames using $NaHCO_3$ powders with different diameters and found that smaller powders were more effective flame suppression agents. Measurements were reported by Dodding *et al.*, (1977) for extinction of methane/air opposed flow diffusion flames with 10 to 20 μm sodium bicarbonate particles added to the oxidizer. However, a key experimental parameter, the strain rate, was not reported. Others have tested the effectiveness of powders in less fundamental geometries. Ewing *et al.*, (1989) reported that approximately 4% (by mass) of $NaHCO_3$ (≈ 10 μm particles) was needed to extinguish heptane pan fires.

In order to study the impact of particle size, the powder was milled and then silica (SiO_2) was added to the powder to improve flow behavior and to prevent agglomeration. The particles were then sized using a centrifuge by VORTEC Industries into several fractions, hereafter referred to as nominally 0-10, 10-20, 20-30, 30-40, 40-50, and 50+ μm. The powder was stored in sealed plastic bags until use.

Particle size distribution was measured using optical microscopy and an average (equivalent sphere) diameter is listed in Table 3. Table 3 also lists the density of the $NaHCO_3/SiO_2$ mixtures which was measured using helium pycnometry (Lum, 1993) and the (mass based) percentage of SiO_2 in each size fraction as measured by X-ray fluorescence (Dow-Corning, 1993).

Table 2. Fuel Properties

Fuel Type	Heat of Combustion (MJ/kg)	Elemental Analysis		
		Mass Percent H	Mass Percent C	Mass Percent O
JP-5	46.3	13.3	85.4	< 0.5
JP-8	46.5	13.9	86.2	< 0.5
5606	44.0	12.6	80.5	2.03
83282	45.1	13.2	79.5	4.78
ethene	50.3	14.3	85.7	0
propane	50.3	18.2	81.8	0
heptane	48.1	16.0	84.0	0

Table 3. Particle Characterization

Nominal Particle Size (μm)	Equivalent Particle Diameter (μm)	SiO_2 % (kg/kg)	Measured Density (kg/m^3)
0 - 10	4.5 $\pm$ 0.5	1.34	2220
10 - 20	7.0 $\pm$ 0.5	0.67	2220
20 - 30	[a]	0.46	2220

[a] Not measured

The remainder of this Section is broken into four parts which include detailed descriptions of the experimental apparatus listed in Table 1. For each configuration, experimental methods, results, and discussion are included. Key findings of the work are compiled in Section 4.6 and reference are listed in Section 4.7.

4.2 Opposed Flow Diffusion Flames

4.2.1 Introduction. An experimental study was conducted to characterize the relative influence of various inhibiting agents in extinguishing diffusion flames burning the liquid hydrocarbon fuels heptane and JP-8. Thirteen gaseous inhibiting agents and $NaHCO_3$ were tested, and their effectiveness in extinguishing diffusion flames burning liquid fuels was compared to CF_3Br. The experimental configuration employed in the study was a diffusion flame stabilized in the mixing layer produced by directing an oxidizing gas stream downward on the burning surface of a liquid fuel. This is referred to in the literature as the OFDF configuration and is a convenient geometry for detailed fundamental studies of the structure and mechanisms of extinction of diffusion flames. In the OFDF configuration,

shown in Figure 1, there exists a stagnation plane, and the stoichiometry of the overall combustion processes is such that the flame (defined as the position where the temperature attains a maximum value) is stabilized on the oxidizer side of the stagnation plane. The oxidizing gas used in the experiments was a mixture of air and the inhibiting agent. To test the influence of the initial temperature of the oxidizing gas stream on the critical conditions of flame extinction, the experiments were performed with the oxidizing stream at temperatures of 25 °C and 150 °C.

Milne *et al.*, (1970) employed the opposed flow technique to evaluate the influence of gaseous inhibiting agents, including CF_3Br and powdered agents, on the critical conditions of extinction of methane-air, propane-air and n-butane-air diffusion flames. These experiments employed the "Tsuji" type opposed flow configuration, where the diffusion flame is stabilized in the vicinity of the forward stagnation line of a porous cylinder from which the gaseous fuel is introduced into the reaction zone. From the experimental measurements it was concluded that on a mass basis some powder agents are approximately ten times more effective than CF_3Br in extinguishing diffusion flames. Kent and Williams (1974) and Seshadri and Williams (1975) studied the inhibiting effect of CF_3Br on opposed flow diffusion flames stabilized over the surface of pools of heptane. The velocity and composition of the oxidizer stream at extinction were measured (Kent and Williams, 1974 and Seshadri and Williams, 1975). The concentration of CF_3Br in the oxidizing stream at flame extinction was compared to the amount of the inert diluent N_2 which must be added to the air stream to extinguish the flame. At selected conditions the flame temperature near extinction was also measured. As mentioned in Section 4.1, interpretation of experimental results of flame extinction using asymptotic theories requires knowledge of the characteristic residence time in the flame, t_{flow}. At a fixed value of the flow velocity of the oxidizer stream, or at a fixed value of t_{flow}, the concentration of CF_3Br in the air stream at extinction was found to be considerably lower than the concentration of N_2 added to the air stream at extinction. In addition, the value of the measured temperature in the vicinity of extinction was higher or the value of the characteristic chemical-reaction time t_{chem} was lower when CF_3Br was added to the oxidizer stream than for nitrogen dilution. Since nitrogen is an inert compound, these results imply that inhibition of chemical reactions by CF_3Br may be responsible for extinguishing the flame at a lower value of t_{chem}. These previously developed techniques (Kent and Williams, 1974; Seshadri and Williams, 1975) are used to interpret the experimental results obtained in the present study.

4.2.2 Experimental Apparatus. Figure 2 shows a schematic illustration of the OFDF burner. The burner consisted of a fuel cup which had a diameter of 50 mm and a depth of 18 mm, and an oxidizer duct through which the oxidizing stream containing the gaseous inhibitor or $NaHCO_3$ powder was introduced into the flame. The fuel cup was cooled by water at the bottom in order to prevent the fuel from boiling, but was not cooled at the rim as that would establish a radial temperature gradient within the liquid fuel. A narrow annulus surrounded the wall of the cup near the rim to catch any overflow of the fuel and prevent it from entering into the exhaust duct. Since, the flame sheet was very sensitive to surface movements, the fuel height in the cup was accurately controlled by a device similar to that designed by Bajpai (1974b). A fine pointer projecting up through the liquid pool was used as an aid in adjusting the height of the fuel surface. Satisfactory repeatability had been obtained by setting the pool at the level at which the pointer just forms a discernible dimple on the fuel surface. The oxidizer duct had an inner diameter of 50.1 mm. For experiments with gaseous inhibitors approximately five layers of fine wire screens (80 mesh/cm) with each layer of the screen separated by a 1 mm split ring were placed in the duct to reduce the scale of turbulence and to ensure a flat velocity profile at the exit of the duct. For experiments with $NaHCO_3$ powder, only two layers of coarse wire screen (8 mesh/cm) were employed to prevent accumulation of the powder on screens. Also, in the experiments with $NaHCO_3$ powder, it was necessary to replace the screens frequently.

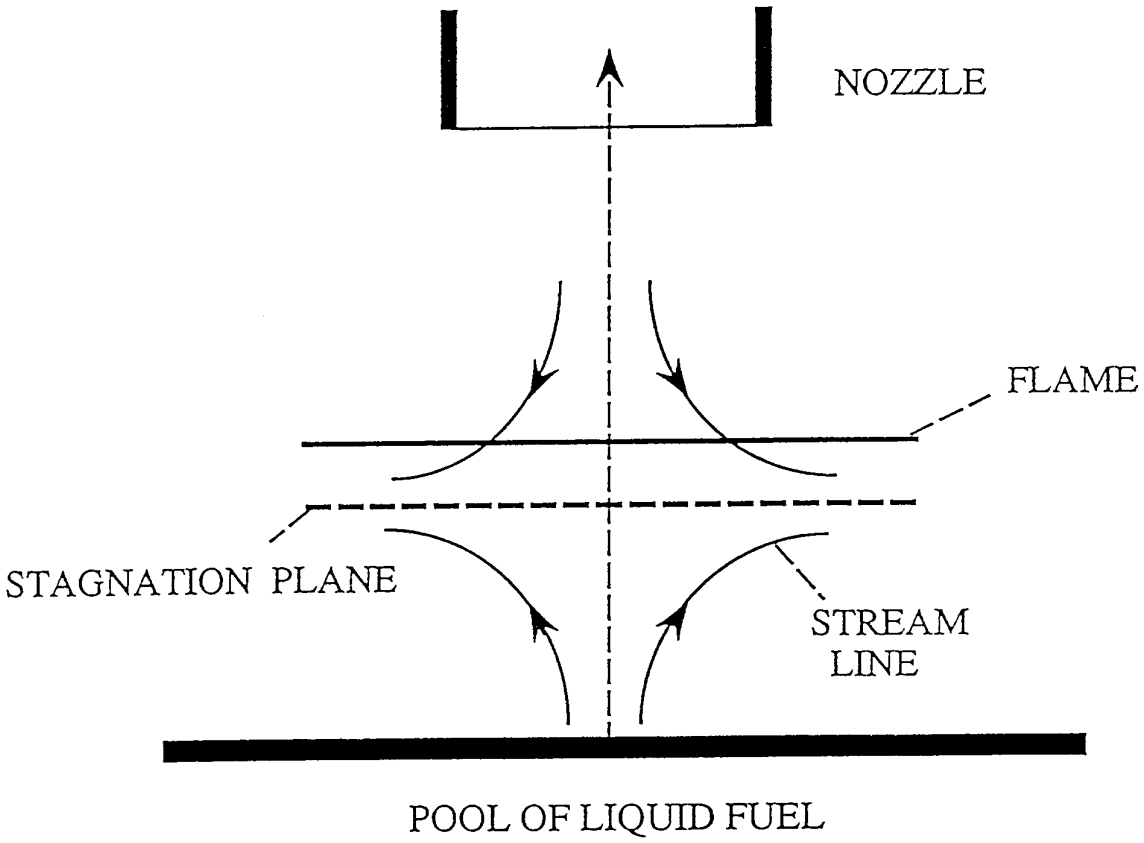

Figure 1. Schematic illustration of the counterflow configuration.

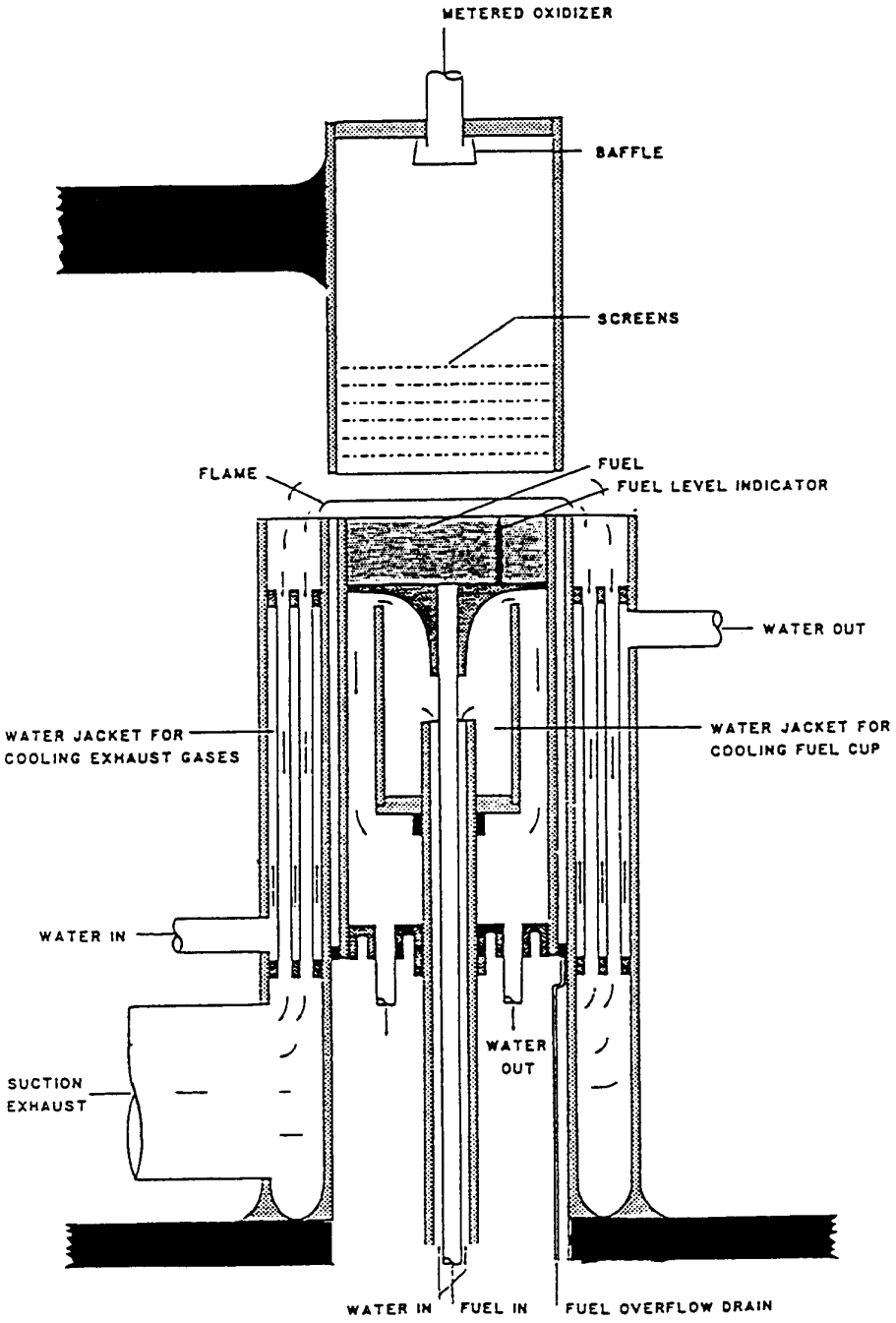

Figure 2. Schematic illustration of the OFDF burner.

The distance between the oxidizer duct and the fuel cup was adjustable and the oxidizer duct could be swivelled to allow access to the fuel cup. Experiments were performed with the separation distance, L, between the surface of the liquid pool and the exit of the oxidizer duct equal to 10 mm. Mild suction was used to pull the products of combustion from the flame into a heat exchanger surrounding the fuel-overflow rim. The cooled gases then flowed into the exhaust. The suction minimized the influence of the ambient air currents on the flame, and prevented after-burning in the heat exchanger. A steady flame like that shown in Figure 3 could be indefinitely stabilized in this apparatus. Measurements were made with the burner enclosed within a plexiglass box with an outlet directly connected to the exhaust to minimize operator exposure to the products of combustion.

The volumetric flow of air, nitrogen and the gaseous inhibitors were measured to $\pm 3\%$ by use of variable area flowmeters. Pressure gauges were arranged in parallel with the flowmeters to insure that the volumetric flow of the gas stream was not affected by fluctuations in the output pressure from compressed gas cylinders or from variations in stagnation pressure caused by adjusting the volumetric gas flows. The flowmeters were calibrated using wet-test meters. The uncertainty in the concentration of agent at extinction are estimated as approximately 10%.

Figure 4 shows a schematic illustration of the device employed to introduce $NaHCO_3$ powder into the flame. This device, originally designed by Williams and Peters (1982), was made of plexiglass and consisted of a bed of powder resting on a porous disk. Air was introduced from the bottom fluidizing tube and passed through a bed of glass beads which distributed the flow in the region between the glass beads and the porous disk. The air passed through the porous disk, lifted the particles and formed a fluidized bed in the region above the bed of powder. The air mixed with powder was removed from the exit tube and introduced into the oxidizing duct of the OFDF burner. The jet ring shown in Figure 4 was used to prevent agglomeration of the particles. The jet ring consisted of a thin tube closed on one end and bent to form a ring. A number of holes were punched along the periphery of the ring and air was introduced from the open end of the tube to raise the particles out of the fluidized bed. The mass fraction of the powder in the mixture of air and the particles flowing out of the exit tube was altered by adjusting the volumetric flows of air in the fluidizing tube and the jet ring.

Particle analysis was done by isokinetic sampling and weighing of the samples. After completion of the experiments, the portion of the OFDF burner containing the fuel cup was removed and a probe with a 10 mm diameter was placed under the oxidizer duct at nearly the same position as that of the fuel cup. A filter was placed inside the probe to collect the particles. The volumetric flows of air in the fluidizing tube and the jet ring were adjusted such that they were identical to those used in the extinction experiments. A wet-test meter was placed downstream to measure the volumetric flow rate of air in the probe. Mild suction was used such that the velocity of the mixture of air and the particles entering into the probe was approximately equal to that at the exit of the oxidizer duct. The flow into the probe was maintained until a measurable amount of powder was collected in the filter. The probe together with the powder was then removed and its weight was measured accurately. The weight of the powder in the probe was calculated from the difference between the weight of the probe with and without the powder. The total weight of the air flowing through the probe was calculated from the measured total volume of air recorded by the wet-test meter. The mass fraction of the particles in the air stream was then calculated from the ratio of the weight of the powder collected in the probe to the sum of the total weight of air and the weight of the particles. An average of three such runs was made at each measured extinction point to determine the mass fraction of powder in the oxidizing stream. The uncertainties in the amount of powder determined using this method was estimated to be approximately 15%.

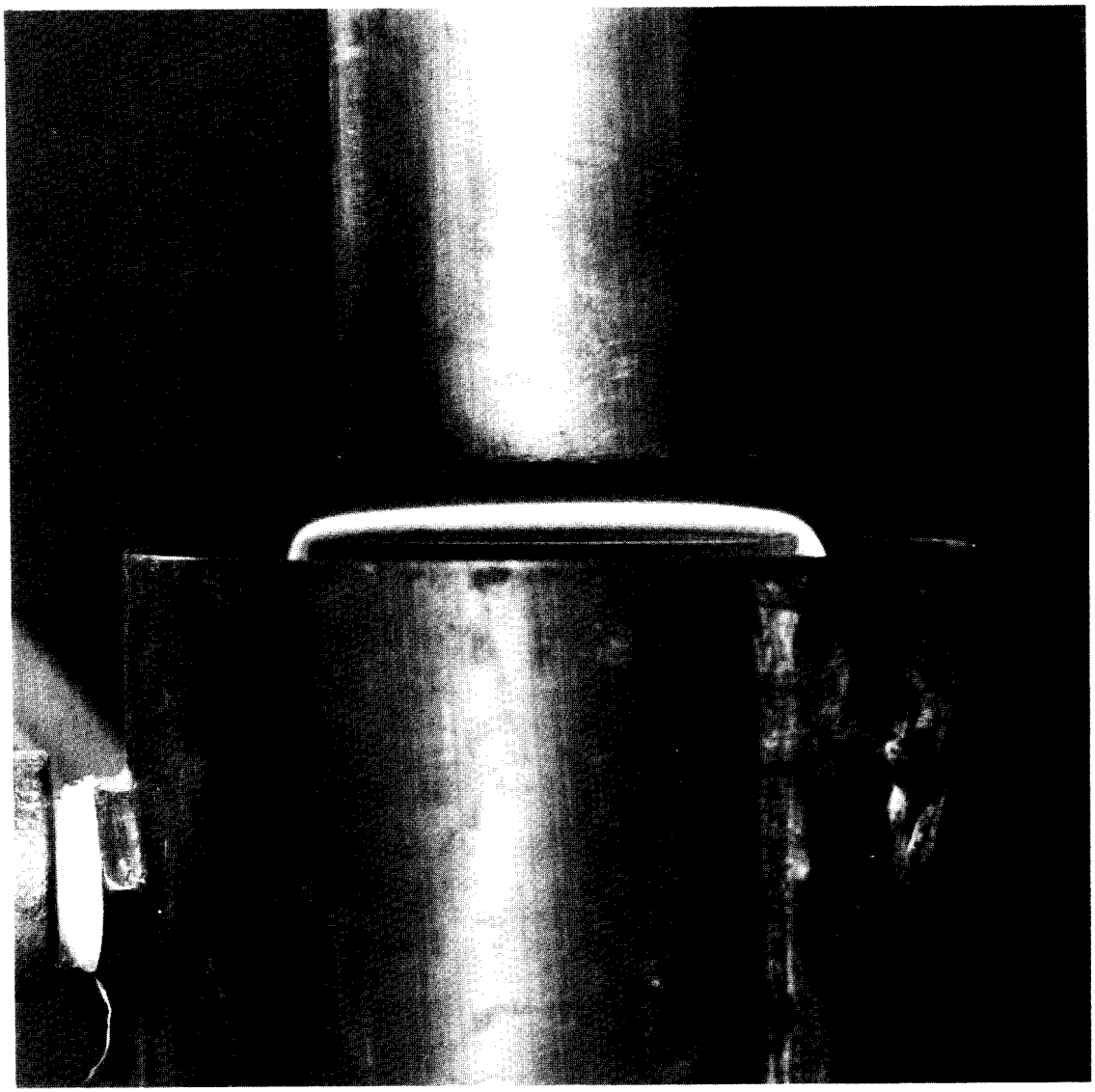

Figure 3. Photograph of uninhibited flame stabilized above heptane pool in OFDF burner.

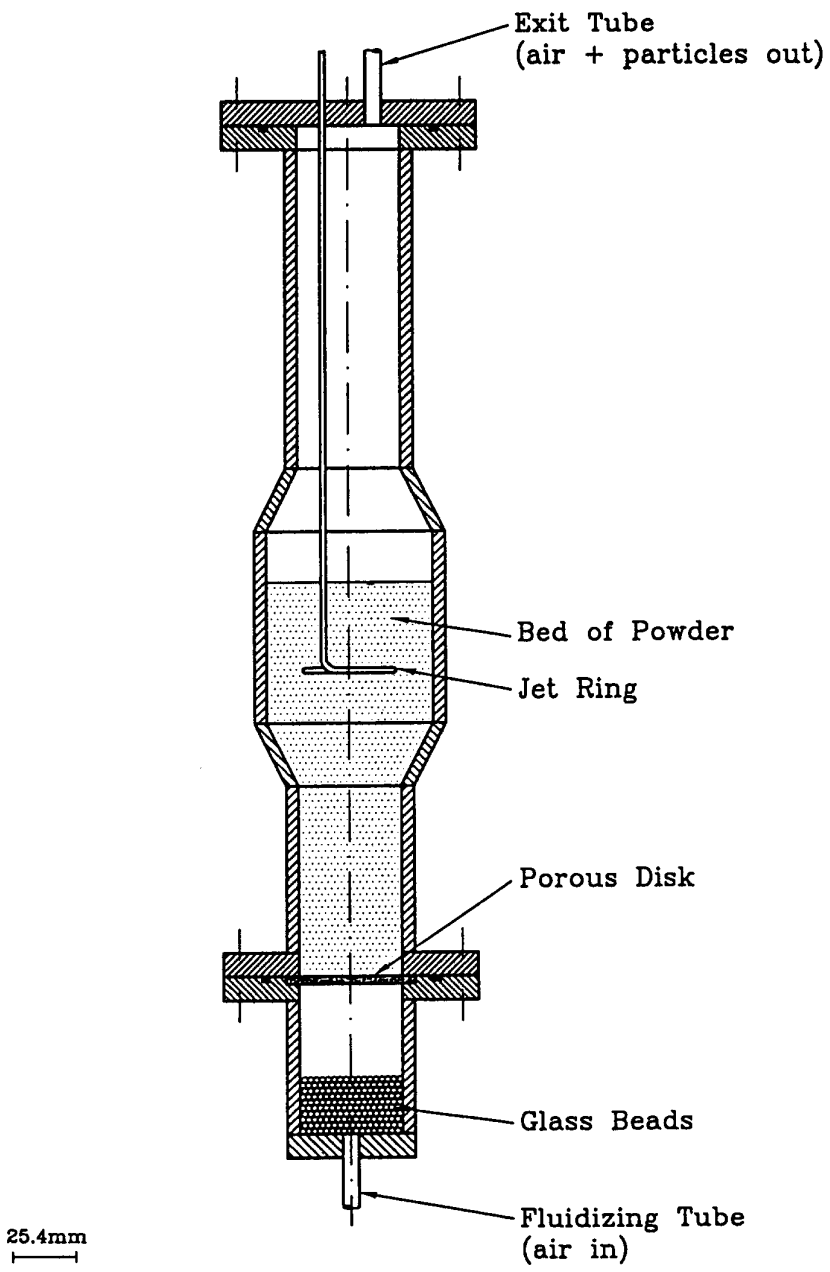

Figure 4. Schematic illustration of the powder dispensing device.

4.2.3 Experimental Procedure. For experiments with gaseous agents the volumetric flow of air through the oxidizer duct was maintained at some predetermined value and the liquid pool was ignited. The inhibitor was then added gradually to the oxidizer stream until the flame extinguished. Care was taken to ensure that the flame attained a steady state after each incremental addition of the inhibitor. The volumetric flows of air and inhibitor at extinction were recorded. The experiments were repeated with a different air flow. The velocity of the oxidizer stream at the exit of the duct, U, was presumed to be equal to the ratio of the total volumetric flow of air and the inhibitor to the cross-sectional area of the oxidizer duct. Following the analysis of Seshadri and Williams (1978b), the strain rate, a, is equal to the ratio of U to L, where L is the separation distance between the surface of the liquid pool and the exit of the oxidizer duct.

For experiments with $NaHCO_3$ powder, the uniformity of the concentration of powder in the oxidizing stream was monitored using the optical arrangement shown in Figure 5. For a given level of powder in the oxidizing gas stream, the attenuation of the He-Ne laser radiation was recorded by the oscilloscope and the strip-chart recorder. For experiments with $NaHCO_3$ powder, two separate air streams flowed into the oxidizer duct. One stream of air, termed the primary air, flowed directly from the flowmeters into the oxidizer duct, and the other stream of air flowed into the fluidizing and jet-ring tube of the powder dispensing device shown in Figure 4.

Initially the volumetric flow of primary air was maintained at some predetermined value and the liquid pool was ignited. Secondary air was then introduced through the fluidizing tube of the powder dispensing device until a sufficient amount of powder was observed to flow through the oxidizer tube. The uniformity of powder concentration in the oxidizer stream was monitored by recording the output of the strip-chart recorder. The flow of air was slowly increased until the flame was extinguished. Care was taken to ensure that the flame attained a steady state after each incremental addition of powder by monitoring the output of the strip-chart recorder. The flowmeter readings for the primary and secondary air as well as the fractions of the secondary air flowing through the fluidizing tube and the jet-ring were recorded. The amount of powder in the oxidizing stream was then determined as described in the previous section. The experiment was then repeated at a different volumetric flow of the primary air.

4.2.4 Experimental Results. Figure 6 shows the mass fraction of the agents as a function of the strain rate, a, at extinction. The fuel was heptane and the initial temperature of the oxidizer stream was 25 °C. For a given agent, the region below the curve represents flammable mixtures. For any value of the strain rate the value of the mass fraction of CF_3Br required to extinguish the flame is lower than the mass fraction of all other agents. Therefore on a mass basis CF_3Br is considerably more effective in extinguishing the flame than all the other agents tested. Figure 6 shows that the relative effectiveness of some of the agents in extinguishing the flame varies with the strain rate. This becomes more clear by examining the results shown in Figure 7, where the data are replotted with an expanded vertical scale. At low strain rates HFC-236 is most effective and FC-116 least effective in extinguishing the flame, whereas at high strain rates HCFC-22 is most effective and FC-318 least effective in extinguishing the flame. In fact at high strain rates only CF_3Br and HCFC-22 are more effective than N_2 in extinguishing the flame. However, the results plotted in Figures 6 and 7 show that with the exception of CF_3Br, the differences in the mass-based effectiveness of the various agent are not large.

Figure 8 is a plot of the same data shown in terms of the mole fraction of the agents. The fuel was heptane and the initial temperature of the oxidizer stream was 25 °C. For any given value of the strain rate the value of the mole fraction of CF_3Br required to extinguish the flame was lower than the mole fraction of all other agents. On a mole basis, at low and high strain rates FC-31-10 was most effective and HFC-32/125 least effective in extinguishing the flame. Note that on a mole basis, all

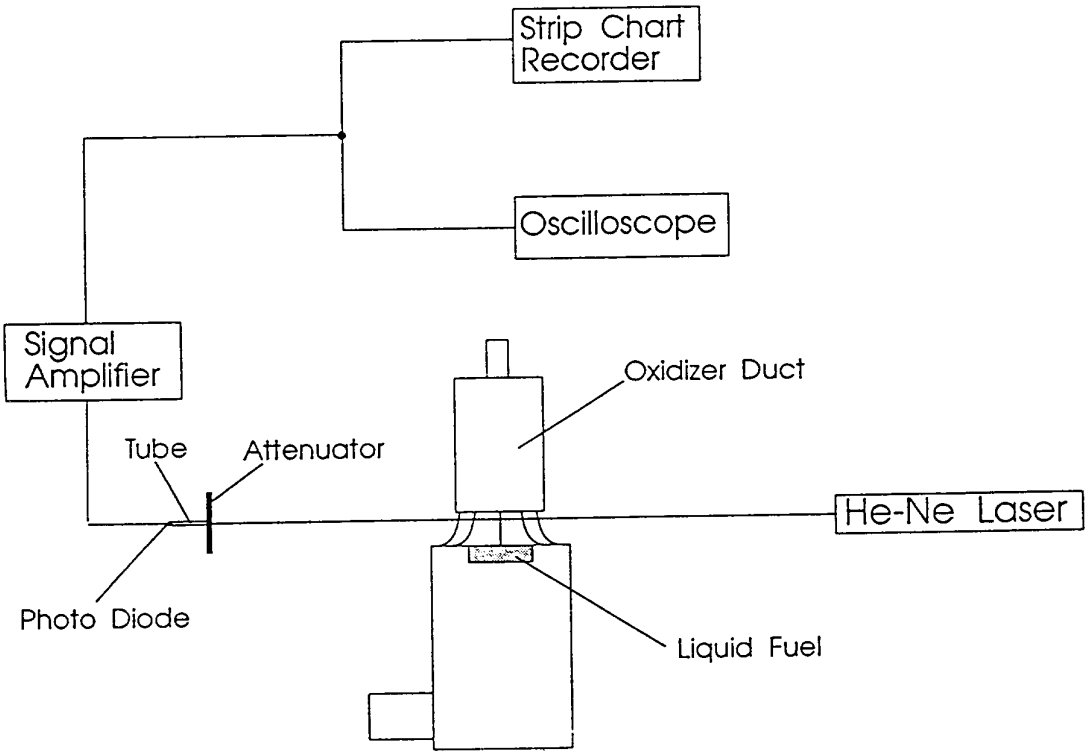

Figure 5. Schematic of the optical arrangement employed for monitoring powder concentration.

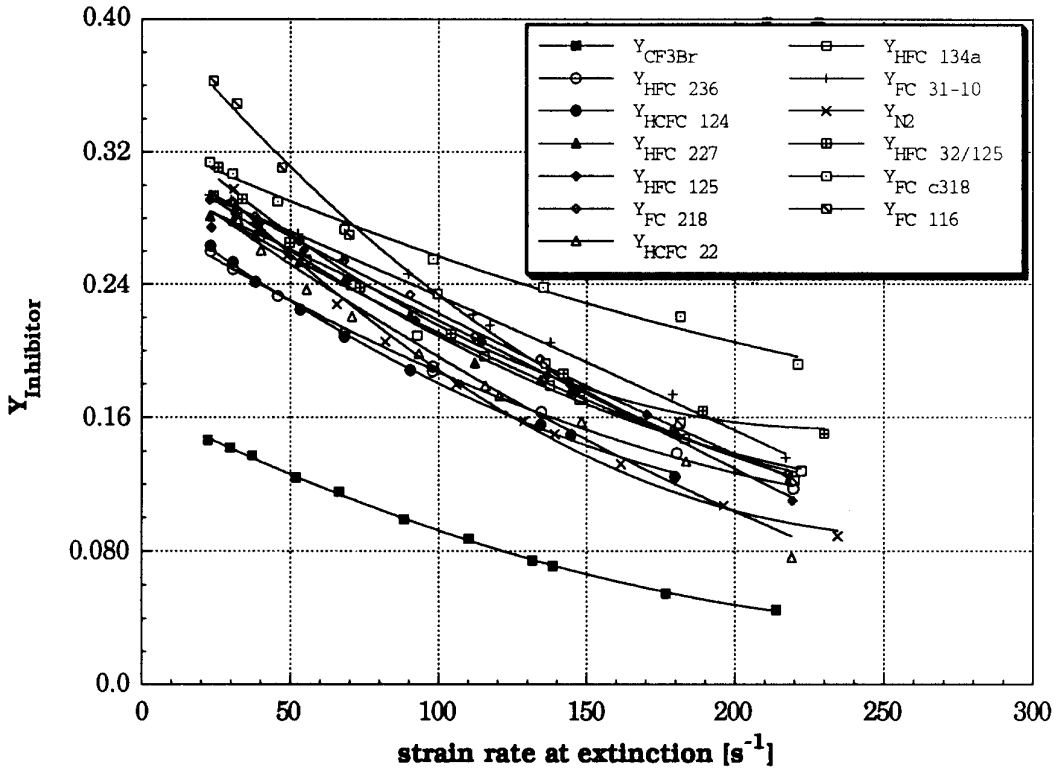

Figure 6. Mass fraction of various agents as a function of the strain rate for heptane flames at extinction, with an oxidizer temperature of 25 °C.

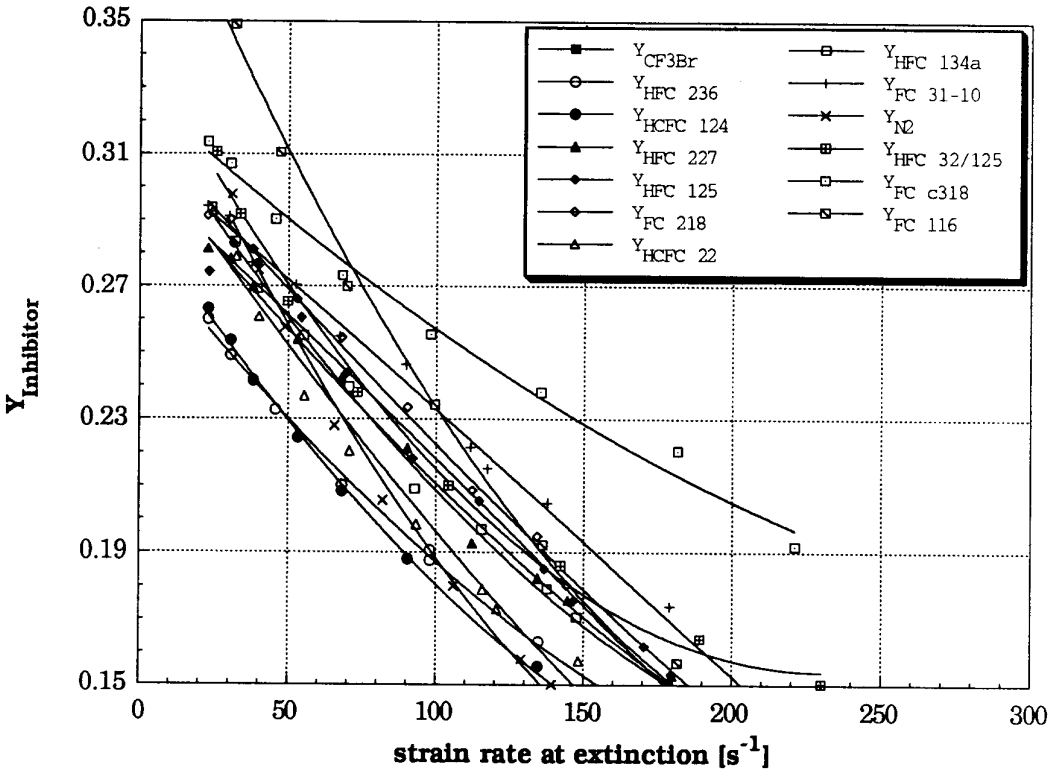

Figure 7. Mass fraction of various agents as a function of strain rate for heptane flames at extinction (expanded vertical scale), with an oxidizer temperature of 25 °C.

the agents tested were more effective than N_2 in extinguishing the flame, which is the inverse of the results when plotted versus mass fraction.

4.2.4.1 Impact of Fuel Type. Figures 9 and 10 show, respectively, the mass and mole fractions of the agents as a function of the strain rate at extinction for JP-8 flames. The oxidizer stream temperature was 25 °C. A comparison of Figures 8 and 10 shows that the JP-8 flames were somewhat easier to extinguish than the heptane flames. The average agent extinction concentration for the JP-8 flames was 65% to 93% of that required to extinguish the heptane flames over the range of strain rates, with the differences being greatest at the highest values of strain rate. The reasons for the variation of this value with strain rate is not clear.

4.2.4.2 Impact of Air Temperature. To clarify the influence of the initial temperature of the oxidizer on the critical conditions of flame extinction experiments were performed with the initial temperature of the air equal to 150 °C. Prior to performing these experiments, radial temperature profiles were measured in the apparatus without igniting the flame using thermocouples in the region between the exit of the gas duct and the surface of the liquid pool. The results are plotted in Figure 11, where the quantity DT refers to the difference between 150 °C and the measured value of the temperature, and r refers to the radial distance in millimeters from the axis of symmetry. Four sets of measurements were made: at the exit of the duct, 2 mm below the exit of the duct, and at approximately the position where the flame was stabilized above the surface of the liquid pool. The latter measurements were made with and without the pool covered with a thin metal sheet. All measurements were made with liquid heptane in the cup. The profiles near the exit of the duct show that the temperature is roughly 18 °C lower than 150 °C in the region near the walls of the duct. However, over a radius of approximately 15 mm from the axis of symmetry, the temperature was nearly uniform and differed from 150 °C by amounts less than 5 °C. The measurements made at the approximate location where the flame would stabilize showed that the radial temperature profile was relatively uniform. The values of the temperature measured with the pool covered were found to be lower than those measured with the uncovered pool, which was attributed to heat losses to the metal sheet. The temperature measurements clearly show the profile to be nearly uniform at the approximate position of the flame, and the value to differ from 150 °C by an amount less than 5 °C.

The relative mass-based effectiveness of the various agents differed slightly for different oxidizer stream temperatures. Figures 12 and 13 show the mass fraction of agent as a function of strain rate for heptane and JP-8, respectively, with an oxidizer temperature of 150 °C. A comparison of the results in Figures 12 and 13 with Figures 6 and 9, shows that an enhanced oxidizer temperature leads to flames which require somewhat more agent to extinguish. This result is consistent with theories of flame extinction. As more enthalpy is added to a flame, it is more difficult to extinguish. Figures 14 and 15 replot the data from Figures 12 and 13 in terms of agent mole fraction.

4.2.4.3 Powder Agent: Impact of Size. Figure 16 shows the mass fraction of $NaHCO_3$ powder with a nominal particle size of 10-20 μm in the oxidizer stream as a function of the strain rate at extinction. The fuel was heptane and the oxidizer stream temperature was 25 °C. For comparison the critical conditions of extinction measured with CF_3Br and N_2 added to the air stream are also shown. For measurements with $NaHCO_3$ powder, the experimental uncertainties are expected to be less than 30%. For any given value of a, the value of the mass fraction of $NaHCO_3$ required to extinguish the flame is lower than the mass fraction of CF_3Br and N_2. Therefore on a mass basis $NaHCO_3$ was more effective in extinguishing the flame than all the agents tested including CF_3Br. Figure 16 shows that at all values of the strain rate tested, the mass of $NaHCO_3$ powder required to extinguish the flame was a factor of three lower than that of CF_3Br. Figure 16 shows the mass

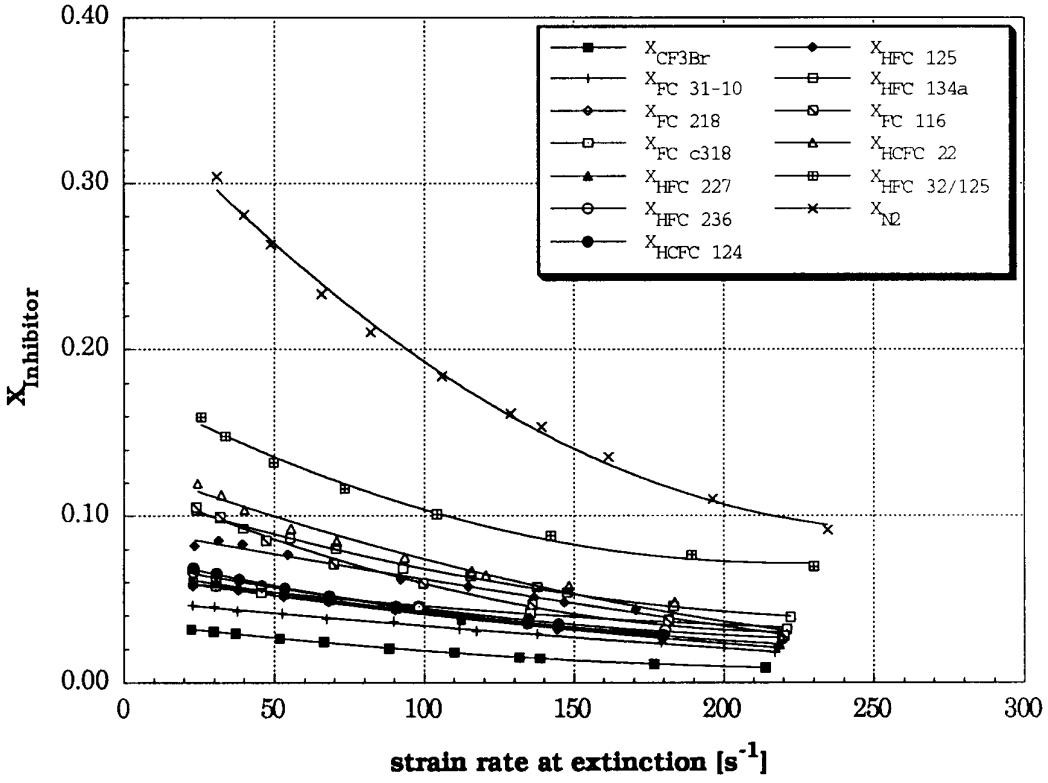

Figure 8. Mole fraction of various agents as a function of strain rate for heptane flames at extinction, with an oxidizer temperature of 25 °C.

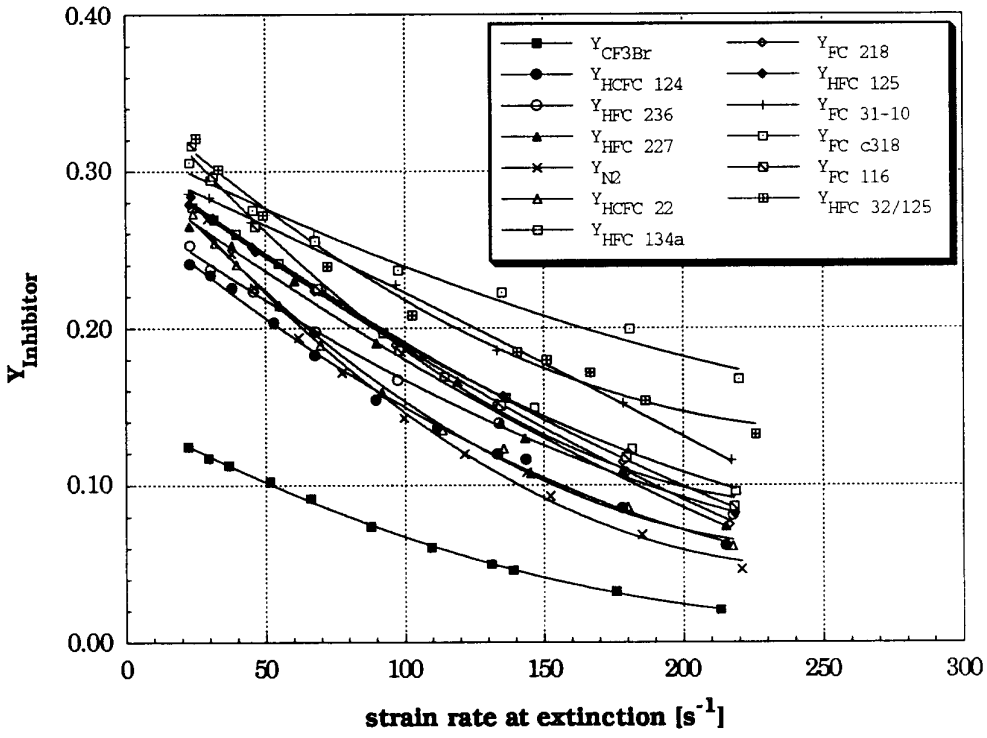

Figure 9. Mass fraction of various agents as a function of strain rate for JP-8 flames at extinction with an oxidizer temperature of 25 °C.

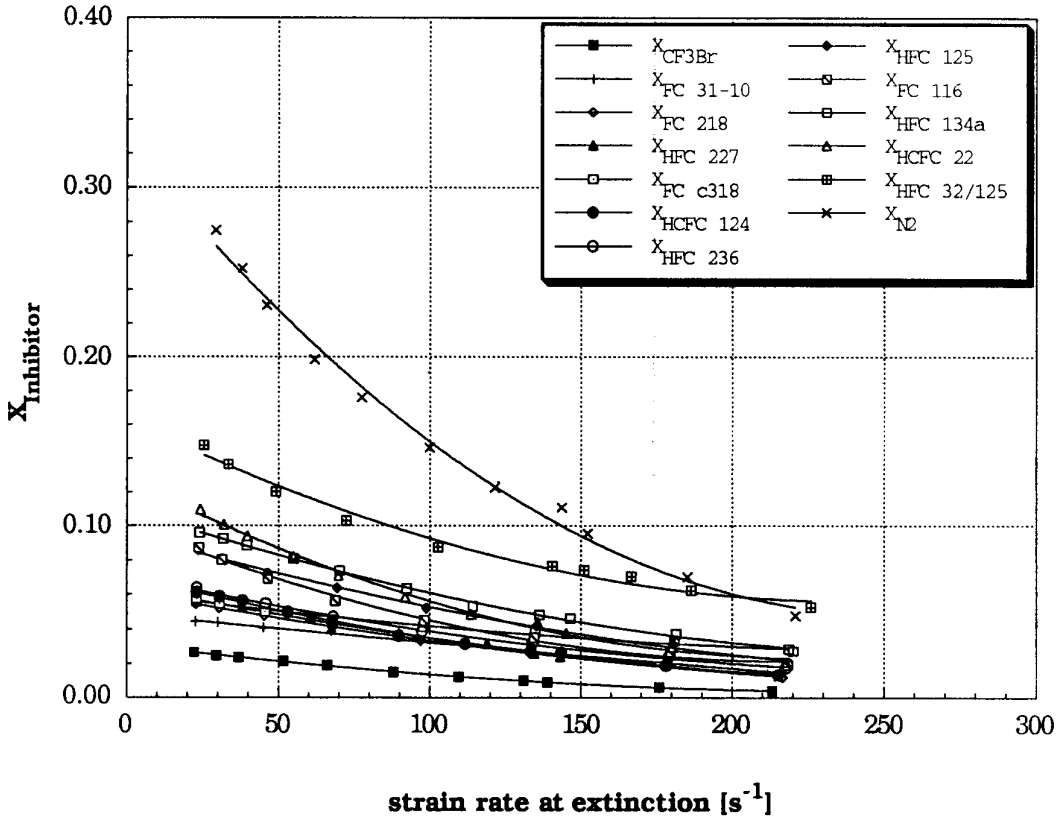

Figure 10. Mole fraction of various agents as a function of strain rate for JP-8 flames at extinction with an oxidizer temperature of 25 °C.

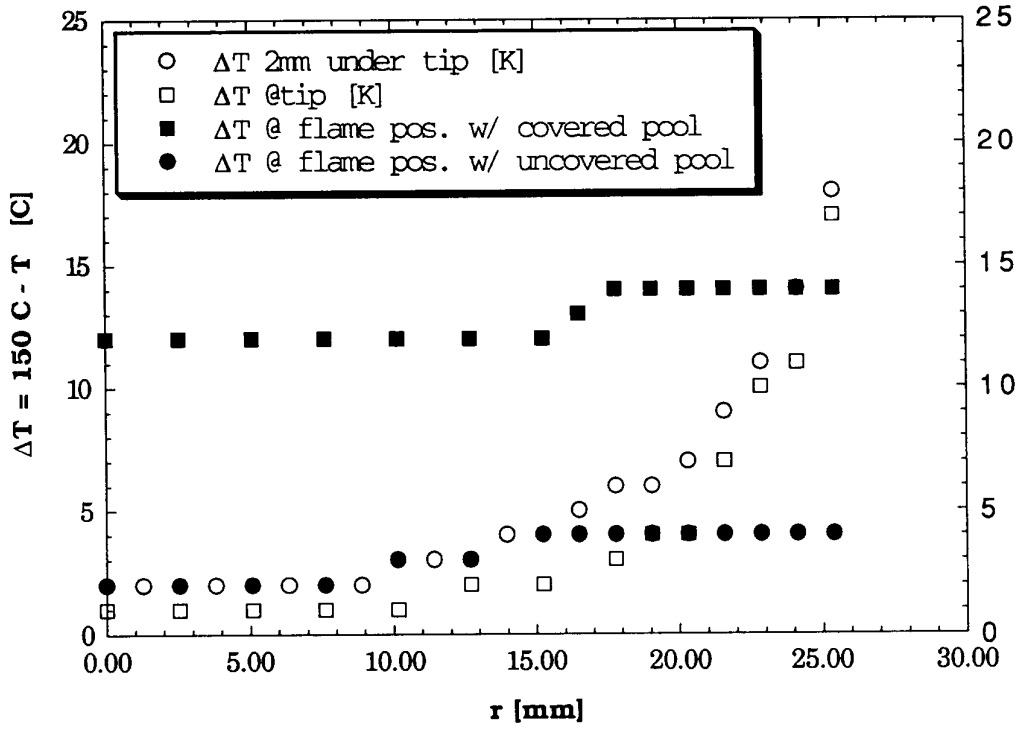

Figure 11. Radial temperature profiles measured without the flame at various locations at the region between the exit of the gas duct and the surface of the liquid pool for an oxidizer stream temperature of 150 °C.

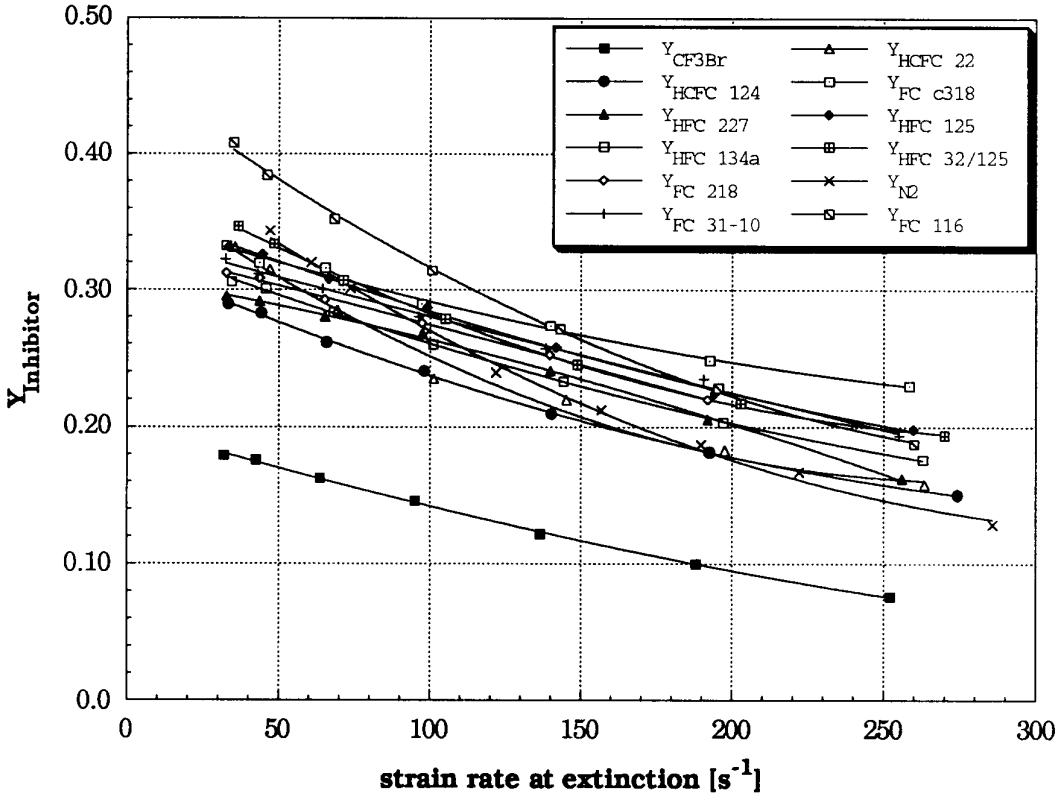

Figure 12. Mass fraction of various agents as a function of strain rate at extinction for heptane flames with an oxidizer temperature of 150 °C.

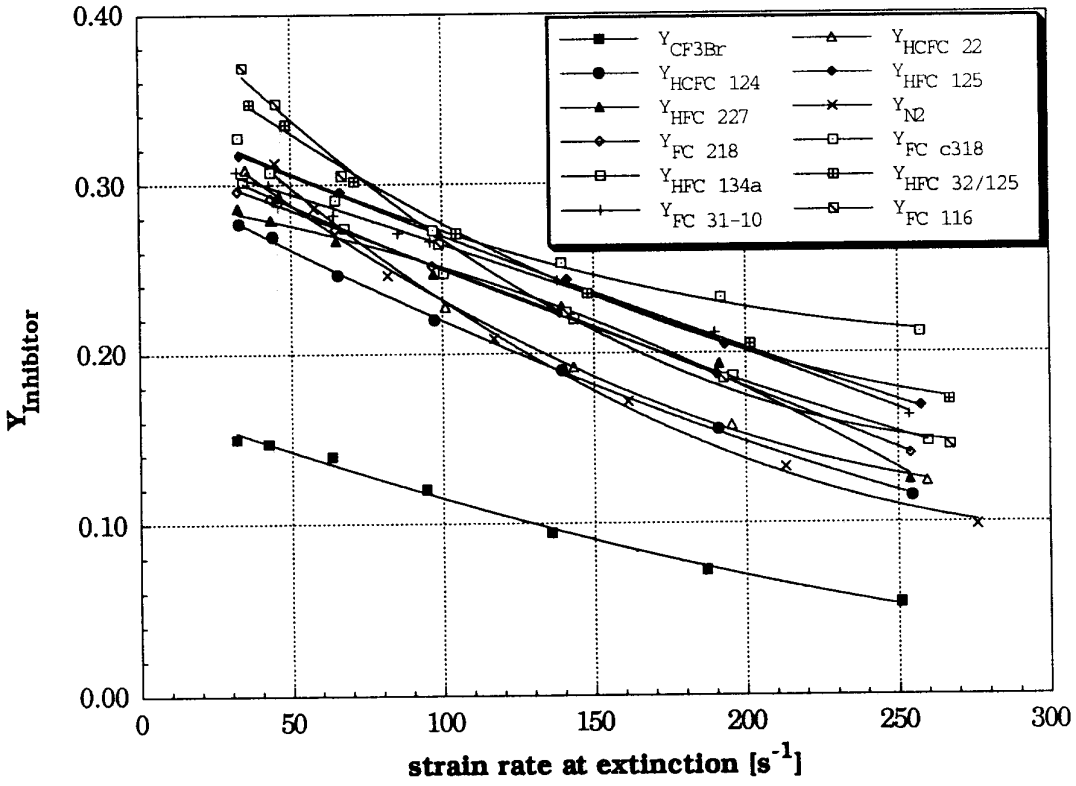

Figure 13. Mass fraction of various agents as a function of strain rate at extinction for JP-8 flames with an oxidizer temperature of 150 °C.

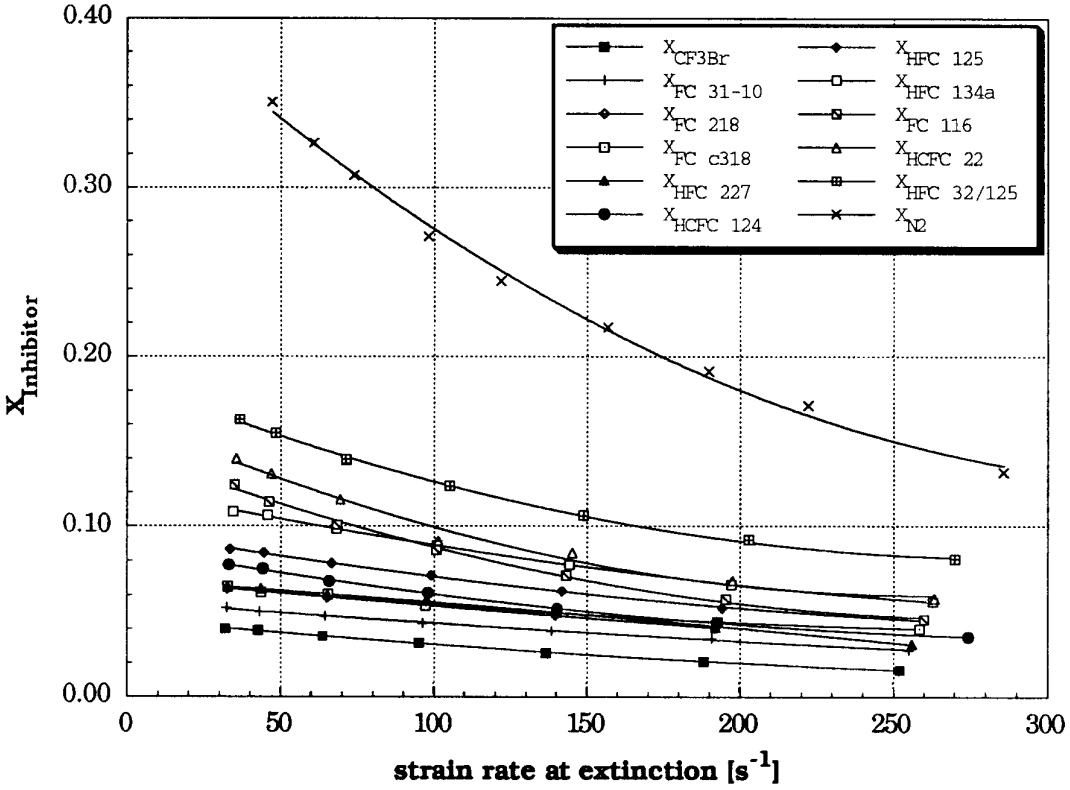

Figure 14. Mole fraction of various agents as a function of strain rate at extinction for heptane flames with an oxidizer temperature of 150 °C.

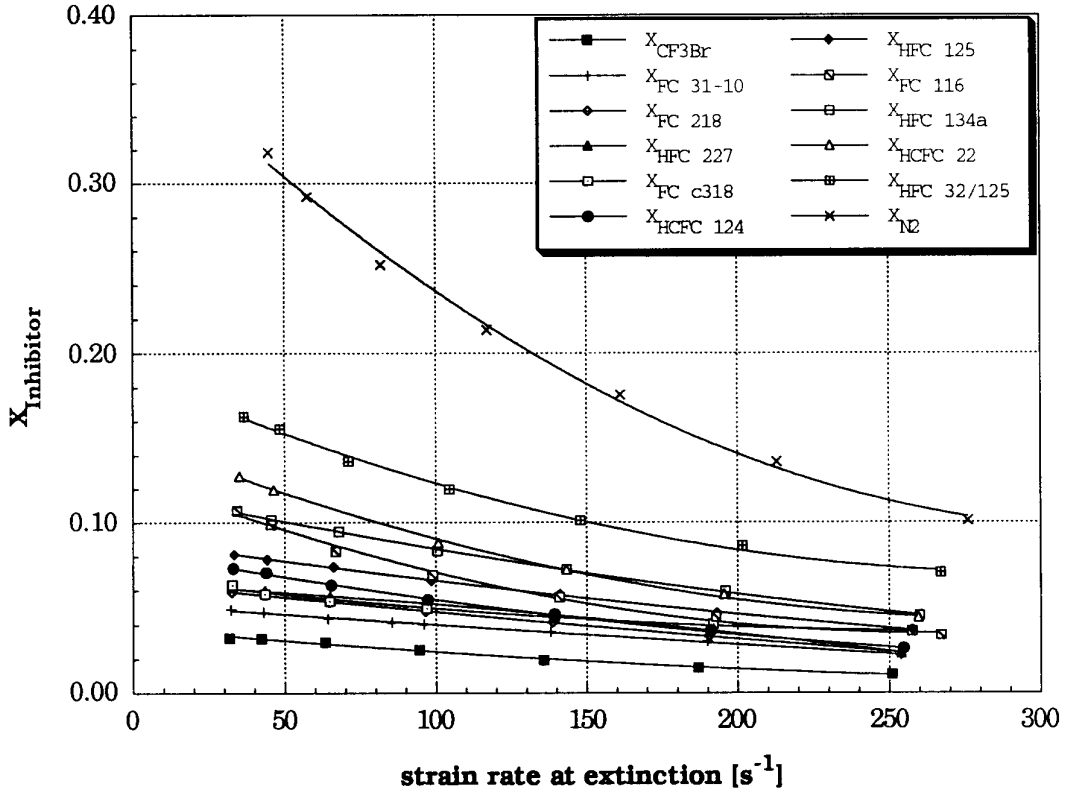

Figure 15. Mole fraction of various agents as a function of the strain rate at extinction for JP-8 flames with an oxidizer temperature of 150 °C.

fraction of $NaHCO_3$ powder (10 - 20 μm) in the oxidizer stream required to extinguish diffusion flames burning heptane and JP-8 as a function of the strain rate. The oxidizer stream temperature was 25 °C. Consistent with extinction data measured using gaseous agents, Figure 17 shows that at any value of the strain rate, the mass of $NaHCO_3$ required to extinguish JP-8 flames was less than that required to extinguish a heptane flame.

Figure 18 shows the influence of initial particle size of $NaHCO_3$ in extinguishing heptane flames. The initial temperature of the oxidizer stream was 25 °C and the nominal particles sizes tested were 0-10, 10-20, and 20-30 μm. The results show that particles between 0-10 μm were more effective than those between 10-20 and 20-30 μm. However, the results show that 20-30 μm particles were more effective than those 10-20 μm. Further studies are required to explain this observation.

4.2.5 Interpretation of the Experimental Results. As mentioned at the beginning of Section 4, in fundamental theories of flame extinction where the gas-phase chemical reaction can be approximated as a one-step process, changes in the value of the Damköhler number, D_n, can be used to qualitatively explain the results of the OFDF suppression experiments. For a given chemical system, flame extinction is predicted to occur at a well defined and experimentally reproducible value of the critical Damköhler number D_n* (Fendell, 1965; Liñan, 1974; Peters, 1982, 1984). The value of t_{chem} (and, hence, D_n) will depend on the relative concentrations of the various reactants including that of the agent and the local gas temperature, and the value of t_{flow} will depend inversely on the strain rate a. In the absence of temperature measurements at conditions close to flame extinction, the calculated adiabatic flame temperature T_f, can be used in Equation (1) to provide a rough measure of the characteristic chemical time. For flames near extinction, the value of t_{chem} decreases with increasing values of T_f for a fixed global activation energy.

The concentration of fuel, air, and agent at extinction in a heptane flame were used (from Figure 6) to calculate the adiabatic flame temperature, assuming complete combustion to stoichiometric amounts of CO_2 and H_2O, and frozen levels of inert agent. Figure 19 is a plot of T_f as a function of strain rate for each of the gaseous agents. The temperatures at extinction concentrations of CF_3Br are higher than the value of T_f calculated using the measured mass fractions of all other agents. Therefore for any value of t_{flow}, the critical conditions of extinction measured with CF_3Br yield values of t_{chem} which are smaller than those for the other agents. Hence the values of D_n* with CF_3Br is higher than the corresponding values of D_n* from the other agents. The values of T_f for N_2 suppression are 100 to 300 K lower than for CF_3Br. The temperatures for agents without chlorine are below nitrogen, and the two containing chlorine have slightly higher calculated temperatures. Since the nitrogen data are representative of a purely thermally acting agent, T_f can be used as a qualitative measure of the thermal versus chemical influence of the agent on the flame.

A global activation energy can be estimated from the theoretical value of D_n* found by performing an asymptotic analysis (Liñan, 1974; Peters, 1982, 1984; Krishnamurthy *et al.*, 1976) of the flame. Knowing the value of D_n at extinction from the analysis, and the flame temperature and strain rate from Figure 19, Equation (1) can be used to estimate the global rate coefficient k. Figure 20 is a plot of the natural log of a function (Krishnamurthy *et al.*, 1976) which is directly proportional to k (see Equation 1), versus $1/T_f$. (The value of T_f was calculated assuming that the agents were chemically inert.) The value of the E_0 for each of the agents can be estimated from the slope of the respective curves. For N_2, E_0 is 167 kJ/mole. Deviations of E_0 from this value for the other agents is a rough measure of the chemical influence of these agents. The value of E_0 calculated using extinction data with CF_3Br is equal to 894 kJ/mole, an unrealistically high value. Clearly the

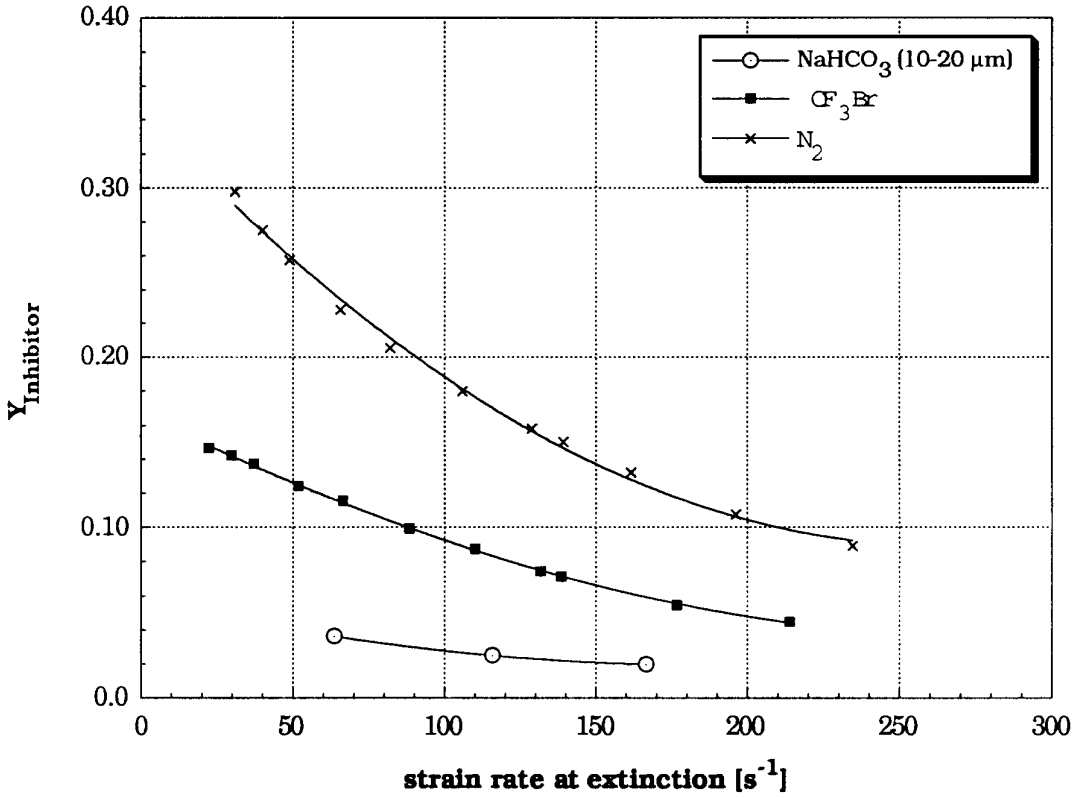

Figure 16. Mass fraction of $NaHCO_3$ (10 - 20 μm) powder in air as a function of the strain rate at extinction for heptane flames with an oxidizer temperature of 25 °C.

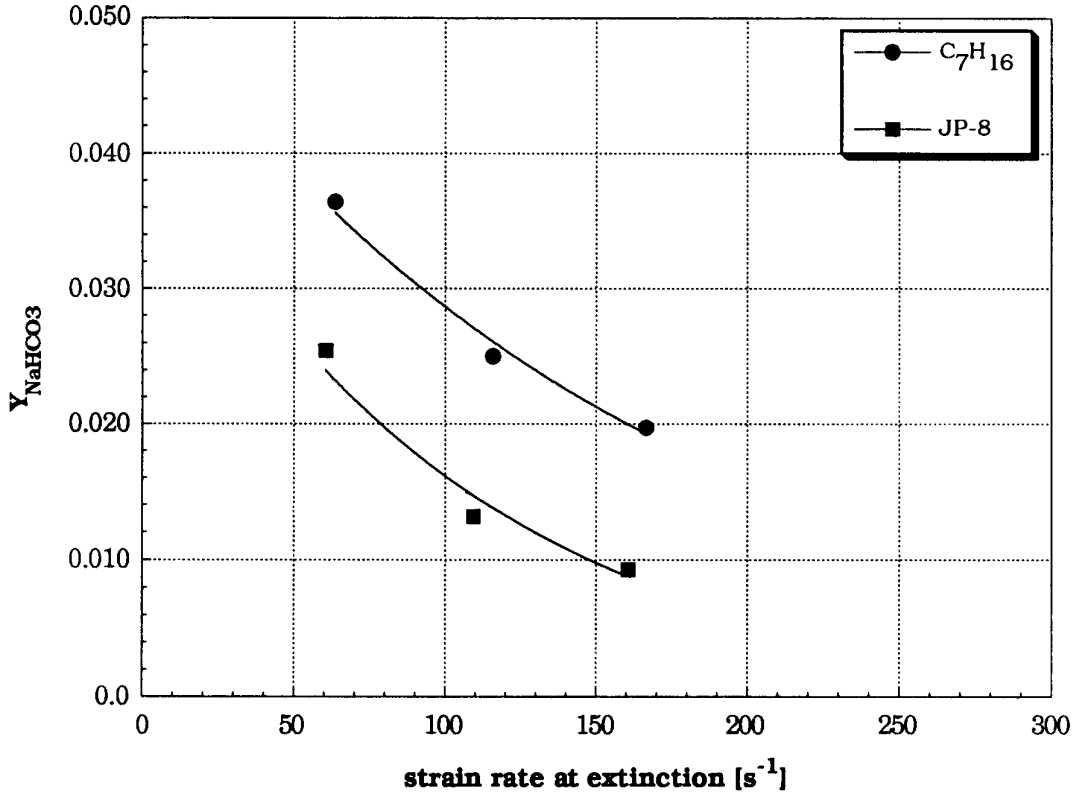

Figure 17. Mass fraction of $NaHCO_3$ (10 - 20 μm) powder in air as a function of the strain rate at extinction for heptane and JP-8 flames with oxidizer temperatures of 25 °C.

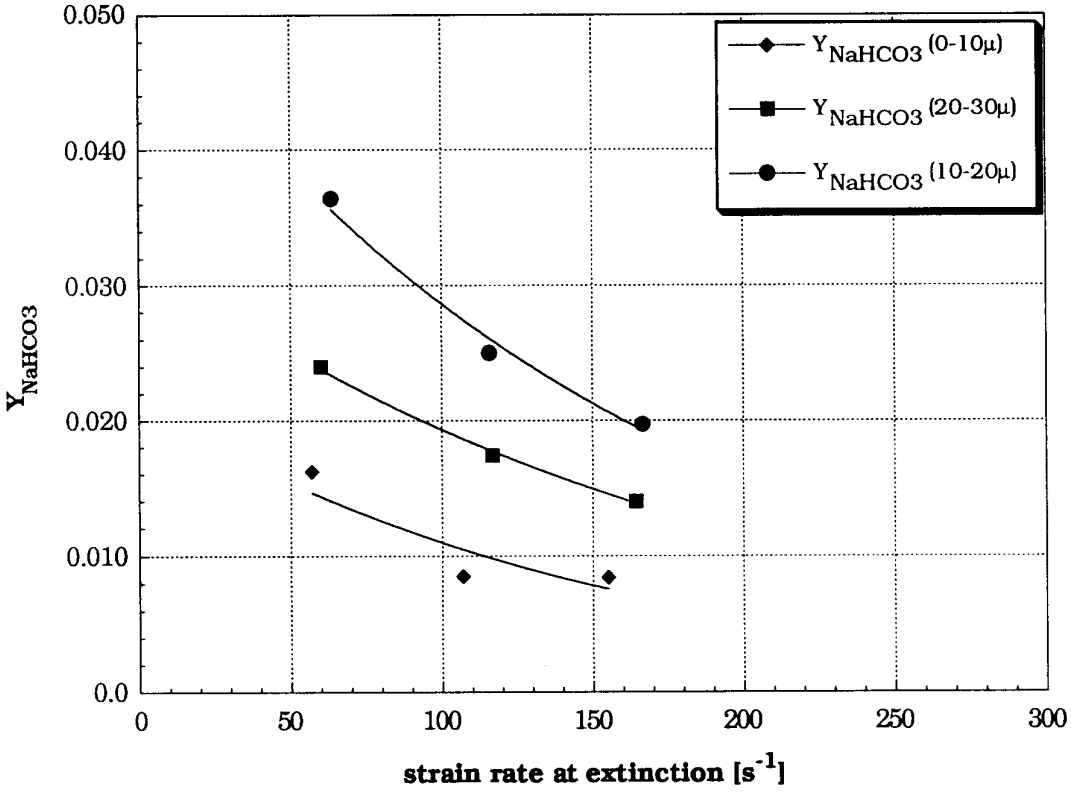

Figure 18. Mass fraction of $NaHCO_3$ (0-10, 10-20, and 20-30 μm) powder in air as a function of the strain rate at extinction for heptane flames with an oxidizer temperature of 25 °C.

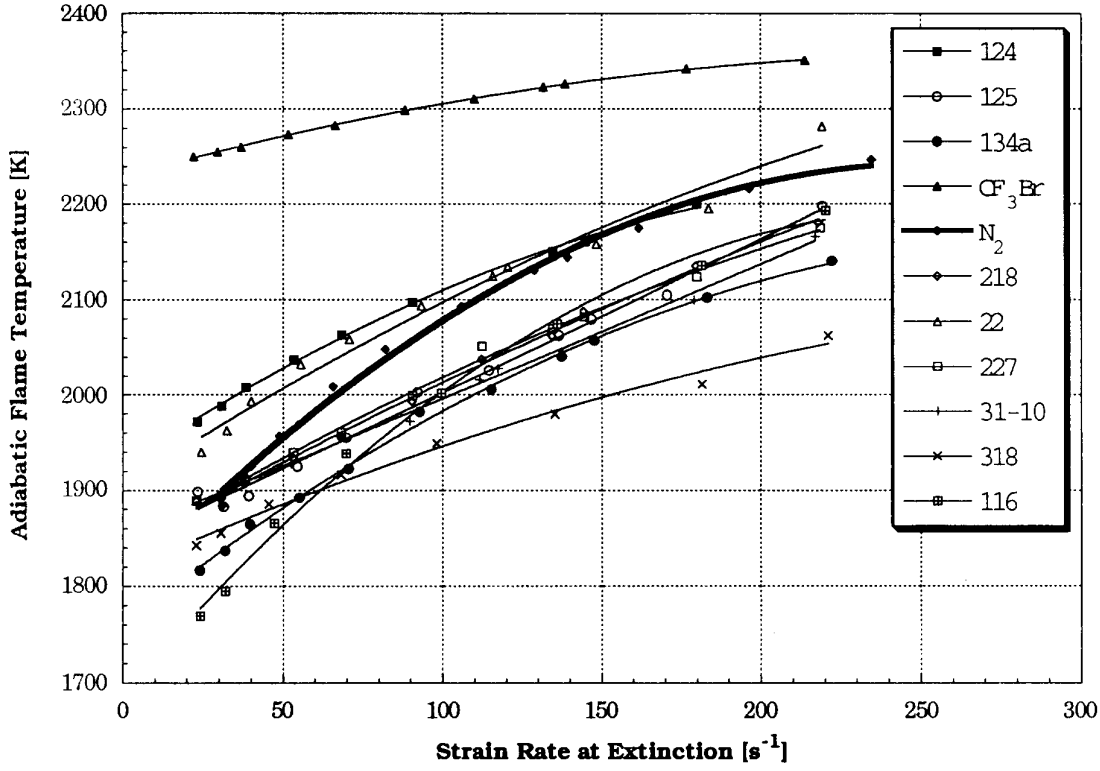

Figure 19. Calculated adiabatic flame temperatures at extinction assuming complete combustion of fuel and frozen composition of agent.

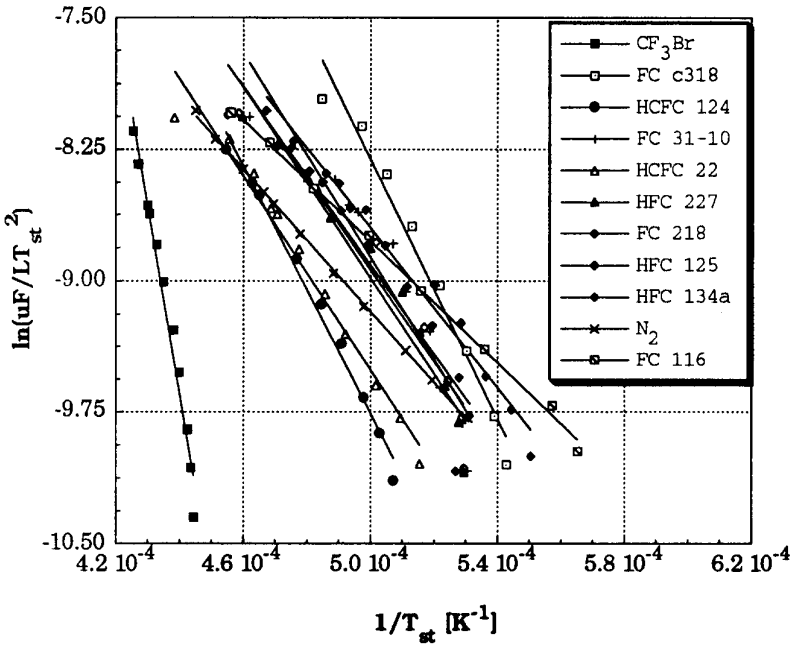

Agent	E_0 [kJ/mol]
CF_3Br	896
FC c318	310
HCFC 124	293
FC 31-10	243
FC 22	230
HFC 227	226
FC 218	218
HFC 125	214
HFC 134a	189
N_2	168
FC 116	142

Figure 20. Arrhenius plots obtained using the extinction data shown in Figure 6. The agents were considered to be chemically inert.

one-step approximation is not valid, and CF_3Br appears to be having a significant influence on the flame chemistry.

Figure 21 shows the adiabatic flame temperatures at different strain rates calculated assuming that the agents and stoichiometric fuel/air mixture react completely to N_2, CO_2, H_2O, HF, HBr, and HCl. The halogenated agents tend to have higher calculated temperatures in Figure 21 as compared to Figure 19 due to the enthalpy associated with conversion to the relatively stable acid gases, which implies that at least part of the chemical behavior exhibited by the agents may be related to simple conversion to equilibrium combustion products, HF and HCl. It is difficult to distinguish between the chemical and thermal influences of these agents on the flame because of possible differential transport effects. These effects are not accounted for in the current analysis.

4.2.6 Conclusions from OFDF Study. The opposed flow configuration was employed to determine the relative effectiveness of various inhibiting agents in extinguishing diffusion flames burning liquid heptane and JP-8. Eleven gaseous inhibiting agents and $NaHCO_3$ powder were tested. The oxidizing gas used in the experiments was a mixture of air and the inhibiting agent at initial temperatures of 25 °C and 150 °C. The following remarks summarize the major conclusions of the study:

1. The OFDF burner can be used to measure accurately the amount of a powdered agent required to suppress a variable strain-rate, laminar flame.

2. The strain rate, agent, fuel type and oxidizer temperature (in decreasing order of significance) all affect the amount of agent necessary to extinguish the opposed-flow diffusion flame.

3. The ranking of relative effectiveness of the various gaseous agents in quenching diffusion flames on a mole basis differs substantially from ranking on a mass basis, due to variation in molecular weight.

4. The rankings of relative mass- and mole-based effectiveness of the various agents are affected somewhat by the strain rate at which the tests are run, but only slightly by the fuel type (JP-8 or heptane) and the oxidizer temperature (25 °C and 150 °C).

5. On a mass or mole basis CF_3Br is considerably more effective in extinguishing the flame than all of the other gaseous agents tested.

6. On a mass basis at low strain rate HFC-236fa is most effective and FC-116 least effective of the gaseous alternatives, whereas at high strain rates HCFC-22 is most effective and FC-318 least effective.

7. On a mole basis, at low and high strain rates FC-31-10 is most effective and HFC-32/125 least effective of the gaseous alternatives.

8. Interpretation of the gaseous agent results based on one-step activation energy asymptotic theories shows that CF_3Br has a significant influence on the flame chemistry, and that the one-step approximation is not realistic. The results also show that all the agents except CF_3Br have a significant thermal influence on the flame. However, it is difficult to distinguish between the two influences accurately because preferential diffusion has not been considered. Further studies using detailed and reduced mechanisms are required to clarify the influence of the gaseous agents on the flame.

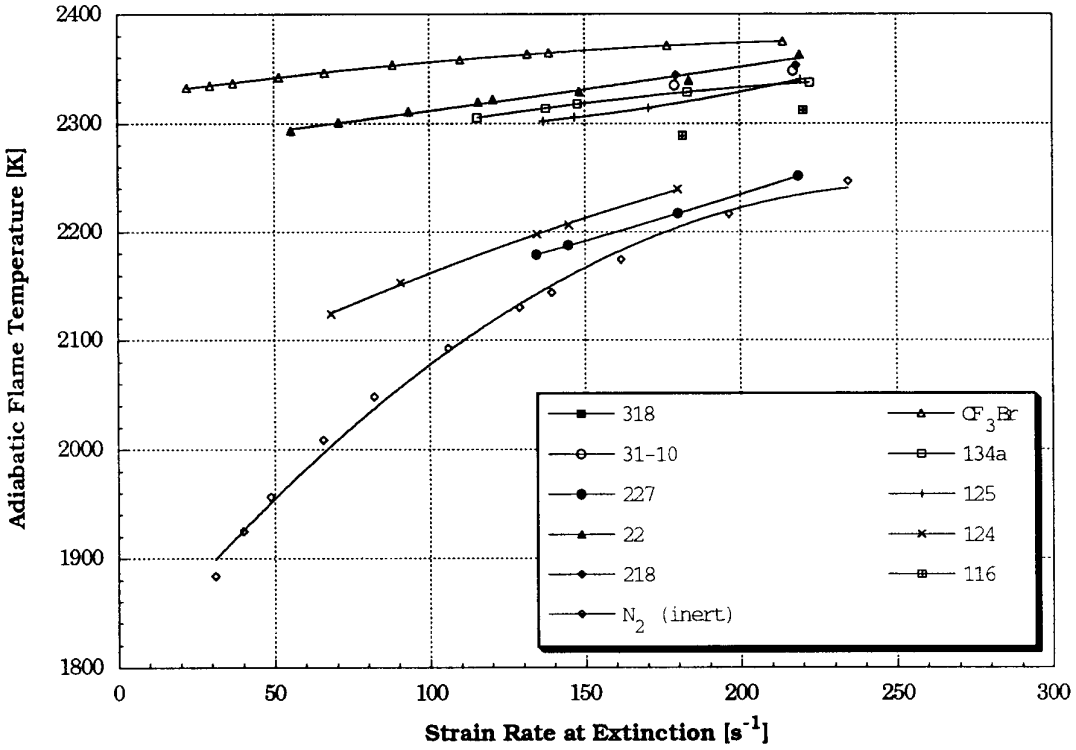

Figure 21. Calculated adiabatic flame temperatures as a function of extinction concentrations and strain rates assuming complete conversion of agents to CO_2, H_2O, HF, HCl, and HBr.

9. The effectiveness of $NaHCO_3$ powder on a mass basis is greater than that of CF_3Br; powder with 0-10 μm particles is more effective than the 20-30 μm, which in turn is more effective than the 10-20 μm. The mechanisms of flame extinction by powders are not well understood and merit further investigation.

4.3 Coflowing Nonpremixed Flames

4.3.1 Apparatus. An experimental study was conducted to rank the relative suppression effectiveness of various inhibiting agents on nonpremixed flames stabilized in a cup burner. The cup burner is a very common test apparatus for screening of suppressants. It is not, however, a standardized test method. A number of different size apparatus exist and various fuels and different air flows have been used (Gann *et al.*, 1990). Nevertheless, the experimental results from the different investigators have shown general agreement. The cup burner was selected as a test apparatus not to determine absolute extinction concentration data, but to rank the relative suppression effectiveness of the various agents. As such, it is an adequate test apparatus.

The concentration of gaseous agent in the oxidizer stream needed to obtain extinction was measured in the cup burner shown in Figure 22. The oxidizer, a mixture composed of dry air and agent, flowed through a 96 mm diameter chimney around a fuel cup. The cup had a 45° ground inner edge (28 mm diameter) and was used for both liquid and gaseous fuels. The ground inner edge minimized heat losses from the flame to the Pyrex cup. A fine wire mesh screen (40 mesh/cm) and small glass beads ($\approx$0.5 mm diameter) were placed inside the fuel cup for the gaseous fuel to flatten the velocity profile. The liquid fuel was gravity fed from a reservoir using a previously developed technique which facilitated an adjustable and constant level in the cup (Bajpai, 1974b).

Figure 23 is a schematic of the oxidizer flow control system. Compressed breathing air was dried by passing it through a two-stage filtering system composed of a silica gel water vapor trap followed by a particle trap. The flows of air and agent were monitored by rotameters which were calibrated with a dry test meter. Rotometer float and pressure readings were both measured. When sufficient agent was available, direct calibration was performed with that agent. Otherwise, an indirect calibration method was performed with dry air. Correction for density and viscosity differences were then applied to determine the flow. A series of tests were conducted with HCFC-22 to compare the precision of the two calibration methods. On average, the indirect method, calibrating with dry air, was within 3% of the direct calibration method. The values of gas viscosity (at 23 °C) for a number of test agents are listed in Table 4 (Reid *et al.*, 1977). For gases where data were not available (HFCs -125, -134a and -227, and HCFC-124) Reichenberg's corresponding states method was utilized. This method is described by Reid *et al.*, (1977). The method requires a number of physical parameters including the critical temperature, molecular weight and group contributions. For the mixture (HFC-32/HFC-125), Wilke's approximation was used. The critical temperatures are listed in Table 1 of Section 2.

4.3.2 Experimental Method

4.3.2.1 Gaseous Agents. A detailed experimental protocol was developed based on previous studies (Gann *et al.*, 1990). The fuel level was carefully set such that the ground lip of the pyrex cup was completely covered with fuel. The air flow was initiated and the flame was ignited with a torch.

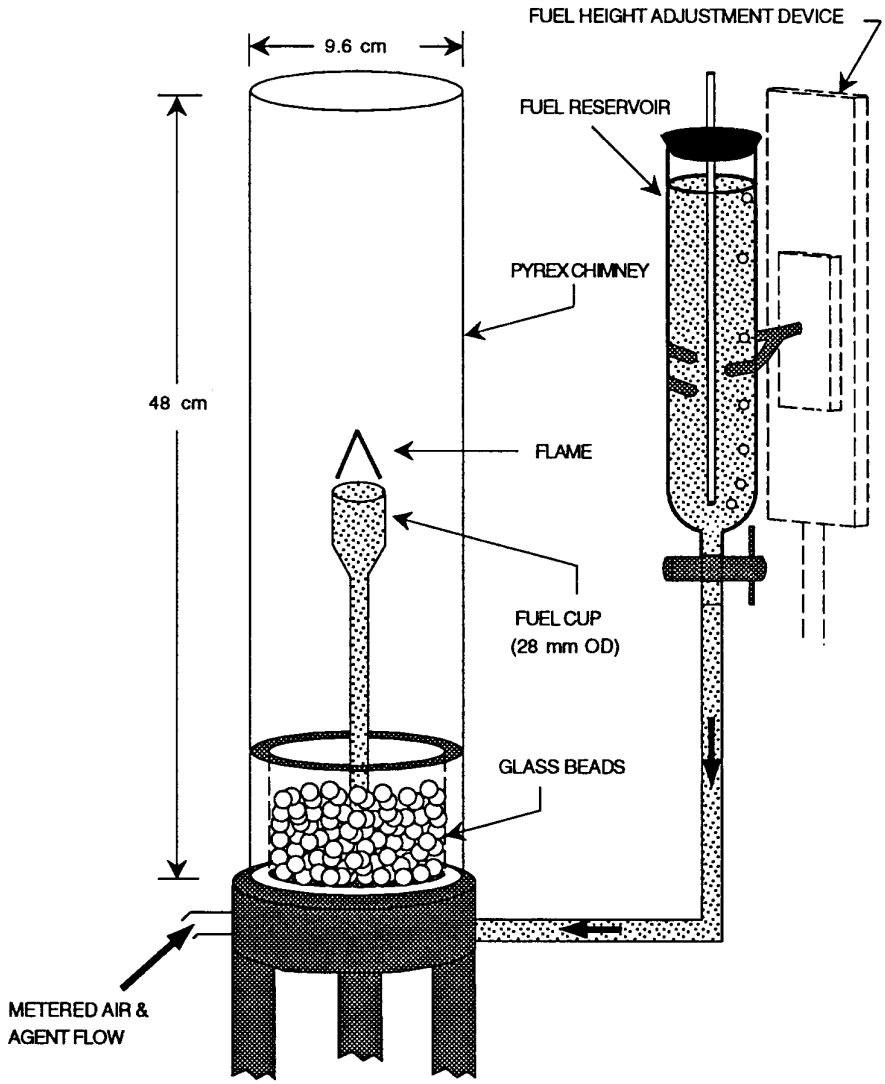

Figure 22. Schematic drawing of the cup burner.

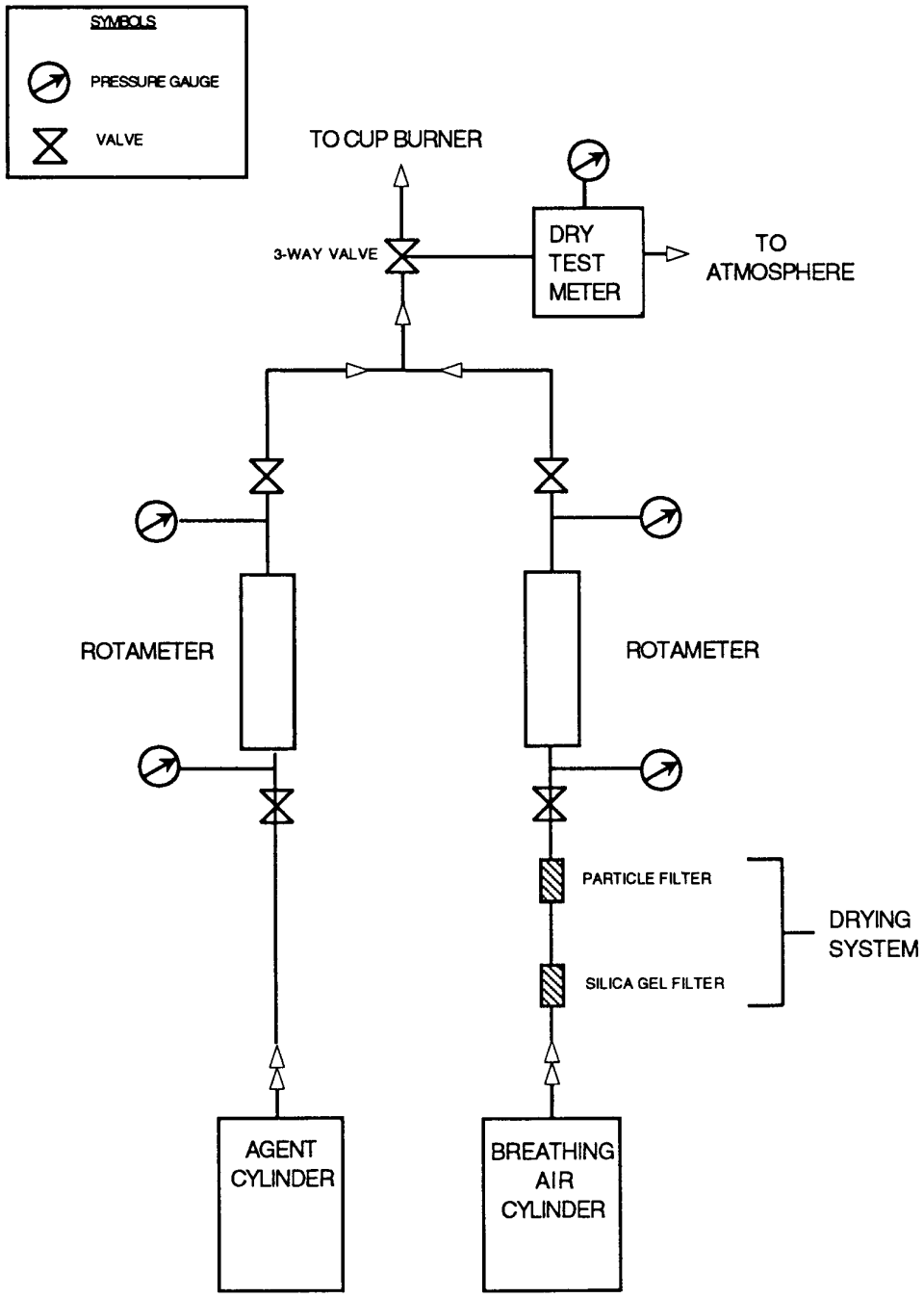

Figure 23. Schematic drawing of the oxidizer flow control system.

Table 4. Absolute Viscosity of Some Agents

Agent	Molecular Weight, g/mole	Absolute Viscosity @ 23 °C, N-s/m^2
HFC-32 (CH_2F_2)	52.1	1.20×10^{-5}
HFC-32/HFC-125 (CH_2F_2/C_2HF_5)	67.3	1.32
HFC-227 (C_3HF_7)	170.0	1.59
HCFC-22 (CHF_2Cl)	86.5	1.29
HFC-134a ($C_2H_2F_4$)	102.0	1.30
FC-116 (C_2F_6)	138.0	1.44
HCFC-124 (C_2HClF_4)	136.5	1.20
HFC-125 (C_2HF_5)	120.0	1.39
FC-128 (C_3F_8)	188.0	1.35
FC-31-10 (C_4F_{10})	238.0	1.25
1301 (CF_3Br)	148.9	1.55
1211 (CF_2ClBr)	165.4	1.36
FC-318 (c-C_4F_8)	200.3	1.18
CO_2	44.0	1.50
N_2	28.0	1.76
Ar	40.0	2.23
He	4.0	1.96
C_3F_6	150.0	1.36
HFC-236 ($CF_3H_2CF_3$)	152.0	1.22
SiF_4	104.1	1.60
C_2BrF_3	160.9	1.36
C_2F_3Cl	116.4	1.28
CF_4	88	1.72

Tests showed that the jet fuels and hydraulic fluids did not readily ignite without the use of a micro-torch. Once ignition occurred, the torch was immediately removed to prevent excess preheating of the Pyrex cup. The chimney was placed about the fuel cup. Figure 24 is a photograph of the flame in the cup burner. A 100 second warm up period was used prior to agent addition to minimize variation in apparatus heat-up during ignition. With the flame established, the agent concentration in the oxidizer stream was incrementally increased until the flame was extinguished. Agent was added to the oxidizer stream in small amounts ($< 1\%$ of flow needed to attain flame extinction), with a waiting a period from five to ten seconds between increases in the agent flow. This allowed time for the changing oxidizer flow to reach the burner and to impact flame stability. The flame was observed

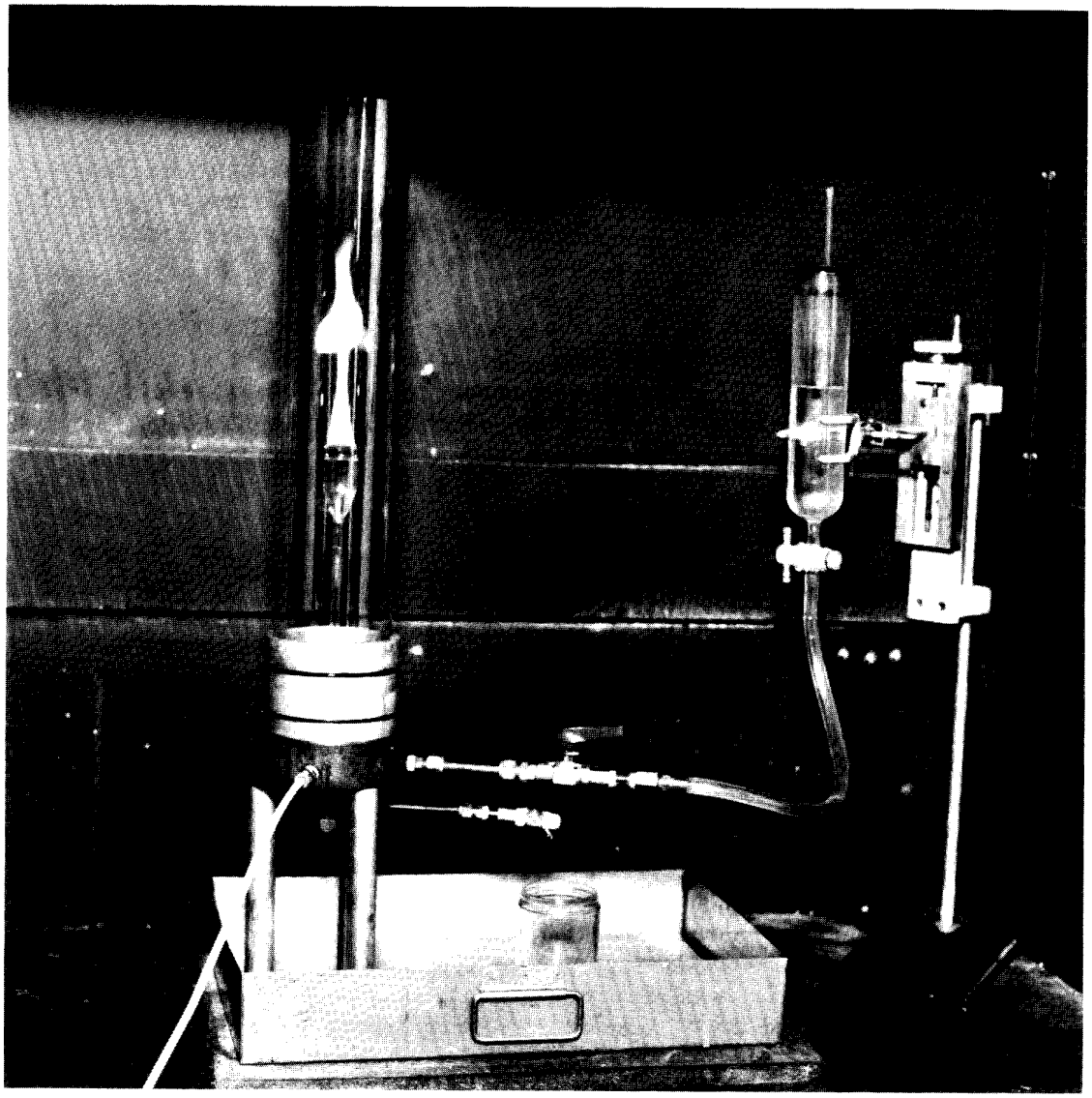

Figure 24. Photograph of cup burner and liquid fuel supply.

during this waiting period. After flame extinction was achieved, the used fuel was drained and the test was repeated several times (with fresh fuel each time) to insure experimental precision. Extinction tests were conducted on six fuels including one gas (propane) and five liquid fuels, which were heptane, two jet fuels (JP-5 and JP-8) and two hydraulic fluids (5606 and 83282) as shown in Table 1.

4.3.2.2 Liquid Agents. A liquid agent was introduced into the oxidizer stream using the delivery system shown in Figure 25. A regulated nitrogen stream flowed into a beaker containing the liquid agent, displacing the agent from the beaker into the heated oxidizer stream. The beaker holding the agent was situated in an ice-water bath. The flow of nitrogen was monitored using a calibrated flowmeter and a pressure gauge above the agent was observed. The liquid density at the bath temperature was needed to calculate the mass of agent addition to the oxidizer stream. The liquid agents CF_2Br_2 and CH_2BrCF_3 had densities of approximately 2.46 and 1.79 g/ml, respectively. A variable voltage regulator allowed control of the temperature of the heated oxidizer lines. A thermocouple above the glass beads inside of the chimney monitored the oxidizer temperature which was typically 10 to 15 °C above ambient. A test, described in Section 4.3.3, was conducted to substantiate the viability of the agent delivery method.

4.3.2.3 Sodium Bicarbonate Powder. The cup burner shown in Figure 22 was modified to foster a controlled, homogeneous flow of powder and to facilitate repeatable extinction measurements using powder agents. Figure 26 is a schematic diagram of the modified cup burner system. the system had five components: the cup burner, the air drying and control system, the powder feed system, the powder monitoring system, and the iso-kinetic sampling system used for calibration of the powder concentration.

A series of wire mesh screens (10 mesh/cm) functioned as flow straighteners. They were placed across the entire cross sectional area of the chimney, below the fuel duct, after cutting the chimney into several sections. Without these screens, non-homogeneous powder flow and recirculation zones were observed near the fuel cup. Flow visualization under non-combusting conditions showed that uniform upward flow was achieved for the powder/oxidizer dispersion for velocities greater than $\approx$ 9 cm/s.

The powder was introduced into the air stream by turning a 9 mm drill bit through a closed container of powder. The drill bit carried the powder through a 12.7 mm tube. The powder was fed into the oxidizer stream via a tee located just below the base of the cup burner where it was swept into the oxidizer flow. The delivery rate was controlled by a variable speed motor and a voltage regulator. Flow visualization showed that the 0-10 and 10-20 μm powder traveled through the chimney as a uniform bulk flow, whereas the 20-30 μm size fraction did not, for flows achievable in our laboratory. Thus, no powder testing was conducted with the larger size fraction. For the powder experiments, the air stream flow was maintained at 40 l/min (in the 96 mm diameter chimney).

The concentration of powder in the flow field at the time of extinction for locations near the flame was quantified by a laser transmission measurement in combination with iso-kinetic vacuum sampling and a wet chemistry technique - sodium ion analysis. The method assumes a uniformly seeded flow field. A 10 mW helium-neon laser beam (632.8 nm) was directed across a $\approx$7 cm chord of the pyrex chimney which traversed the flow field. The beam was positioned $\approx$ 2 cm below the fuel duct to avoid light attenuation by soot particles or other combustion products. The laser signal was monitored by a silicon photo-detector with a 10 nm bandwidth line filter and connected to a data acquisition system (4 Hz sampling rate). This allowed monitoring of the line-of-sight integrated $NaHCO_3$ concentration as a function of time. Increased powder concentration in the flow field was indicated by increased laser attenuation as represented by the following equation:

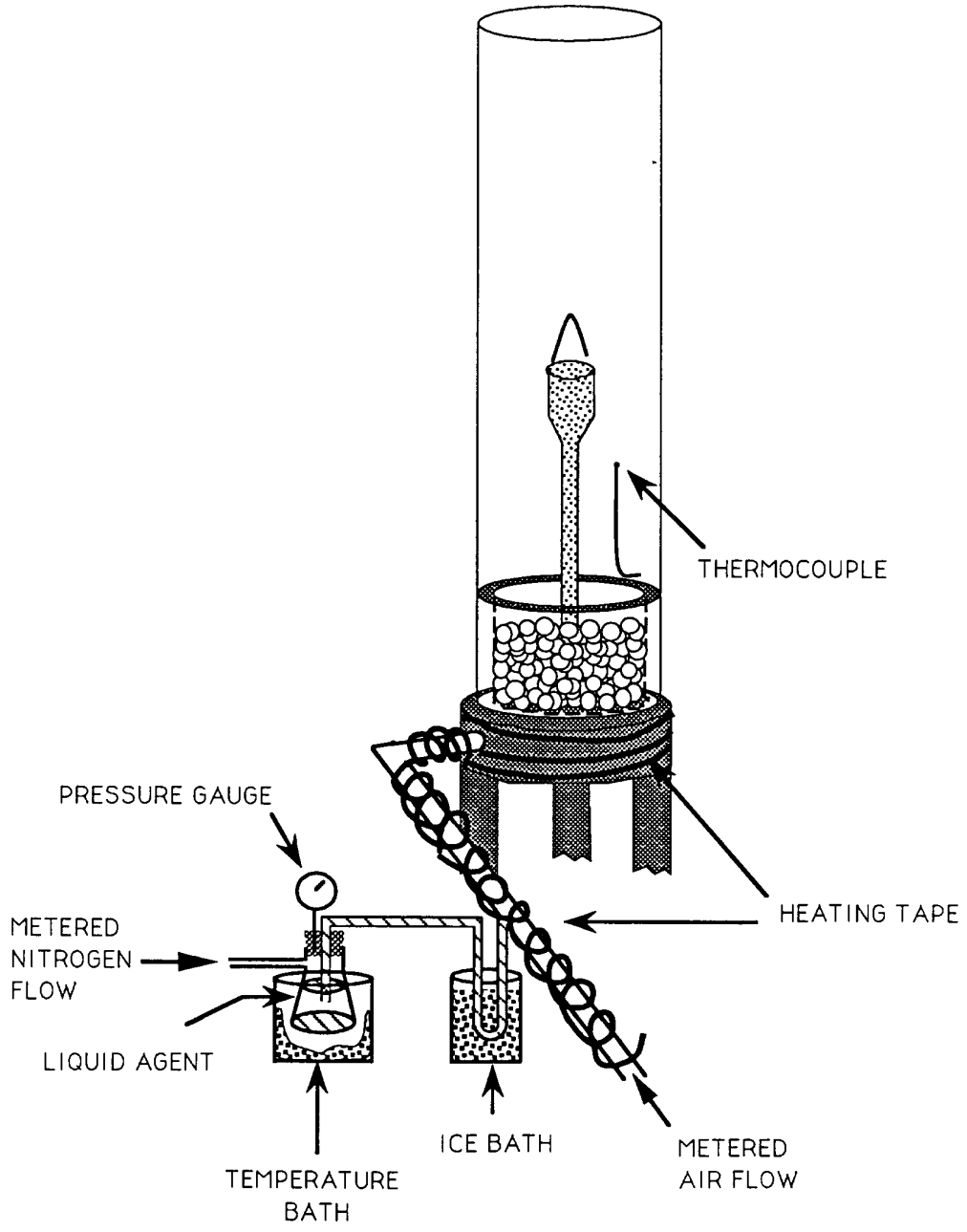

Figure 25. Schematic drawing of the cup burner modified for delivery of liquid agents.

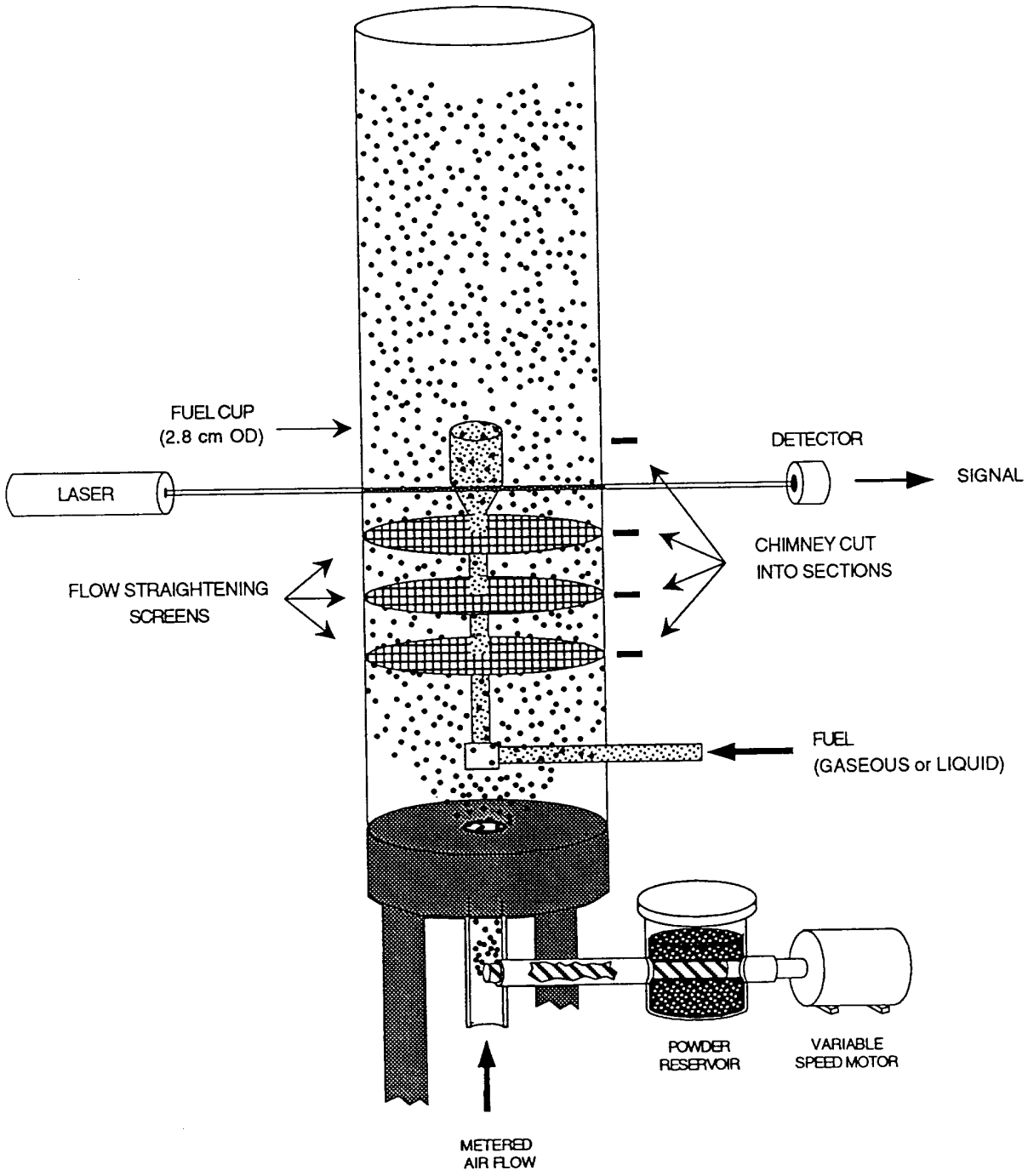

Figure 26. Schematic drawing of the cup burner modified for delivery of a solid powder.

$$\frac{I}{I_o} = \exp(-K \cdot [NaHCO_3] \cdot L) \quad (3)$$

where I_0 is the unattenuated laser signal, I is the attenuated signal, [$NaHCO_3$] is the powder concentration, L is the path length, and K is an absorption/scattering coefficient which is dependent on particle diameter, and shape as well as a number of other parameters. At the moment of flame extinction, a signal was sent to the data acquisition system, the laser transmission was monitored and the flow system was immediately shut off. This prevented further powder agglomeration on the chimney walls and allowed determination of the laser signal (I_0), unattenuated by powder in the flow field. Laser attenuation was related to mass percent of powder in the oxidizer by iso-kinetic vacuum sampling in combination with a sodium ion electrode/analysis system.

For calibration, small holes (2 mm) were drilled in the chimney for passage of the laser beam, eliminating the possibility of laser attenuation due to powder adsorption on the chimney walls. Flow visualization showed that a negligible amount of powder escaped through the orifices. During calibration, the top section of the chimney was removed and the probe/collection system was positioned at the plane defined by the rim of the fuel cup, where the flame was typically anchored. This avoided possible losses of powder to the chimney walls, which would have occurred if the sample was extracted at the top of the chimney.

Calibration of the $NaHCO_3$ mass flow in the oxidizer stream was determined by iso-kinetically sampling a portion of the $NaHCO_3$/air dispersion into a vacuum collection system while simultaneously monitoring the laser signal (I) for different powder loadings as shown in Figure 27. The absorption/scattering coefficient K was assumed to be invariant during the extinction and calibration measurements. The powder/oxidizer dispersion was iso-kinetically collected through a 20 mm diameter tube connected to a 20 l/min vacuum pump. The sample passed through $\approx$25 cm of polyvinyl tubing into a 200 ml glass impinger filled with deionized water which captured the water soluble powder particles. After approximately a 30 second sampling time, the sample probe and lines were washed with deionized water, combined with the impinger contents, and diluted with deionized water to 500 ml. A calibrated sodium ion-selective electrode was then used to determine the ion concentration in the powder/water solution. In this manner, a calibration curve was developed covering an appropriate range. Typically, 0.5 to 2 g of powder were collected over the sampling period, which was completely salable in the 500 ml water solution.

4.3.3 Assessment of Operating Parameters. A series of preliminary measurements tested the effect of a number of parameters on the agent concentration in the oxidizer stream at extinction. The parameters tested include the fuel cup diameter, the oxidizer flow, the chimney diameter, and the preburn time. The oxidizer flow was found to have a negligible effect on the concentration of agent at extinction, once a minimum flow was achieved, as seen in Figures 28 and 29 for N_2 and HCFC-22 suppressing JP-5, JP-8, 5605, and 83282 flames. The effect of varying chimney diameter (96 and 113 mm diameters) was also tested. The chimney size was found to have a negligible effect once a minimum flow velocity was achieved as shown in Figure 30 for HCFC-22 extinguishing 5606 and JP-8 flames. Two fuel cup diameters (12 and 28 mm) were tested as shown in Figure 31 and found to have a negligible impact on the agent concentration (HCFC-22) at extinction of JP-8 flames. Because fuel consumption in the two cups was expected to be different, this implies that the fuel burning rate had a minimal impact on the measured extinction concentration. In order to directly test this, flames burning a gaseous fuel (propane), where the fuel flow was an independently controlled experimental parameter, were used. The results presented in Figure 32 show only a small variation in

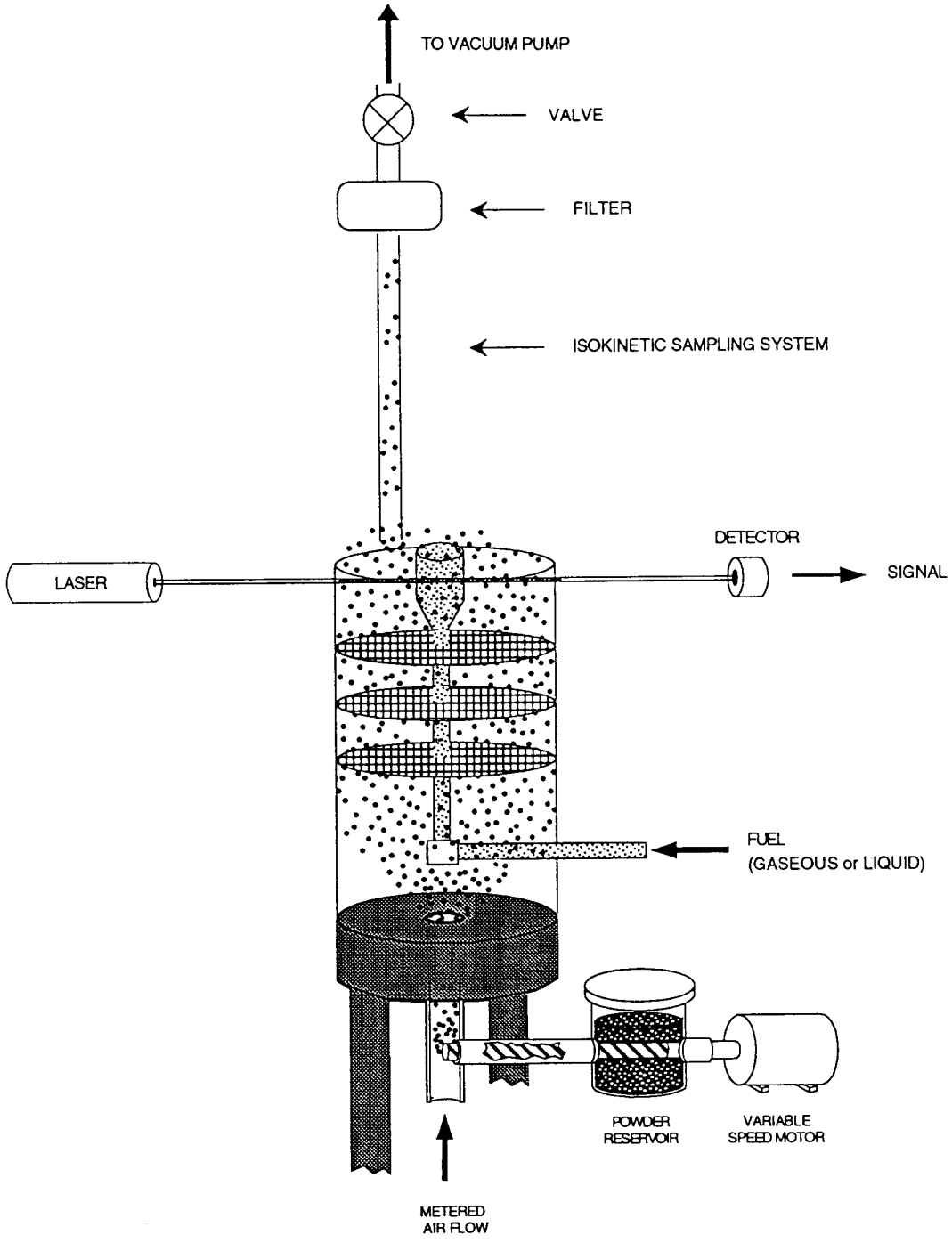

Figure 27. System used to calibrate powder flow in cup burner.

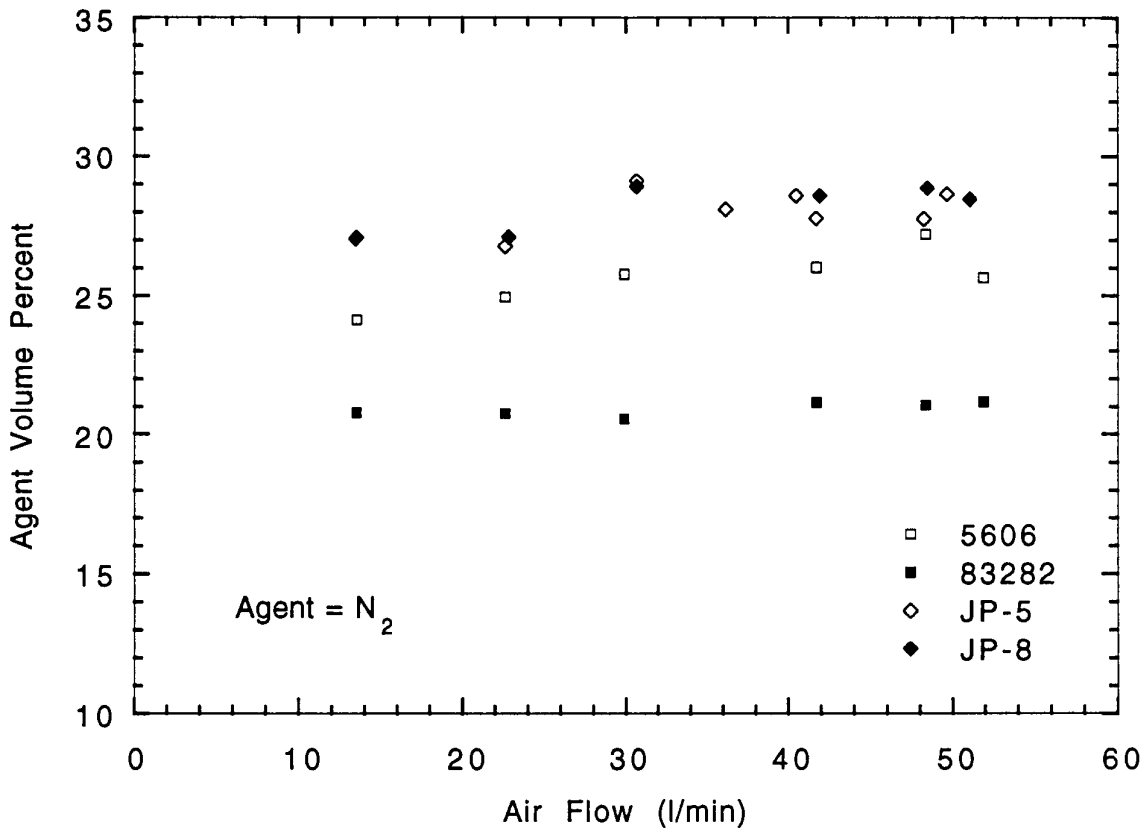

Figure 28. N_2 concentration at extinction as a function of air flow.

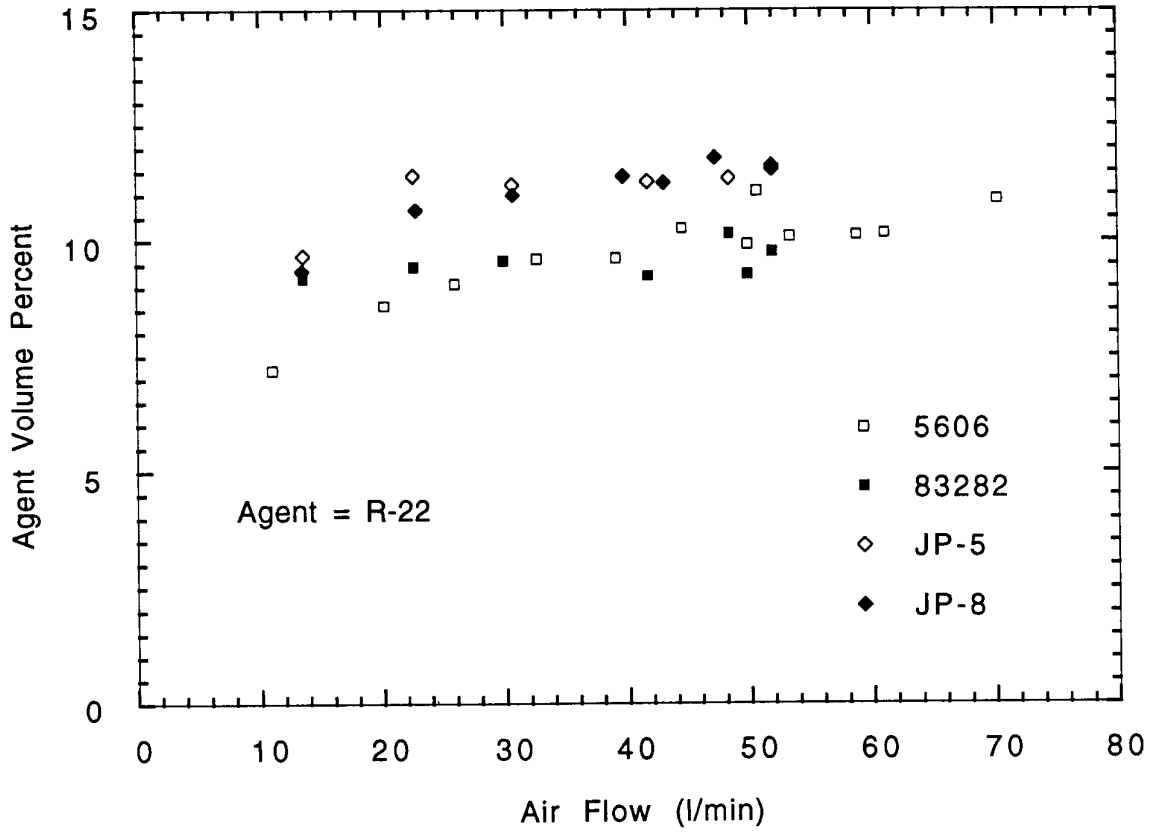

Figure 29. CHF_2Cl concentration at extinction as a function of air flow.

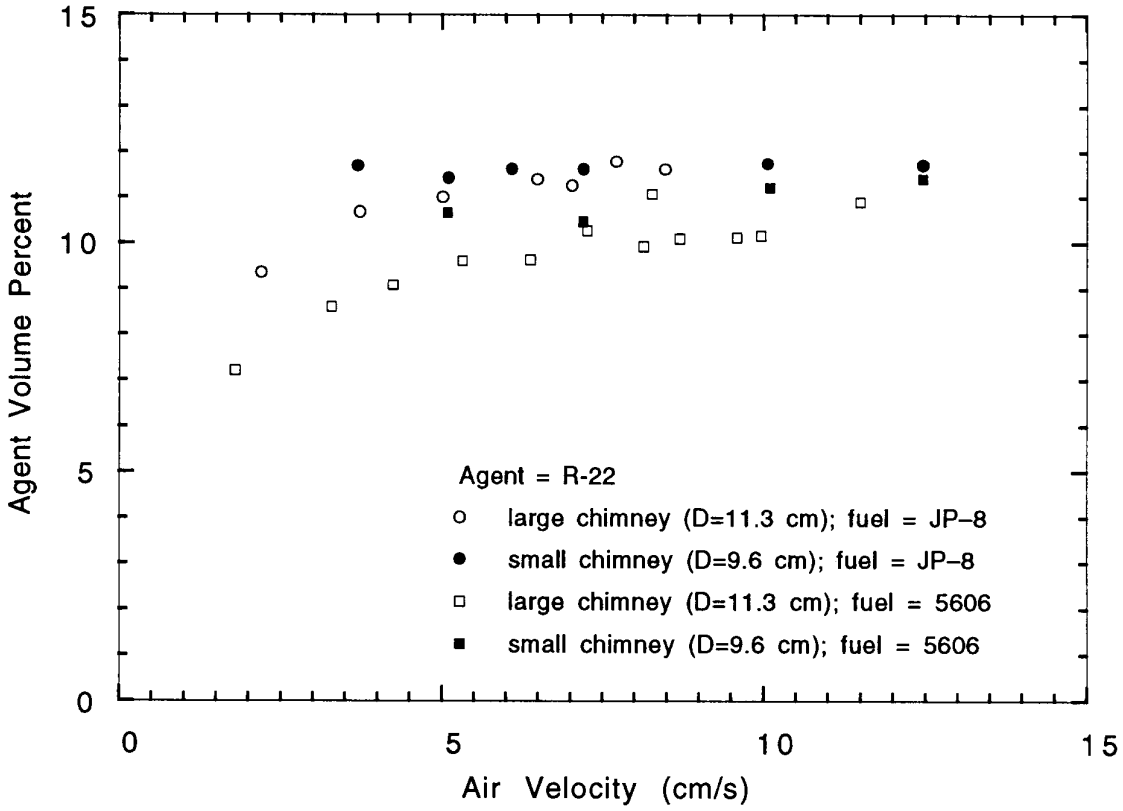

Figure 30. CHF_2Cl extinction concentration as a function of air velocity for different chimney sizes.

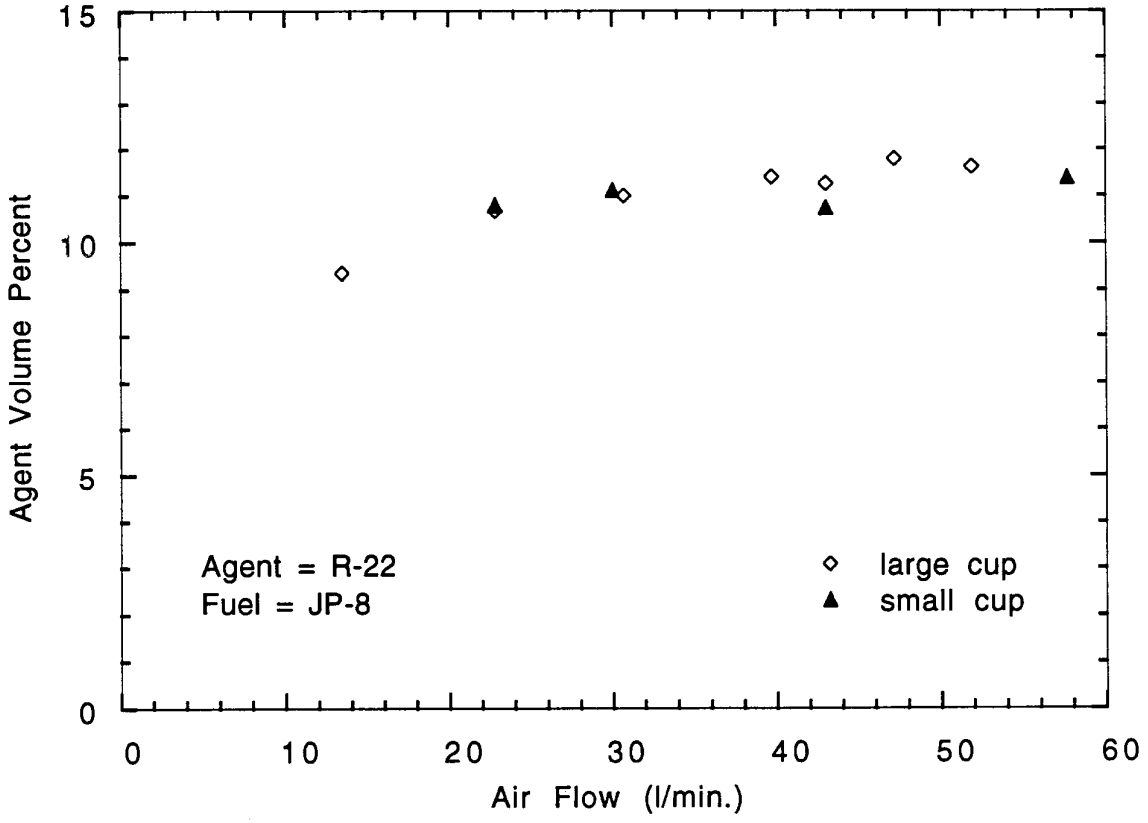

Figure 31. CHF_2Cl extinction concentration as a function of air flow for different fuel cup sizes.

the N_2 and HCFC-22 extinction concentration with the propane flow. In order to test if the global equivalence ratio was a factor in these results, a particular fuel flow (0.11 l/min) was used and the effect of increasing air flow on the agent extinction concentration was tested and found to be negligible. Thus, the fuel flow had only a small effect on the agent concentration at extinction. This effect may be related to flame liftoff and air/agent premixing with the fuel near the lip of the fuel cup. Further study is needed to investigate the mechanism responsible for these effects.

A number of the fuels contained multiple components. Thus, preferential distillation effects might have led to differences in the agent extinction concentration as a function of time after ignition. This effect was tested and found to be negligible for preburn times from 50 to 400 s. However, because the fuel burning rate was found to be unsteady at times less than 100 s, the experimental protocol required a 100 s preburn time after ignition and before agent was added. In addition, all extinction experiments were completed in less than 300 seconds. For all measurements, the 96 mm chimney was used. For the gaseous and liquid agents, an air velocity in the chimney of approximately 5 cm/s was used. For the extinction measurements with $NaHCO_3$, an air velocity of approximately 10 cm/s was used to insure that the powder travelled uniformly through the chimney.

Measurement variance and a propagation of error calculation considering the air and agent flows, yielded an estimate of the combined standard uncertainty in the gaseous agent concentration at extinction as $\pm$ 10%. The combined standard uncertainty in the measurement of the $NaHCO_3$ concentration at extinction was found to be approximately 25% on average and was always less than 40%. This value was dominated by measurement variance.

In order to test the impact of heating the liquid agent delivery system, the concentration of N_2 needed for extinction of a propane flame was tested with and without a heated (to 35 °C) oxidizer stream. The extinction concentration showed negligible difference.

As agents were added to the oxidizer stream the color of the flame changed. With the addition of an inert non-halogenated agent such as He or N_2, the flame lifted off the burner, became narrower and blue in color. With the addition of halogenated agents, the flame lifted off the burner, and became more intensely yellow in color for all of the fuels studied. At large agent concentrations, copious amounts of soot were produced, covering the pyrex chimney. A greenish luminosity was emitted from the flame when a chlorinated agent was used.

4.3.4 Experimental Results

4.3.4.1 Core Agents. Figure 33 shows the cup burner extinction results for N_2, CF_3Br and the core gaseous agents on a mole basis for flames burning propane, heptane, JP-8, JP-5 and the hydraulic fluids 5606 and 83282. The propane flames were the most difficult to extinguish, followed by heptane, the jet fuels, and the hydraulic fluids. The measurements compare favorably to previous results as shown in Table 5 for heptane flames. Consistent with our results, Hirst and Booth (1977) also found propane more difficult to extinguish than heptane. Cup burner extinction measurements using the jet fuels and the hydraulic fluids have not been previously reported.

The different agents in Figure 33 had dissimilar suppression effectiveness. For all fuels, CF_3Br was a highly effective suppressant as compared to the other gaseous agents, being approximately an order of magnitude more effective than N_2 in extinguishing the cup burner flames. Other agents had intermediate effectiveness as compared to halon 1301 and N_2. On a mole basis, the larger molecular weight FC, HFC, and HCFC compounds had a higher suppression effectiveness. The most efficient agent was C_4F_{10}, followed by cyclo-C_4F_8, C_3F_8, and C_3HF_7. The chlorinated agents (CHF_2Cl and $CHFClCF_3$) did not exhibit flame suppression behavior superior to the non-chlorinated agents.

Figure 34 replots the mole based results shown in Figure 33 on a mass basis. The most efficient gaseous agent was halon 1301 requiring approximately 15% by mass in the oxidizer stream to

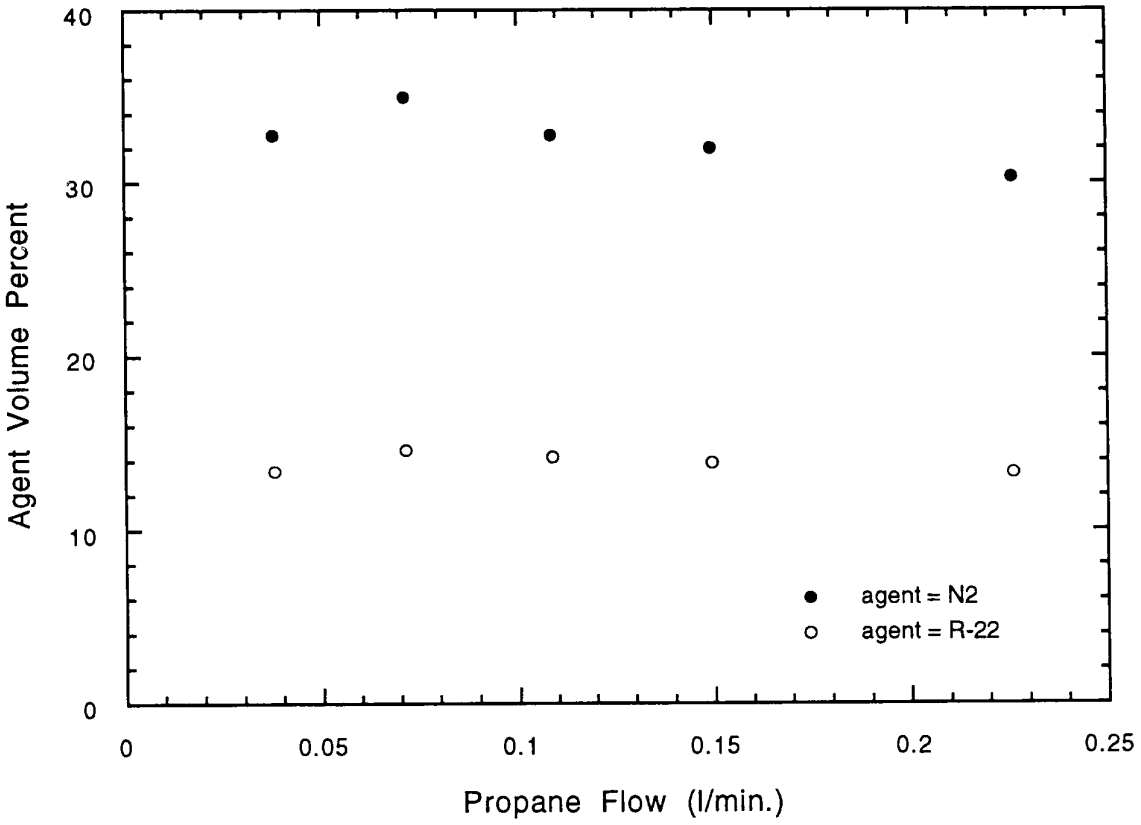

Figure 32. N_2 and CHF_2Cl extinction concentration as a function of the propane fuel flow rate.

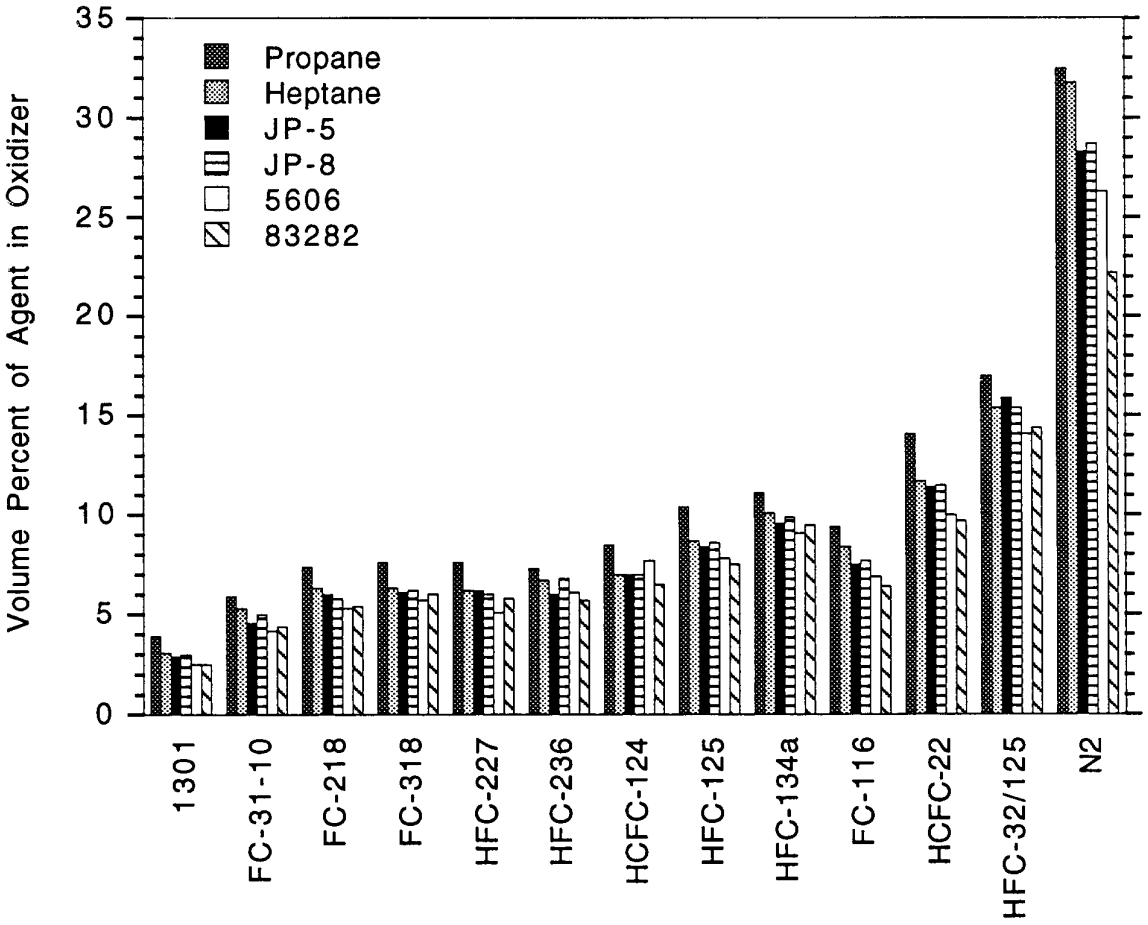

Figure 33. Agent (volume percent) concentration at extinction.

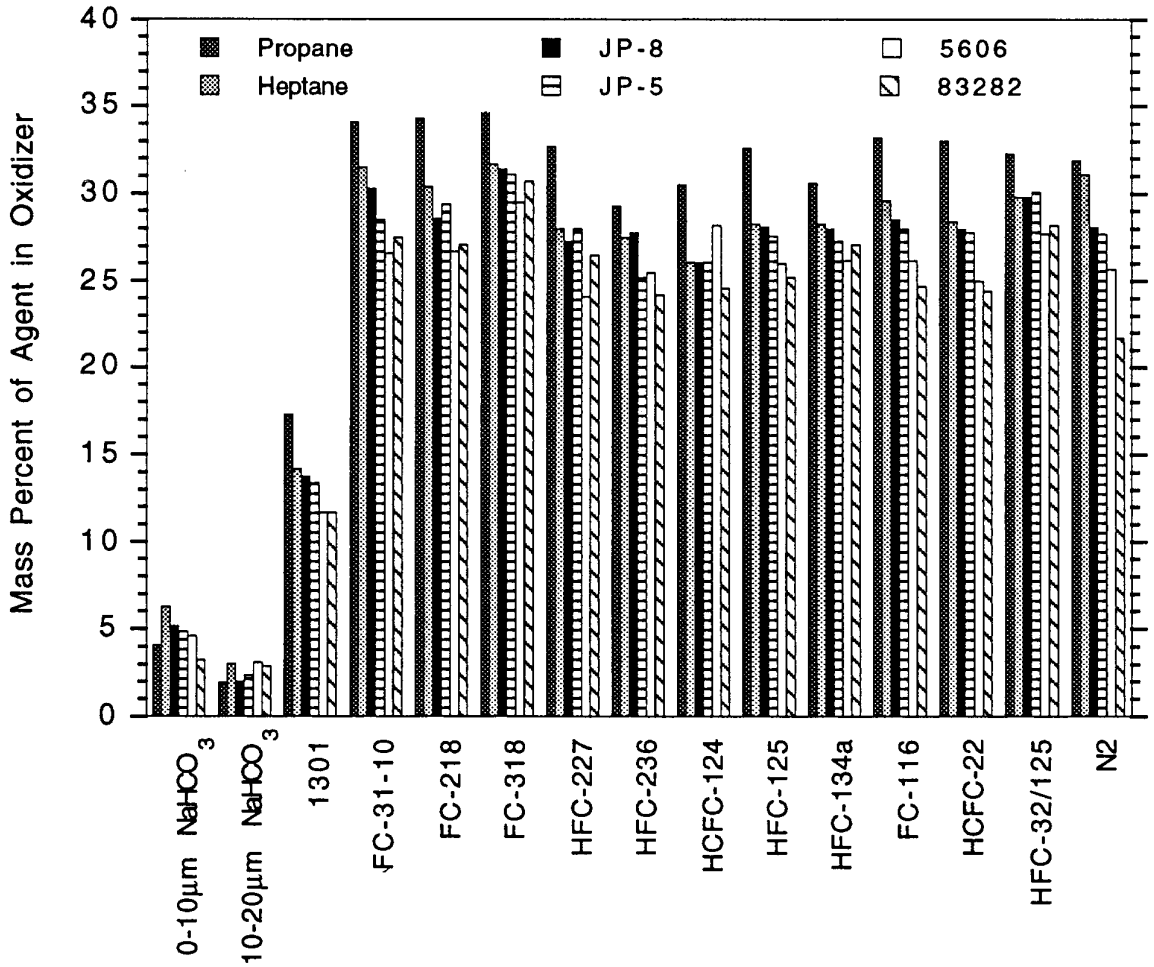

Figure 34. Agent (mass percent) concentration at extinction.

Table 5. Comparison of (mole based) Extinction Measurements with Previous Work. Fuel is Heptane.

Agent	Halon 1301	CF_3I	C_2F_6	N_2
this study	3.2%	3.2%	8.1%	32%
Hirst and Booth, 1977	3.5%	[a]	[a]	30.2%
Harrison, 1992	3.5%	[a]	[a]	[a]
Bajpai, 1974a	3.3%	[a]	[a]	[a]
Sheinson *et al.*, 1978	3.1%	3.2%	7.9%	30%

[a] Not measured

extinguish the cup burner flames. The perfluorinated agents all had approximately the same effectiveness as N_2 on a mass basis. This is directly related to the agent heat capacity, as listed in Table 6, which shows that all of the perfluorinated agents have approximately the same heat capacities at flame temperatures.

4.3.4.2 Sodium Bicarbonate Powder. The color of the flame became bright yellow with the addition of even minute amounts of $NaHCO_3$ into the flame. Equilibrium calculations (Gordon and McBride, 1970) indicate that at flame temperatures, the sodium containing species in the flame with the highest concentrations are Na^+ and NaOH. The intense yellow luminosity was likely due to high temperature Na^+ ion emission in the flame. As the powder concentration in the oxidizer stream was increased, the flame became thinner and less luminous. Near extinction only a small luminous region was apparent.

For suppression of the liquid fuel flames, some powder was observed to accumulate inside of the fuel cup and submerge. The effect of $NaHCO_3$ powder on the extinction resistance of the fuels was tested by measuring the extinction concentration of N_2 in the oxidizer stream for flames burning fuels with and without powder sprinkled on the fuel surface. No differences were determined for any of the five liquid fuels tested.

Experiments showed that flame extinction using SiO_2 was not possible for powder loadings achievable with our delivery system. With as much silica as could be delivered by our apparatus, the cup burner flames appeared unaltered. The SiO_2 concentration attainable by the delivery system was not quantified.

Figure 34 shows that the concentration of $NaHCO_3$ required to extinguish the cup burner flames for two powder size fractions. Approximately 4% by mass of $NaHCO_3$ in the oxidizer stream was necessary to extinguish the heptane cup burner flames. A comparison shows that in general, $NaHCO_3$ was a factor of three to five times more efficient than halon 1301 on a mass basis depending on fuel type and powder size. Unlike the gaseous agents, propane flames were less difficult to extinguish than heptane for both powder sizes. The reason for this warrants further study.

There were some inconsistencies between the 0-10 and the 10-20 μm powder results. Ewing *et al.*, (1992) observed enhanced extinction effectiveness with decreasing powder size in heptane pool

Table 6. Agent Heat Capacity in the Oxidizer Stream and Calculated Adiabatic Temperature near Extinction for Heptane Cup Burner Flames

Agent	C_p[1627 °C] (J/g-°C)	T_f (°C)
CF_3Br (1301)	0.0406	1981
CO_2	0.0779	1567
N_2	0.0731	1586
C_3HF_7 (HFC-227)	0.0822	1614
CHF_2Cl (HCFC-22)	0.0678	1689
CH_2FCF_3 (HFC-134a)	0.0946	1567
C_2F_6 (FC-116)	0.0726	1628
$CHFClCF_3$ (HCFC-124)	0.0717	1706
CHF_2CF_3 (HFC-125)	0.0836	1615
C_3F_8 (FC-218)	0.0764	1597
C_4F_{10} (FC-31-10)	0.0764	1569
cyclo-C_4F_8 (FC-318)	0.0798	1560
Ar	0.0296	1607
He	0.296	1747
CF_3H	0.0831	1685
CF_4	0.0683	1522

fires, until a critical powder size (≈ 30 μm for $NaHCO_3$), when the effectiveness was nearly a constant. The results reported here are not consistent with these findings. Figure 34 shows that the larger diameter particles were more efficient than the small size fraction. It is possible that the 0-10 μm size fraction was exposed to heat or water vapor under preparation or storage, causing the $NaHCO_3$ to react and form Na_2CO_3, a reaction which is known to begin at 50 °C. This possibility is being currently investigated. In any case, $NaHCO_3$ is three to five times more efficient than halon 1301 on a mass basis.

4.3.4.3 Additional Agents. The mole and mass-based heptane extinction results for all gaseous agents tested are shown in Table 7, grouped by molecular type (inert, a silicon containing compound, a sodium containing compound, perfluorinated agents, and chlorine, bromine, and iodine containing compounds). On a mass basis, the most efficient agent was the solid powder, $NaHCO_3$. The most efficient gaseous agent was He, followed by $CHCl_2F$, CF_3Br, and CF_3I. The most efficient gaseous agent on a mole basis was the liquid agent CF_2Br_2, followed by CF_3Br, CF_3I, CH_2BrCF_3, and $CHCl_2F$.

A number of agents, especially those with a large percentage of hydrogen atoms, proved to be flammable. As CF_2H_2, for example, was added to the oxidizer stream, an independent premixed

flame was established in the pyrex chimney. The location of the premixed flame in the chimney depended on the oxidizer flow velocity which was related to the flame speed of the CF_2H_2-air mixture.

One agent, NF_3, behaved as an oxidizer, creating an intensely luminous flame with increasing agent concentration. A simple thermodynamic analysis shows that stoichiometric combustion of NF_3 in conjunction with a hydrocarbon fuel and air yields rather than demands O atoms. Thus, NF_3 should act as a hydrocarbon oxidizer.

A detailed discussion of the results for the additional agents can be found in Section 5 of this publication.

4.3.5 Discussion of Results. The heat capacities of the agents are approximately equal on a mass basis as shown in Table 6. Table 7 and Figure 34 show that on a mass basis, CF_3Br and CF_3I were very effective compared to the other gaseous agents tested. The remainder of the agents exhibited essentially the same suppression performance, which was not significantly more efficient than N_2. Some investigators have found that interpretation of the results are facilitated by flame temperature calculations (Tucker *et al.*, 1981; Sheinson *et al.*, 1989).

Table 7 shows the results of such calculations assuming (a) that the agents behave as an inert, (b) that the combustion process is stoichiometric, with only H_2O and CO_2 as products, (c) that there is no dissociation, and (d) that the agent and O_2 diffuse into the flame at the same rate. Both of the inert non-halogenated agents, CO_2 and N_2, had adiabatic flame temperatures approximately 1587 °C. All of the fluorinated agents had calculated adiabatic flame temperatures near 1590 °C, actually between 1557 and 1617 °C. Halon 1301 had a very high calculated temperature, suggesting an amount of chemical suppression by this compound. The chlorinated agents, HCFC-22 and HCFC-124, also had relatively high calculated temperatures compared to the inert agents and to the perfluorinated agents, indicating some measure of chemical activity. From an energy balance it is possible to quantify the percentage of physical and chemical action associated with each of these agents.

This interpretation of the data, however, is problematic when considering results for the inert monatomic gases (helium and argon). The high calculated flame temperature associated with helium in Table 6 is likely due to large preferential diffusion or Lewis Number effects. An interpretation of Lewis Number effects on coflow extinction studies has not been addressed. Understanding preferential diffusion effects could be an important parameter for predicting the effectiveness of a replacement agent and understanding the relative importance of an agent's chemical activity to its transport properties.

Figure 35 compares the mole fraction of agent needed for extinction of heptane flames burning in the cup (from Figure 33) and OFDF burners (from Figure 8). The relative agent suppression ranking and even the absolute values of agent concentration at extinction show excellent agreement between the low strain rate OFDF results and the cup burner results. It is conjectured that the strain rate near extinction in the cup burner flame is characterized by a low strain rate.

Table 8 shows the results of a statistical analysis considering all of the agents tested which indicates that propane flames were the most difficult to extinguish, followed by heptane, the jet fuels, and the hydraulic fluids.

4.3.6 Summary and Recommendations. An apparatus and methodology were developed to test the suppression effectiveness of gaseous, liquid and solid powder agents in a simple, coflowing flame burning gaseous and liquid fuels. The major findings were:

Table 7. Agent Fraction in the Oxidizer Stream at Extinction of Heptane Cup Burner Flames

Agent Type	Agent	Mass Percent	Volume Percent
inert	N_2	31	32
	CO_2	32	23
	He	6.0	31
	Ar	38	41
nitrogen containing	NF_3	[a]	[a]
silicon containing	SiF_4	36	13
sodium containing	$NaHCO_3$ (10-20 μm)	3.0	[b]
HFC	CF_3H	25	12
	CF_2H_2	[c]	[c]
	CF_2H_2/C_2HF_5	30	15
	CH_2FCF_3	29	10
	CHF_2CF_3	29	8.7
	$CF_3CH_2CF_3$	27	6.5
	C_3HF_7	28	6.2
FC	CF_4	37	16
	C_2F_6	30	8.1
	C_3F_6	29	7.3
	C_3F_8	30	6.3
	c-C_4F_8	32	6.3
	C_4F_{10}	32	5.3
chlorine containing	CHF_2Cl	28	12
	$CHCl_2F$	32	11
	CH_3CF_2Cl	[c]	[c]
	CF_2=CHCl	[c]	[c]
	CF_2=CFCl	31	10
	$CHFClCF_3$	26	7.0
bromine containing	CF_3Br	14	3.1
	CF_2Br_2 (l)	16	2.6
	CH_2BrCF_3 (l)	17	3.5
	CH_2=CHBr	[c]	[c]
	CF_2=CFBr	27	6.3
	CF_2=CHBr	24	6.0
iodine containing	CF_3I	18	3.2

[a] acted as an oxidizer, promoted flame stability
[b] solid powder not expressed in volume percent
[c] agent observed to be flammable

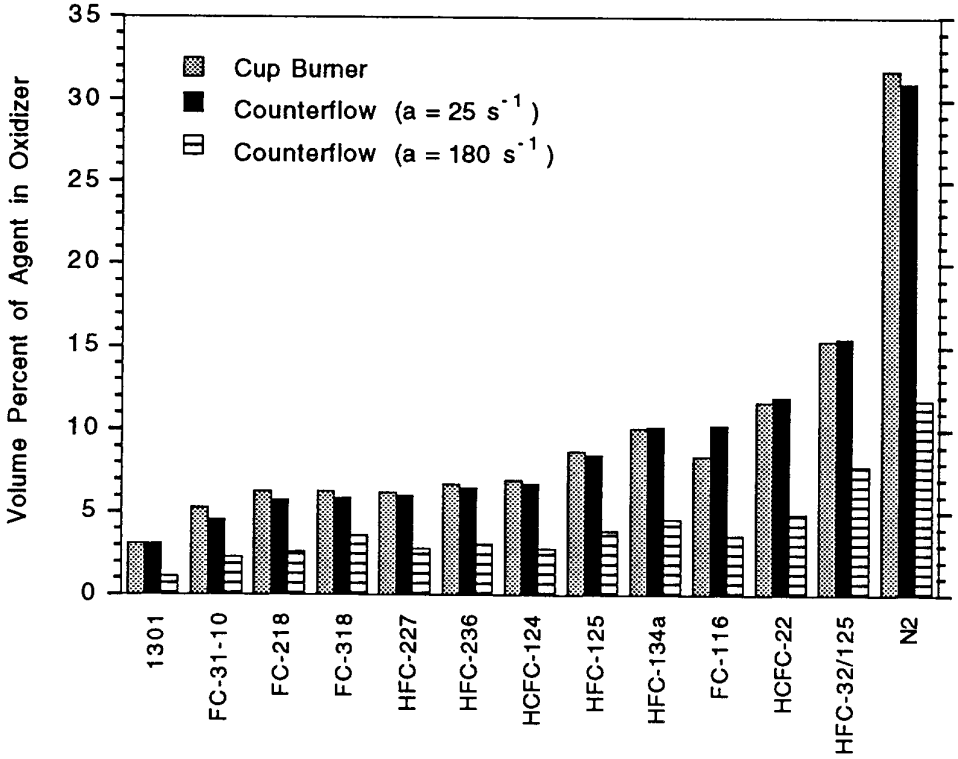

Figure 35. Comparison between the volume percent of agent required to suppress heptane flames in the OFDF and the cup burner.

Table 8. Relative Difficulty in Extinguishing Different Fuels in the Cup Burner

Fuel	Resistance to Extinction
Propane	1.00
Heptane	0.87
JP-8	0.84
JP-5	0.82
5606	0.76
83282	0.74

1. The measurements showed that a mass-based agent ranking of agent suppression effectiveness significantly differed from a mole based ranking. On a mass basis the FC, HFC, and HCFC compounds had essentially the same suppression effectiveness, whereas on a mole basis the higher molecular weight compounds were more effective.

2. Propane flames were most difficult to extinguish (required highest agent concentration), followed by heptane, the jet fuels, and the hydraulic fluids.

3. The relative extinction effectiveness of the agents was essentially unchanged for all fuels tested.

4. $NaHCO_3$ powder was the most effective of all agents tested on a mass basis.

5. Several agents (CF_2H_2, CH_3CF_2Cl, $CF_2{=}CHCl$, and $CH_2{=}CHBr$) behaved like fuels, as characterized by the appearance of an independently stabilized premixed flame inside the burner. Another agent (NF_3) behaved like an oxidizer.

6. CF_3I and the bromine containing compounds were generally very effective on both a mole and a mass basis.

7. The relative rankings of the effectiveness of various gaseous agents in extinguishing the opposed flow diffusion flame burner at low strain rates agree with the cup-burner studies. In addition, at low strain rates, the absolute agent concentration at extinction was found to agree well with measurements made in the cup-burner. Although it is very likely that flame stretch in the cup burner is similar to the low strain rate generated in the OFDF, a systematic study to show this correspondence should be undertaken.

4.4 Turbulent Spray Flames

4.4.1 Background. A fuel spray provides a unique opportunity for a fire. Small droplets quickly evaporate and the momentum from the spray efficiently entrains the air necessary for combustion. A ruptured high pressure fuel, lubricant or hydraulic fluid line can supply a steady flow of fuel for a fire stabilized behind obstacles in the engine nacelle, or create a cloud of droplets from a punctured fuel tank adjacent to a dry bay. Extinguishment of the burning spray will occur when the critical level of agent is mixed with the air that gets entrained into the primary reaction zone. The process is affected by the velocity of the flow, the rate of mixing, the system temperature, and the agent and fuel concentrations and properties.

Neither the cup burner nor the OFDF can simulate the combined droplet evaporation and turbulent mixing which occur in a realistic spray flame. The objective of this portion of the investigation was to develop a laboratory facility which could capture some of the additional critical elements that could exist within an engine nacelle or dry bay fire. The apparatus is useful as a screening device only if the flame and agent injection process can be precisely controlled and operated in a reliable and repeatable manner. In addition to the flexibility offered by a reduced scale facility, the laboratory spray burner provides an opportunity to separate the effects of agent transport and vaporization from flame suppression effectiveness, and to control independently the rate at which the agent enters the flame.

No standard laboratory setup for evaluating the effectiveness of an agent for extinguishing an aircraft in-flight spray fire existed when this study was initiated. The design described in the next section was based upon the desire to maintain flame stability over a reasonable dynamic range, and to accommodate the application of gaseous and powdered agents. A coaxial jet with a spray nozzle typical of a simple oil furnace or gas turbine combustor was chosen for the spray flame apparatus.

4.4.2 Experimental Facility. The spray burner facility consisted of an air delivery system, a fuel delivery system, an agent injection system, and a combustion zone, as laid out in Figure 36. Figure 37 shows a cross-sectional view through the combustion zone. Air at atmospheric pressure co-flowed around a 6 mm diameter fuel tube within a 0.5 m long, 50 mm diameter stainless steel pipe. A pyrex tube with a 65 mm inner diameter, supported on a Teflon ring, contained the flame for 75 mm beyond the outer steel casing. The fuel was injected along the centerline through a pressure-jet nozzle (Delevan model 0.5-45-B) that formed a 45° solid-cone spray. The exit of the nozzle was flush with the open end of the surrounding pipe. The flame was stabilized on a 35 mm diameter steel disk attached to the nozzle body.

The air was supplied by a high capacity compressor at 800 kPa, and its flow was monitored with a sonic-orifice. Temperatures from ambient to in excess of 150 °C, measured with a type-K thermocouple 1.1 m upstream of the fuel outlet, could be obtained using a 60 kW electric air heater. Average velocities across the burner cross-sections reached 50 m/s. The fuel (JP-8 or hydraulic fluid MIL-H-83282C) was stored in an 18 liter tank and delivered to the burner with an electric pump at pressures controllable to 1.0 MPa-g. The nozzle was designed to deliver fuel oil at a rate of 0.5 ml/s when the fuel line gauge pressure is 687 kPa. The flow was calibrated at the actual operating temperatures and pressures for each of the fuels.

The gaseous agents were injected impulsively into the air 0.54 m upstream of the nozzle. Uniform dispersion across the air stream was enhanced by injecting the gas in a radial direction into a reduced diameter (25 mm) section of the air pipe through two 6 mm diameter tubes. Screens with 50% open area were placed 40 and 80 mm downstream of the injection point to ensure complete mixing between the air and agent prior to encountering the flame zone.

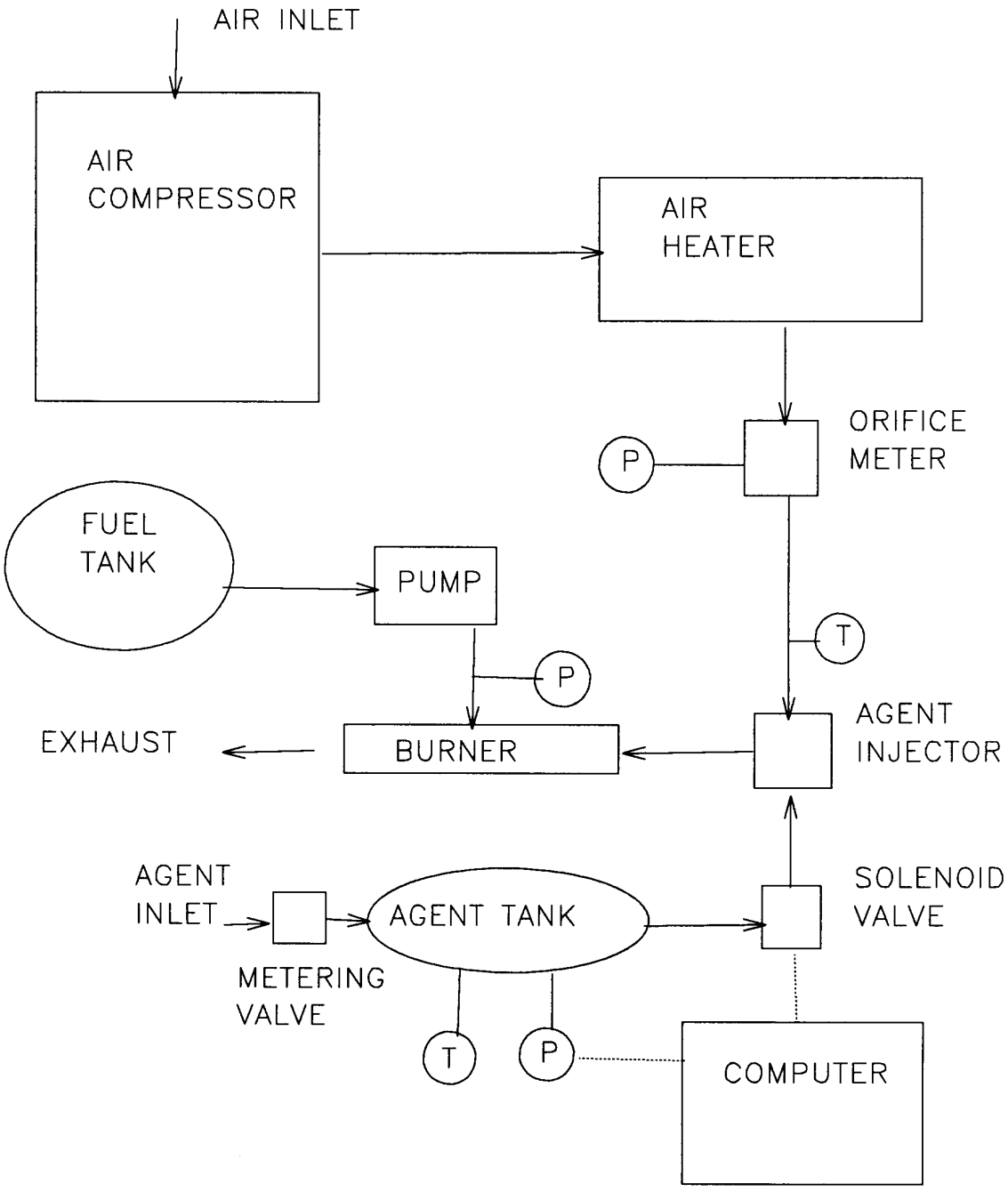

Figure 36. Block diagram of turbulent spray burner facility.

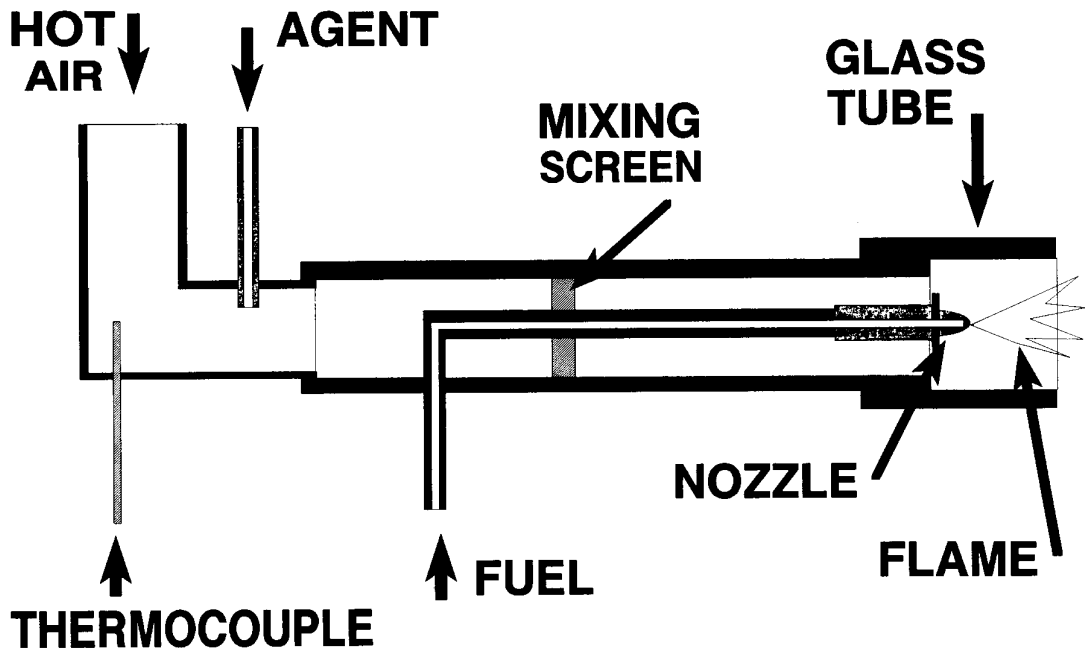

Figure 37. Cross-section of combustion zone of spray burner facility.

A photograph of the overall facility is shown in Figure 38.

The injection mechanism, shown in Figure 39 (a), consisted of the agent supply bottle connected to a stainless steel storage vessel through a metering valve, and to the burner through a computer controlled solenoid valve. The storage volume, including the one liter pressure vessel and associated plumbing, was 1040 $\pm$ 10 ml and the agent pressure was adjustable up to 687 kPa-g. The agent temperature and pressure in the storage vessel were measured with a type-K thermocouple and a pressure transducer located upstream of the solenoid valve. The amount of injected agent was controlled by varying the initial pressure and the time that the valve was open. The controlling computer acquired the digital signal from the pressure transducer at 700 Hz. The actual mass delivered was determined from the difference between the initial and final pressures in the storage vessel using the Redlich-Kwong equation of state (Van Wylen and Sonntag, 1978).

Figure 39 (b) shows how the gaseous injection system was modified to accommodate powders. The powder was loaded into two nylon tees downstream of the computer-controlled solenoid valve. Straight-through ball valves isolated the powder from the burner to minimize back-flow and powder loss during loading. Aluminum caps were machined to reduce any excess volume within the storage tees. Compressed air stored in the agent vessel was used to propel the powder into the burner.

4.4.3 Experimental Parameters and Procedures. The independent parameters which were controlled in the spray burner facility were the air flow and temperature, the fuel flow and type, the agent composition, and the mode of injection (fixed time or fixed pressure). For powder agents there were two additional independent parameters: the particle size distribution and the transport gas pressure. The primary dependent parameters were the mass and the rate of injection required for suppression. Table 9 lists the range of independent parameters investigated, and other relevant operating conditions derived therefrom.

The air and JP-8 fuel flows were varied to ascertain how flame stability was affected by the operating conditions. The fuel pressure was fixed at 687 $\pm$ 10 kPa-g (corresponding to a mass flow rate of around 0.42 g/s). The spray was ignited without the air flowing using a propane torch. The flame extended well beyond the exit of the pyrex tube and was highly luminous under these conditions. As the air flow was increased, the flame attached itself to the stabilizing disc and the plume length decreased until the flame was stationed within the horizontal tube passage. At high air flows little soot radiation was observed beyond the exit plane, although the flame itself maintained some luminosity. A moderate amount of soot formed on the nozzle face in a matter of minutes. A stable flame was sustainable until the air flow rate exceeded 73 g/s. The average gas velocity across the air duct was about 33 m/s at the above-mentioned mass flow, which translated to an estimated residence time in the recirculation zone behind the stabilizing disc of 5 ms. Blowout experiments were repeated for fuel nozzle pressures of 515 and 858 kPa-g. At the reduced pressure the fuel flow rate decreased by about 14%, which resulted in an equivalent decrease in the amount of air necessary to extinguish the flame. The higher nozzle pressure had no appreciable affect on the blowout limit. The operating conditions chosen for baseline measurements were a mass flow of JP-8 equal to 0.42 g/s and an ambient temperature and pressure air flow of 33 g/s, resulting in an average inlet air velocity of 14 m/s. This produced an 18 kW flame with an overall equivalence ratio of about 0.17.

4.4.3.1 Gaseous Agents. The injection system under idealized conditions (incompressible flow, massless valves, no pressure losses) was designed to deliver a square-wave pulse of agent to the burner for the amount of time programmed by the computer controller. The actual flow deviated substantially from this scenario. There was a 15 ms delay between when the solenoid was triggered and the flow of agent actually began. When the valve started to close, pressure waves were created which reverberated in the injection system at the acoustic velocity, causing the flow rate to modulate.

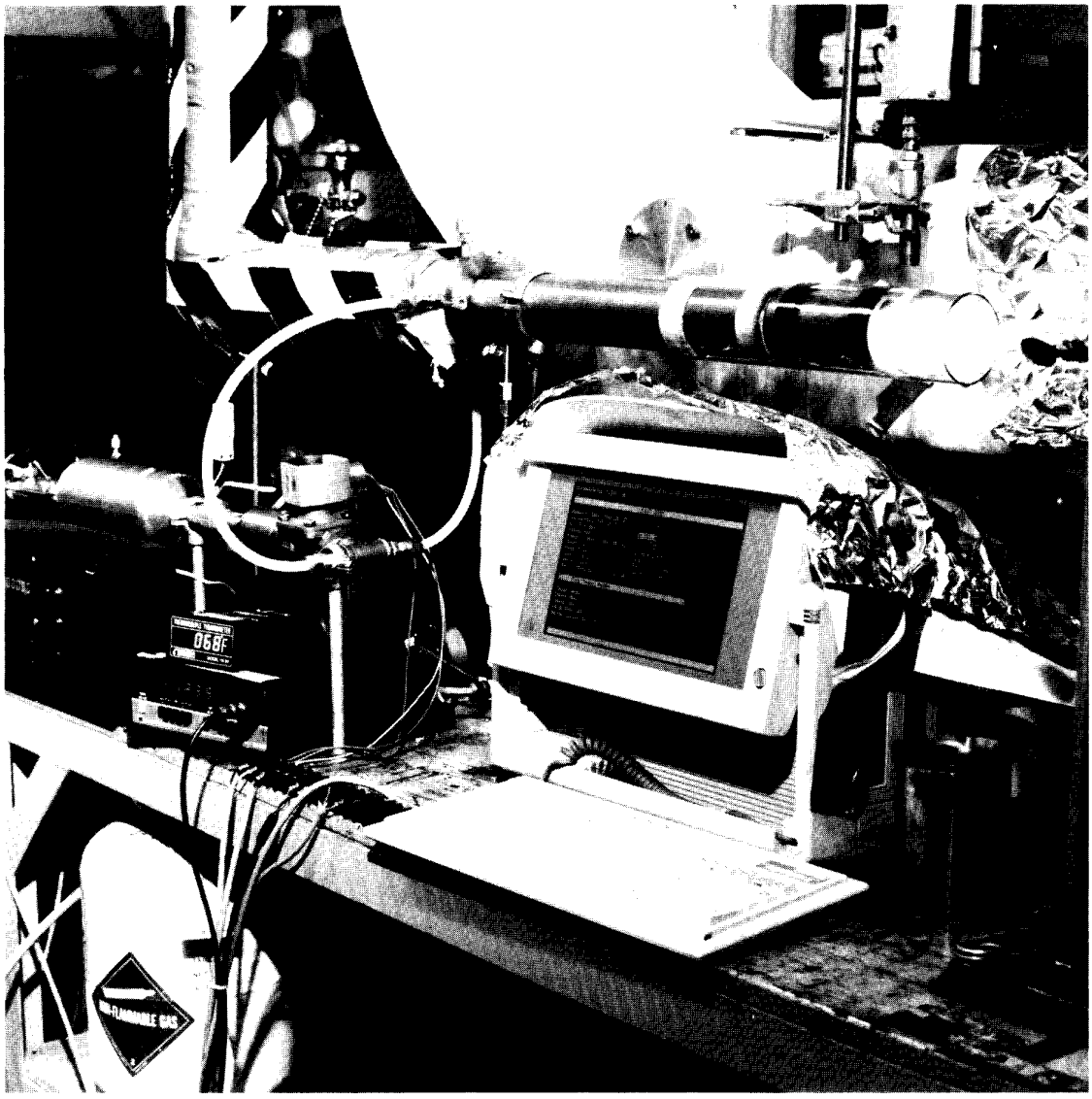

Figure 38. Photograph of turbulent spray burner facility.

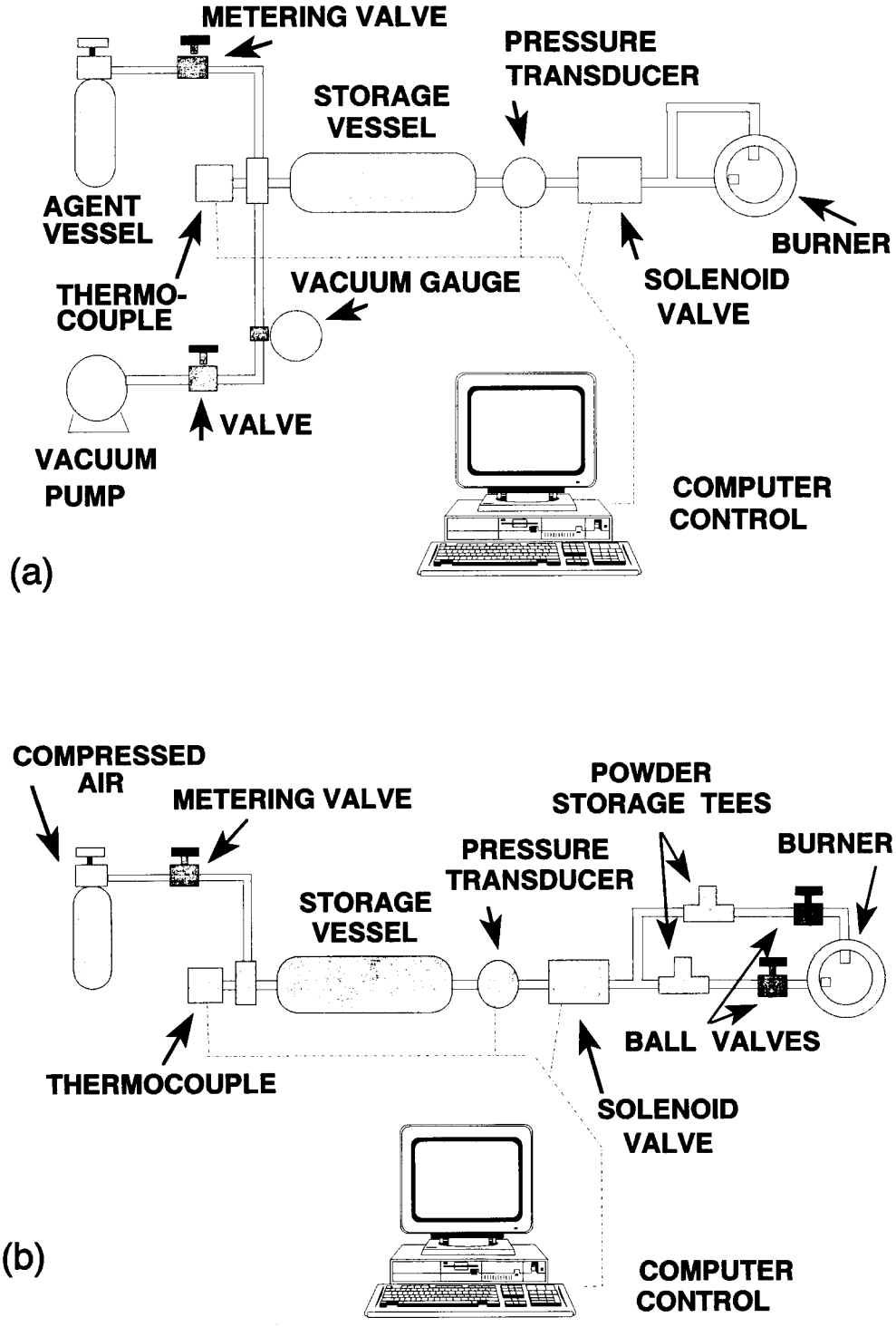

Figure 39. Schematic of agent injection mechanism for (a) gases, and (b) powders.

Table 9. Operating conditions in turbulent spray burner

Parameter	Fuel		
	JP-8		MIL-H-83282C
Air Temperature	19 - 25 °C	146 - 153 °C	118 - 123 °C
Air Pressure	ambient	ambient	ambient
Air Flow	22 to 73 g/s	33±1 g/s	30±1 g/s
Nominal Air Velocity	10 to 33 m/s	20 m/s	18 m/s
Fuel Temperature	19 - 25 °C	< 150 °C	< 120 °C
Fuel Pressure	515 to 858 kPa-g	1034±10 kPa-g	896±10 kPa-g
Fuel Flow	0.43 to 0.55 ml/s	0.46±.05 ml/s	0.65±.05 ml/s
Thermal Input	15 to 20 kW	16±2 kW	[a]
Equivalence Ratio	0.14 to 0.19	0.15	[a]
Gaseous Agents	core 11, N_2, CF_3Br, CF_3I	core 11, N_2, CF_3Br	core 11 (except FC-31-10), N_2, CF_3Br
Powder	$NaHCO_3$ + silica (0-10 μm, +50 μm)	none	none
Agent Temperature	20 - 25 °C	20 - 25 °C	20 - 25 °C
Agent Pressure	20 - 687 kPa-g	20 - 60 kPa-g	20 - 60 kPa-g
Injection Interval	20 to 900 ms	75±10 ms	75±10 ms

[a] molecular composition and enthalpy of formation not provided

An example of these pressure modulations and the injection timing sequence is seen in Figure 40. The curve labeled P2 is the voltage from the pressure transducer between the solenoid valve and the metering orifice and P1 relates to the pressure upstream of the orifice.

The mass of agent, m, contained in the vessel of volume V, at pressure P and temperature T, was determined from the Redlich-Kwong equation of state,

$$m = \frac{PVM}{RT}\left[\frac{1}{1-bm/V} - \frac{am/(VRT^{3/2})}{1+bm/V}\right]^{-1} \quad (4)$$

M is the molecular weight of the gaseous agent, R is the gas constant, and a and b are constants dependent upon the critical properties of the agent (Van Wylen and Sonntag, 1978). The initial temperature was measured, and the final temperature was determined by assuming that the expansion occurred isentropically following the relation

$$\frac{T_f}{T_i} = \left(\frac{P_f}{P_i}\right)^{\frac{\gamma-1}{\gamma}}. \tag{5}$$

Gamma is the specific heat ratio for the gas. Thus, by measuring the change in pressure, Equation (4) can be used in an iterative fashion to determine the total amount of mass injected into the burner. Equation (5) assumes the gas is ideal. (From Equation (4) the deviation from ideal gas behavior was found to be a maximum of 7% for the gaseous agents.) The pressure data were collected at a rate of 700 Hz, with the initial and final conditions found from the average of at least 100 points measured one-half second prior to the release of the agent, and one second after the solenoid valve closed, respectively. Figure 41 presents an example under minimum suppressing conditions of the calculated mass delivered as a function of time using Equations (4) and (5) for six different trials at the same computer setting.

A figure of merit for extinguishing the flame, ß, can be defined in terms of the mass flows of agent, m_i, and air, m_{Air}:

$$\beta \equiv \frac{\dot{m}_i}{\dot{m}_i + \dot{m}_{Air}}. \tag{6}$$

A small value for ß is desirable. The mass of agent added to the flame is determined from Equation (4), and the actual time interval of agent injection into the burner is estimated from the linear portion of the slope in the mass-time curve. (*e.g.*, see Figure 40).

The storage vessel was pressurized with air to 687 kPa-g, and the solenoid valve was opened for successively longer periods of time, up to a maximum of 910 ms. Figure 42 presents the cumulative increase in mass delivery with set time. The results indicate that the mass of air (solid symbols) increased almost linearly with time in the range between about 25 and 250 ms. For short time settings, less mass was delivered because the valve did not have sufficient time to fully open. The deviation from linear behavior when the valve was open for a long period resulted from depletion of the entire mass ($\approx$ 10 g) contained in the injector storage vessel. Figure 42 also presents the time over which the pressure decreased in the vessel (open symbols). There was a minimum time for the solenoid valve to respond due to inertia, which explains the greater measured time for settings below 25 ms.

A number of experiments were carried out with the burner operating at baseline conditions and with air as the extinguishing agent to ensure that the flame could not be suppressed simply by blowing it out. When air was injected into the burner, the flame was observed to fluctuate momentarily, but was never extinguished even when the storage pressure and injection period were at their maximum values (*viz.*, 687 kPa-g and 910 ms, respectively).

The protocol used in the experiments with the gaseous agents was to ignite the fuel spray and set the air flow to the desired level. The flame was allowed to burn for several minutes to ensure steady operation. If the air was at an elevated temperature, it was necessary to wait until the temperature of the air at the burner stabilized, which took as long as 20 minutes in some cases. The storage vessel was evacuated and then flushed several times with the agent under investigation to purge contaminating gases from the system. The pressure in the vessel was adjusted with the solenoid valve closed using the inlet metering valve. Initially a pressure was chosen which was expected to be insufficient to extinguish the flame. The computer control/data acquisition was begun and the response of the flame to the injection process was observed. If the flame was not extinguished, the pressure in the agent vessel was increased and the experiment was repeated immediately. Eventually a pressure was

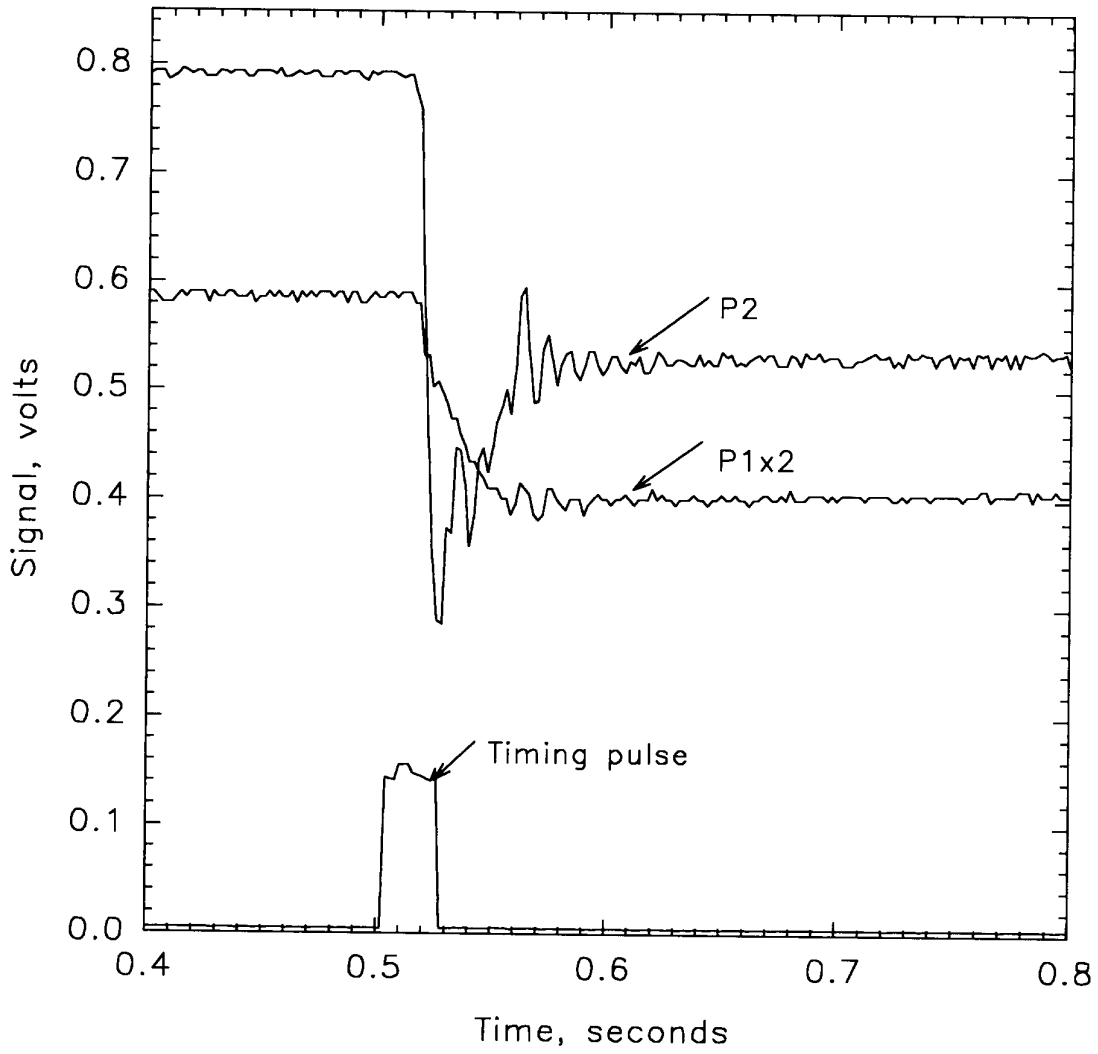

Figure 40. Pressure during injection of nitrogen; 6.4 mm metering orifice, time = 23 ms.

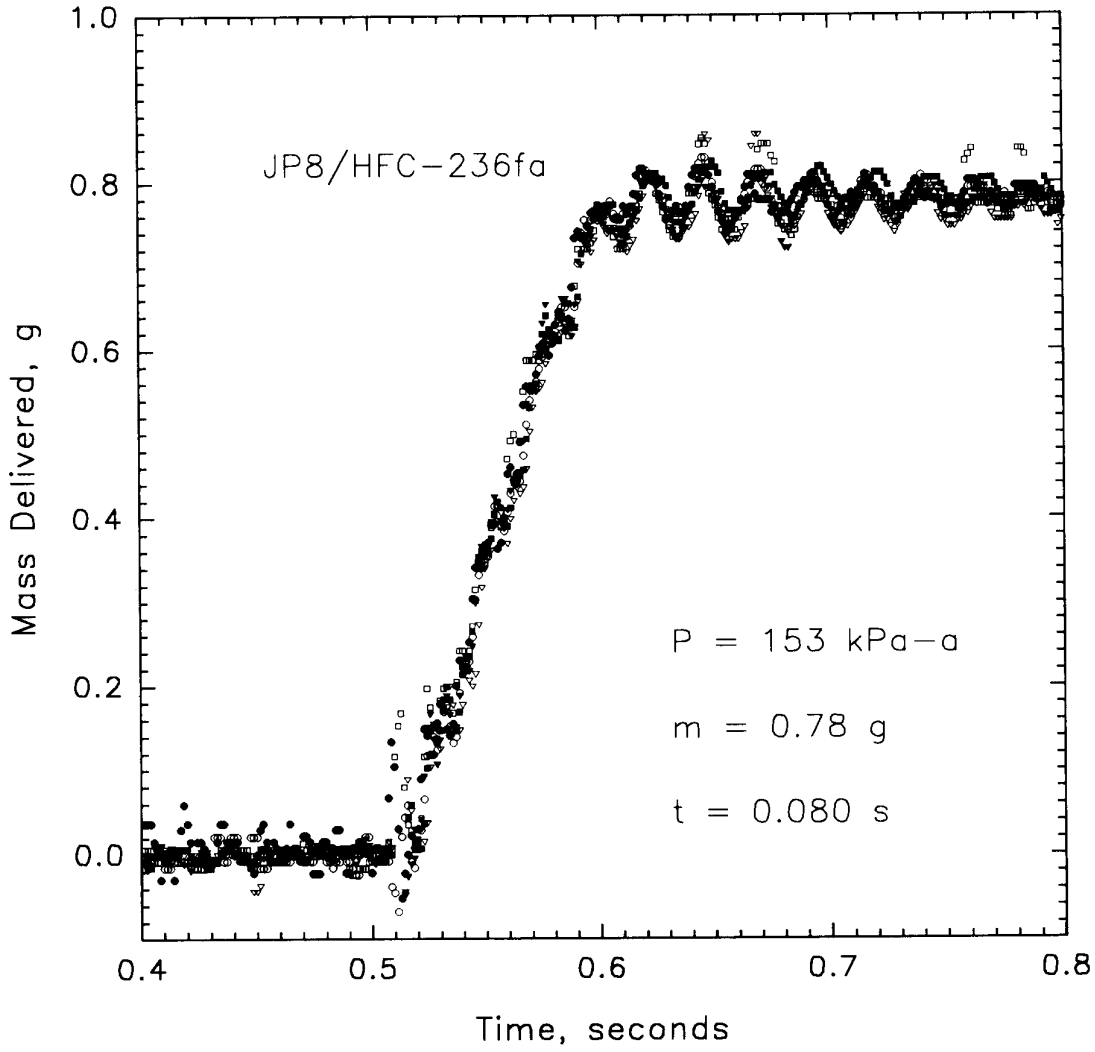

Figure 41. Mass delivered to burner as a function of time; HFC-236fa/hydraulic fluid flame.

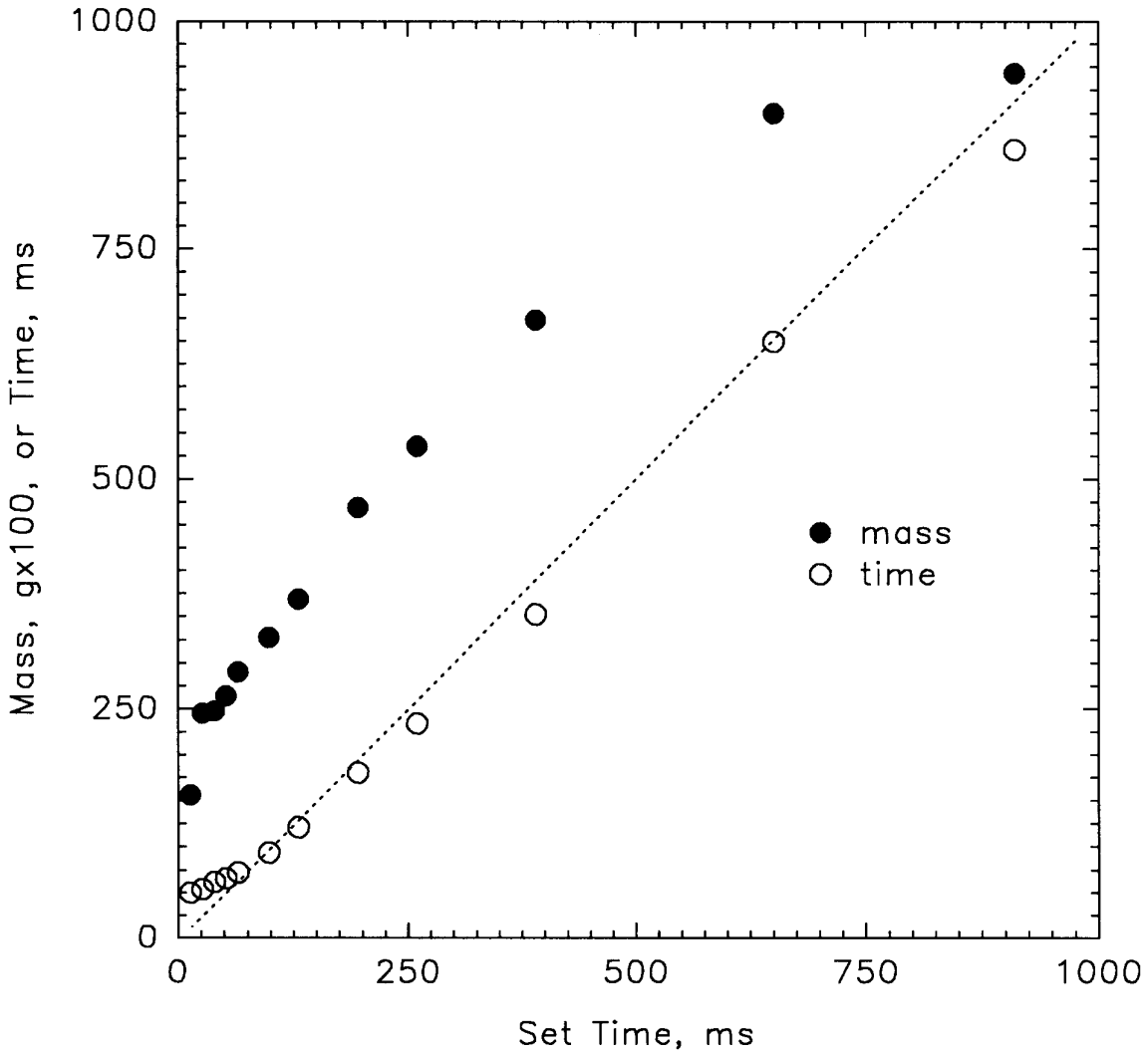

Figure 42. Injection period (open circles) and mass of air delivered (solid circles) as a function of set time. Initial pressure is 687 kPa-g.

found which was sufficient to suppress the flame. This procedure was normally repeated four times for each agent.

4.4.3.2 Powder Agents. Two powder samples and two different pressures were used to determine the effects of particle size and pressure on suppression performance. $NaHCO_3$ powder was mixed with silica gel and classified by size as described earlier in Section 4. The two distributions used were 0-10 μm and +50 μm. Two air pressures were selected for powder delivery, 172 and 241 kPa-g. Lower pressures were avoided because of poor delivery performance in preliminary testing.

The storage vessel was filled to the desired air pressure with the solenoid valve closed using the inlet metering valve. With both downstream ball valves closed, a preweighed amount of powder, expected to be insufficient to extinguish the flame, was loaded into the storage tees (see Figure 39 (b)). Once loading was complete, both ball valves were opened, the computer control/data acquisition was begun, and the flame response to the injection process was observed. The nominal injection period was set for 65 ms in all the experiments presented here. If the flame was not extinguished, any powder accumulation within the injection mechanism and the burner was removed. Total removal was accomplished by using a minimum of five high pressure air injections (> 240 kPa-g) and by increasing the burner air flow to at least 60 g/s for approximately 20 minutes. Preliminary testing showed that this procedure was necessary to properly clean the injection mechanism. The storage vessel was again pressurized to the same injection pressure, a larger preweighed amount of powder was loaded into the storage tees, and the experiment was repeated. Eventually an amount of powder was found which was sufficient to suppress the flame. This procedure was normally repeated three times for each powder sample and pressure.

Once the powder suppression mass was determined the delivery tubes were disconnected from the burner and a series of tests were run to determine powder injection efficiency. This was done by loading a preweighed amount of powder into the storage tees and injecting it into a one liter plastic bag. The injection was performed according to the previously discussed experimental procedure. The plastic bag was weighed before and after the injection to determine the weight gain. Five air injections at 240 kPa-g were also performed in a different plastic bag to determine the amount of residue left in the injection mechanism after the first injection. This procedure was repeated a minimum of five times to determine reproducibility. The percentage of powder injected was determine by dividing the plastic bag weight gain by the preweighed amount of powder loaded into the injection mechanism. The percentage of powder residue was calculated in the same manner, using the plastic weight gain from the five high pressure injections. The results are summarized in Table 10. Powder losses within the burner itself were not quantified; however, inspection of the burner walls and mixing screens showed almost no powder accumulation beyond a very thin layer of dust.

4.4.4 Experimental Results

4.4.4.1 Characterization of Facility. The influence of air velocity, injection period, and injection pressure on the amount of N_2 required to extinguish the JP-8 spray flame and on the value of ß was investigated as a means to validate the operation of the experimental facility. The storage vessel was pressurized with nitrogen to 113 kPa-g and the turbulent burner set to baseline conditions (ambient temperature, air flow equal to 33 g/s). The fuel flow was kept constant at 0.42 g/s. The injection interval was increased one millisecond at a time until the flame was extinguished. Flame extinguishment occurred between 23 and 26 ms for five different runs, delivering an average of 0.33 $\pm$ 0.03 g nitrogen at a mean flow rate of 11.2 $\pm$ 0.5 g/s. From Equation (6), the figure of merit

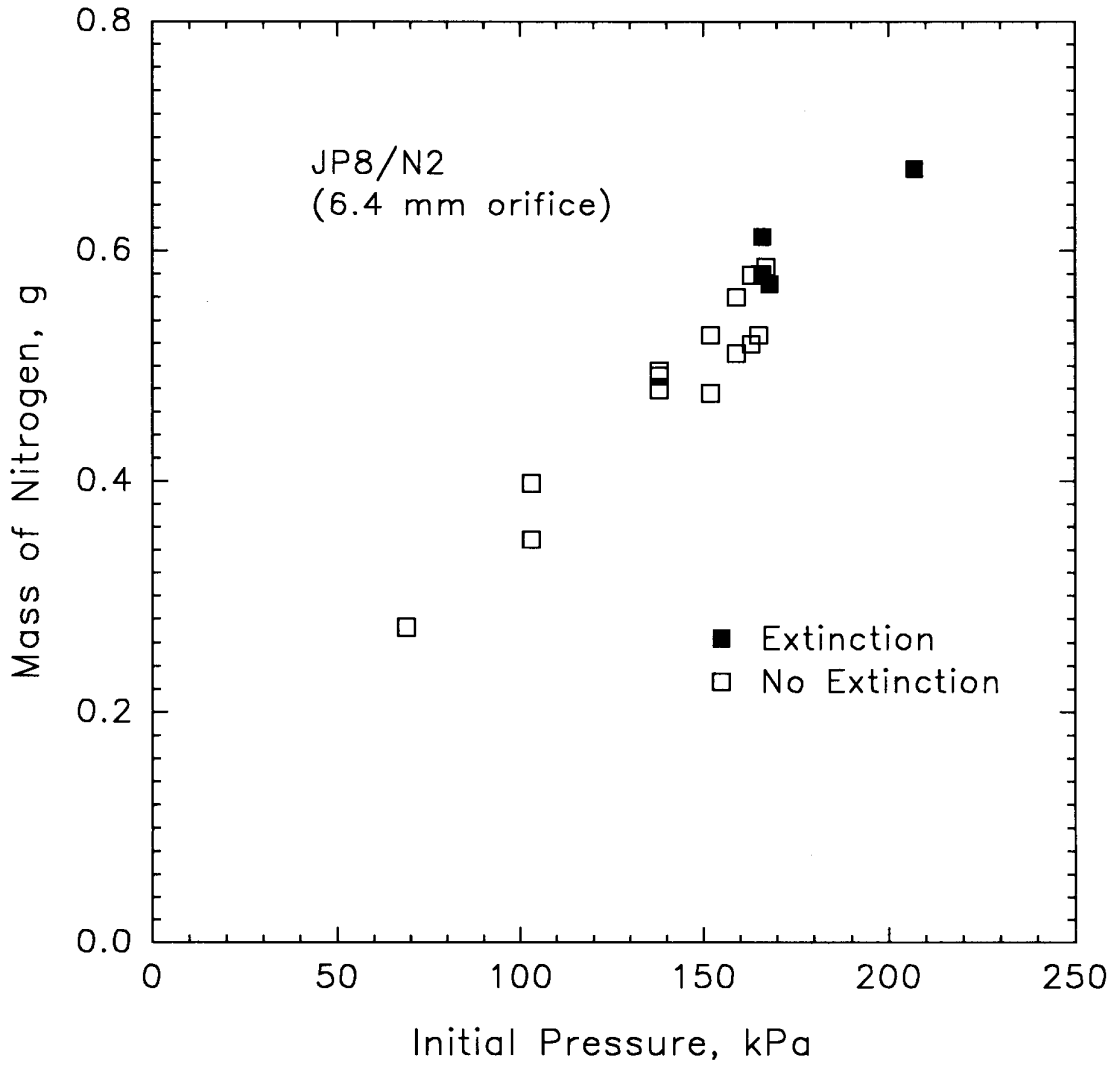

Figure 43. Effect of vessel pressure on extinguishment of JP-8 spray flame by nitrogen. Solid symbols indicate extinction; open circles indicate no extinction.

Table 10. Powder injection efficiency

Particle Size (μm)	Powder Injected (%)	Powder Residue (%)	Air Injection Pressure (kPa)
0-10	81.2 ± 3.0	17.8 ± 3.4	172
0-10	88.8 ± 1.2	10.7 ± 1.7	240
+50	82.3 ± 3.4	17.9 ± 4.4	172
+50	93.8 ± 1.5	7.5 ± 0.1	240

varied between 0.24 and 0.26. This value compares to a figure of merit for nitrogen of 0.28 measured in the cup burner apparatus with JP-8 as the fuel.

Additional experiments were carried out for air flows of 44 g/s and 22 g/s. The high velocity (19 m/s) required an average total nitrogen mass of 0.29 g at a rate of 11.5 g/s. The amount of nitrogen required to extinguish the lower air velocity flame was 0.32 g, with an average flow of 10.7 g/s. In this case, doubling the air flow reduced the mass of nitrogen required by 10%. The high air flow case yielded ß = 0.21 and the low air flow case yielded ß = 0.33.

A series of experiments was carried out with the air and fuel flow rates at baseline conditions, and the time interval was fixed as the nitrogen pressure was increased. Figure 43 is a plot of the mass of nitrogen delivered to the burner as a function of initial vessel pressure for an injection interval set to 65 ms. The open squares indicate that the flame remained lit; the solid squares correspond to successful extinguishments. The minimum vessel pressure necessary to extinguish the flame 100% of the time was 167 kPa-g. The amount of nitrogen delivered at this pressure and time interval was 0.58 ± .03 g.

The injection time interval had an effect on the minimum amount of nitrogen required to extinguish the flame. The open squares plotted in Figure 44 illustrate this effect. For these experiments, the pressure was fixed and the injection time interval was gradually increased until extinction occurred. The minimum mass of nitrogen was about 0.32 g, for a set injection period of 23 ms. Reducing the set time to 6 ms had no impact on the amount of nitrogen required to quench the flame because, as shown in Figure 42, the actual period of injection did not change appreciably. Injection times longer than 23 ms lead to delivering greater amounts of N_2, with more than three times as much N_2 required when the injection time was set to 260 ms. A limit was reached at long time intervals where the transient mass addition was insufficient to extinguish the flame.

Nitrogen was allowed to flow continuously in one experiment, with the rate increasing until the flame was extinguished. The figure of merit was found from Equation (6) to be 0.11, and is indicated by the continuous flow arrow in Figure 44. This compares to a value of 0.28 found in the cup burner with the same fuel/agent combination. Less nitrogen was required for extinguishment of the spray flame because of the greater turbulence levels and reduced time available for the combustion to occur. The solid squares also plotted in the figure are values of ß that correspond to the different injection time intervals. As the time was shortened, ß increased, reaching a limiting value of about 0.28. (It is a coincidence that this value is identical to the value of ß measured in the cup burner.)

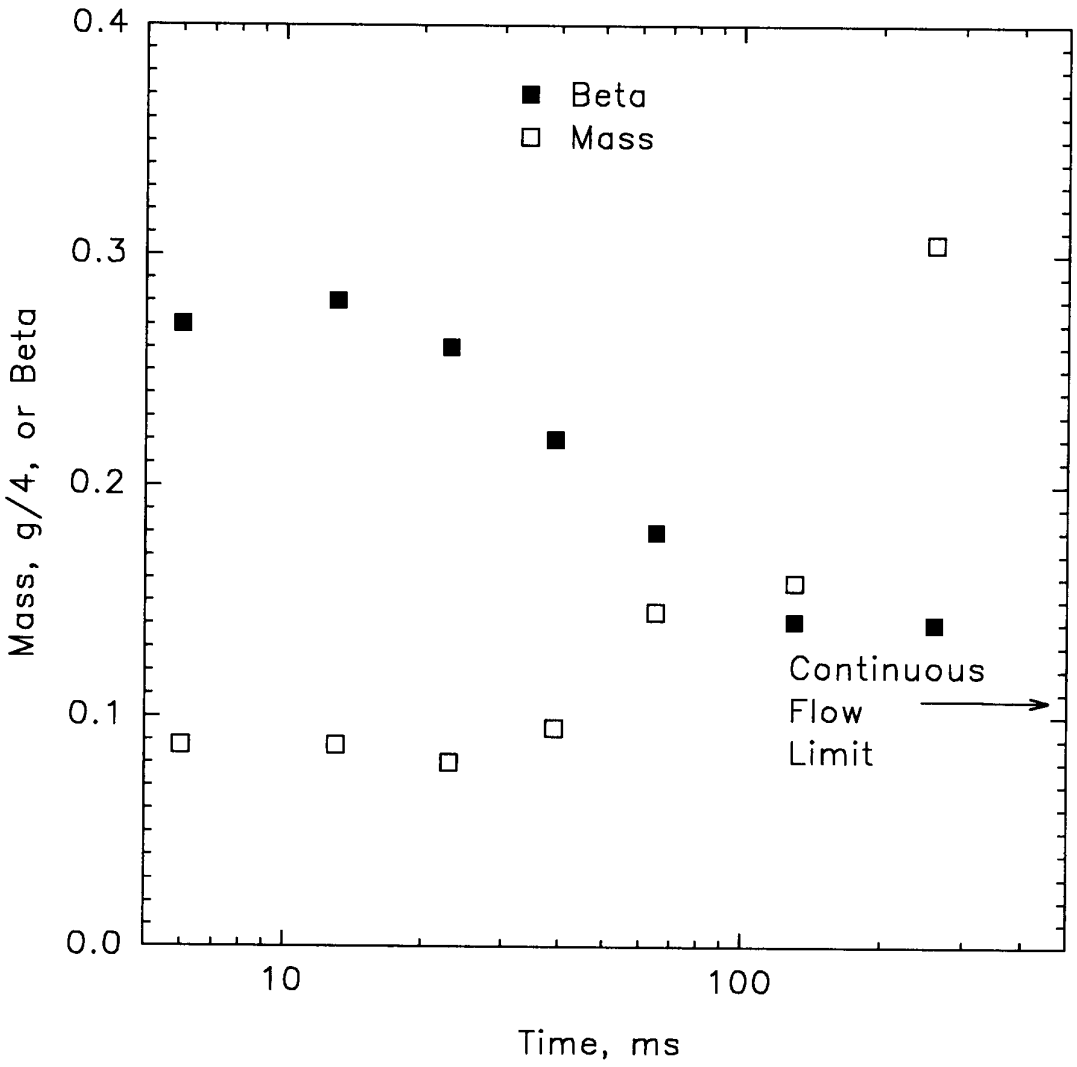

Figure 44. Effect of injection time interval on mass of nitrogen (open squares) required to extinguish JP-8 spray flame; solid squares: β.

If the value of ß were the sole criterion for evaluating an extinguishing strategy, one would chose to inject the agent over an extended period of time. However, as seen in Figure 44, this has the undesirable effect of greatly increasing the amount of agent required to put out the flame. For an agent that is to be used in a transient manner, the total mass must also be considered. This is distinct from the quasi-steady state measurements taken with the cup burner apparatus, for which ß is a reasonable measure of performance for a total flooding agent.

4.4.4.2 Gaseous Agents/JP-8/Ambient Air Test Series. A fixed injection time of 65 ms was chosen to compare the performance of the alternative agents. This value is intermediate between the estimated residence time in the spray flame (5 ms) and a typical time interval for injection in an actual engine nacelle (500 ms). At this setting, an initial pressure of 167 kPa-g was necessary to extinguish the flame with nitrogen. Nitrogen is considered chemically inert during suppression, and has a much lower molecular weight than halon 1301 and the alternative gaseous agents that were evaluated. As a result, the initial pressure in the vessel required for flame extinction was much less for the alternative agents. The 6.4 mm flow-metering orifice was therefore replaced with a 4.8 mm orifice to increase the required pressure and reduce the per cent uncertainty in the pressure change measurement. Extinguishment experiments were performed using halon 1301 to establish a performance reference (Grosshandler *et al.*, 1993). An average over five experiments led to a required initial CF_3Br pressure of 24 kPa-g to extinguish the flame, which translates to a mass of 0.44 $\pm$ .04 g and a β of 0.15.

The repeatability of the experimental technique is demonstrated in Figure 41, which is a plot of the mass of agent delivered to the burner as a function of time for six different trials where the mass of the agent, HFC-236fa, was just above the extinction threshold. The average mass injected was 0.78 g with a range of $\pm$0.02 g. The initial pressure needed to cause extinction was 52 $\pm$ 2 kPa-g, and the calculated injection interval was 80 $\pm$ 8 ms, as compared to the set time of 65 ms. The difference between the average injection interval and the computer setting was slightly larger than that found using nitrogen. This was attributed to the lower initial pressure used in the HFC-236fa experiments, which was less effective in causing the solenoid valve to close.

The results of the ambient temperature air/JP-8 flame suppression experiments for all of the gaseous chemicals examined are summarized in Table 11. The CF_3I required the least mass (0.54 g) and had a figure of merit of β = 0.16, close to that of CF_3Br. Nitrogen was only slightly less effective. Of the core agents, HCFC-22 required the least (0.65 g) and FC-31-10 required the most (1.00 g) material to extinguish the flame. FC-31-10 had the poorest figure of merit, 0.27.

4.4.4.3 Effect of Air Temperature and Fuel Type. The air was preheated to 150 °C (+3/ -5 °C) and the experiments were repeated with all of the gaseous agents except for CF_3I (Vazquez *et al.*, 1994). The increase in temperature affected the flame stability in several ways. First, since the mass flow of air remained fixed, the average velocity across the air duct increased about 50% because of the drop in density. The JP-8 in the line was also heated as it flowed through the heated air annulus. The higher temperatures and lower fuel density required the fuel pressure to be increased to deliver the same amount. However, even at a maximum fuel line pressure of 1.03 MPa-g, the mass of fuel was only 90% of the ambient temperature condition, resulting in a slightly leaner flame. The increase in air velocity and decrease in equivalence ratio destabilized the flame; but this was counteracted by the increase in enthalpy of the reactants due to the higher initial temperature.

As seen in Table 11, increasing the temperature, on average, increased the amount of alternative agent required to suppress the JP-8 spray flame by 0.04 g. The halon 1301 remained the most effective, but in relative and absolute terms, required the largest increase in mass of all the chemicals investigated. The nitrogen remained better than the other halogenated compounds, and FC-31-10

Table 11. Amount of agent required to suppress turbulent spray flames

	JP-8, T_{air}=20 °C		JP-8, T_{air}=150 °C		Hydraulic Fluid T_{air}=120 °C	
Agent	mass	β	mass	β	mass	β
halon 1301	0.44	0.15	0.53	0.19	0.44	0.16
CF_3I	0.54	0.16	[a]	[a]	[a]	[a]
nitrogen	0.58	0.18	0.63	0.19	0.42	0.16
HCFC-22	0.65	0.20	0.70	0.23	0.70	0.24
HFC-125	0.73	0.22	0.77	0.24	0.78	0.26
HCFC-124	0.74	0.22	0.75	0.22	0.70	0.23
FC-116	0.75	0.22	0.74	0.23	0.73	0.23
HFC-134a	0.76	0.24	0.78	0.23	0.79	0.26
HFC-236fa	0.78	0.23	0.84	0.25	0.78	0.24
HFC-227	0.80	0.24	0.81	0.24	0.82	0.26
HFC-32/125	0.81	0.24	0.89	0.26	0.82	0.25
FC-218	0.89	0.24	0.87	0.25	0.86	0.28
FC-318	0.97	0.25	0.99	0.26	1.08	0.30
FC-31-10	1.00	0.27	1.02	0.25	[a]	[a]

[a] not measured

remained the least effective. It can be speculated that the relatively poorer behavior of the halon 1301 is attributable to the decreased residence time of the agent in the flame, such that the bromine has less opportunity to scavenge the chain carrying radicals.

A flame could not be stabilized using Mil-H-83282C hydraulic fluid and ambient temperature air. By increasing the fuel volume flow by 27% over the JP-8 flame and the air temperature to 120 °C (±3 °C), sufficient stability could be maintained. A bluish appearance of the hydraulic fluid spray flame suggested that less soot was being formed.

There was little difference in the amount of halogenated agent necessary to suppress the hydraulic fluid spray when compared to the JP-8 flames. (See Table 11, and note that neither FC-31-10 nor CF_3I was tested with the hydraulic fluid.) In particular, the amount of halon 1301 was identical to the unheated jet fuel experiments. About 10% more FC-318 was used to suppress the hydraulic fluid. By contrast, 28% less nitrogen extinguished the hydraulic fluid flame. An explanation for this unique behavior is not available.

4.4.4.4 Sodium Bicarbonate Powder Experiments. There was a definite particle size effect on the efficiency of the powder as a fire suppression agent. Table 12 summarizes the results. The smallest particle size powder was 2.4 to 3.0 times more effective in its fire suppression capability than the large particle size powder. There was no significant difference in performance created by changing injection pressure in the small size range. On the other hand, increasing pressure increased the effectiveness of the large particle size by more than 20%. The β values indicate a very effective agent for small particles, and a rather average agent for the large particle size.

High speed movies of injection of the 0-10 μm particles showed what appears to have been a uniform powder cloud passing through the burner in about 80 ms. This compared to an injection interval equal to 75 ms based upon the recorded air pressure in the storage vessel. The photographs also showed that flame extinction happened within the first 50 ms from the time the powder reached the flame. This time was independent of injection pressure, and was close to the 40 ms estimated from high speed photographs of HCFC-22 suppressing a similar flame.

4.4.5 Discussion of Results. If the agents are ranked according to the mass required to inhibit the flame, the order does not change by more than plus or minus one position for the three series of experiments. The exception is HFC-125, which drops two positions in both of the high temperature tests. Expressing the results in terms of the flame suppression number (FSN) is a convenient way to compare the performance of the different agents in the three series of experiments. The FSN is defined as the mass of agent relative to the mass of halon 1301 used to suppress the equivalent flame. Figure 45 summarizes the results in this fashion, using (a) ambient temperature air and JP-8 (open bars), (b) 150 °C air and JP-8 (cross-hatch bars), and (c) 120 °C air and hydraulic fluid (solid bars). The superior performance of the 0-10 μm $NaHCO_3$ powder is evident in the figure.

A flame suppression number also can be defined in terms of β, the mass fraction of agent in the flowing mixture, with β for halon 1301 used to normalize the results. The FSN computed on a mass flow basis can be seen in Figure 46. For the ambient temperature JP-8 flame, the cup burner mass flow FSN is about 2.0 ($\pm$0.15) for the various agents, which is about 0.5 greater than the FSNs plotted in Figure 46. The implication is that it takes a significantly lower mass fraction of agent to extinguish the turbulent spray flame than the cup burner flame. The cup burner was not operated at elevated temperatures, but one series of tests were run using ambient temperature hydraulic fluid. The same trend was observed when the cup and turbulent spray extinguishing mass fractions were compared: a measurable decrease in agent concentration was required for the turbulent spray flame (in spite of the fact that the higher reactant temperatures were expected to stabilize the spray flame, everything else being equal).

Minimizing the storage volume on board the aircraft is as critical as minimizing the mass of agent. There are a number of densities which one could use to convert the required mass of agent to the required volume, including the dispersed gas density and the density of the saturated liquid agent at ambient temperature. The former scales with molecular weight. The latter density also has practical significance. It provides a logical conversion from the mass required to the storage volume because the saturated liquid condition at ambient temperature is close to the condition maintained when the fire bottle is filled (assuming negligible solubility of the pressurizing gas). The volume factor, VF, is defined as the volume of the agent, computed with either of the above densities, normalized by the equivalent volume of halon 1301. Figure 47 compares the dispersed volumes. Figure 48 displays the volume factors under storage conditions. Nitrogen requires a storage volume 36 times that of halon 1301, and is off the scale in Figure 48 because it does not liquify under typical bottle conditions. The FC-116 also rates poorly on volume factor because its critical temperature is less than the ambient. In the figure, the density of FC-116 was calculated at 20 °C and 4.1 MPa, a typical bottle pressure. The remainder of the agents have storage volume factors between 1.5 and

Table 12. Sodium bicarbonate powder results

Particle Size, μm	Air Injection Pressure, kPa	Powder Mass, g	β
0-10	172	0.20	0.08
0-10	240	0.19	0.07
+50	172	0.59	0.20
+50	240	0.46	0.16

2.5, depending on the agent, fuel and temperature. Of these, the HFC-32/125 mixture has the highest volume factor, and HFC-227, HCFC-124 and HCFC-22 have the lowest. The powdered agent was not compared on a volume basis since the volume depends upon the pressurizing method as much as on the volume of the powder.

4.4.6 Conclusions from Turbulent Spray Burner Study. The turbulent spray burner has been found to be suitable for comparing the performance of gaseous and fine powder extinguishing agents in transient operation. The facility is not overly sensitive to the air or fuel flows, and the agent delivery system is able to control accurately the injection period between 20 and 910 ms.

The following conclusions can be made regarding the ability of different agents to extinguish the spray flame:

1. The mass fraction, total mass, and minimum volume of agent required to extinguish a given flame must all be considered when ranking the performance of different fire fighting agents.

2. Of the chemicals evaluated in the turbulent spray burner, $NaHCO_3$ was the only compound more effective than halon 1301. CF_3I required the least mass and volume of the gaseous agents to extinguish the flame, followed by nitrogen (FSN only) and the chlorinated agents, HCFC-22 and 124.

3. The larger perfluorocarbons, FC-31-10 and 318, required the greatest mass. On a volume basis, nitrogen was the poorest performer. The mixture of HFC-32 and HFC-125 had the largest volume factor of the condensible agents.

4. No statistically significant difference in agent performance was found between the room temperature JP-8 and hydraulic fluid flame testing, indicating little fuel effect.

5. The majority of the agents required slightly more mass to extinguish the higher temperature JP-8 flame, indicating a small temperature effect. This trend is not completely unexpected since a higher enthalpy flame is normally more stable. However, the temperature effect did not alter the ranking on agent performance, with the exception of HFC-125.

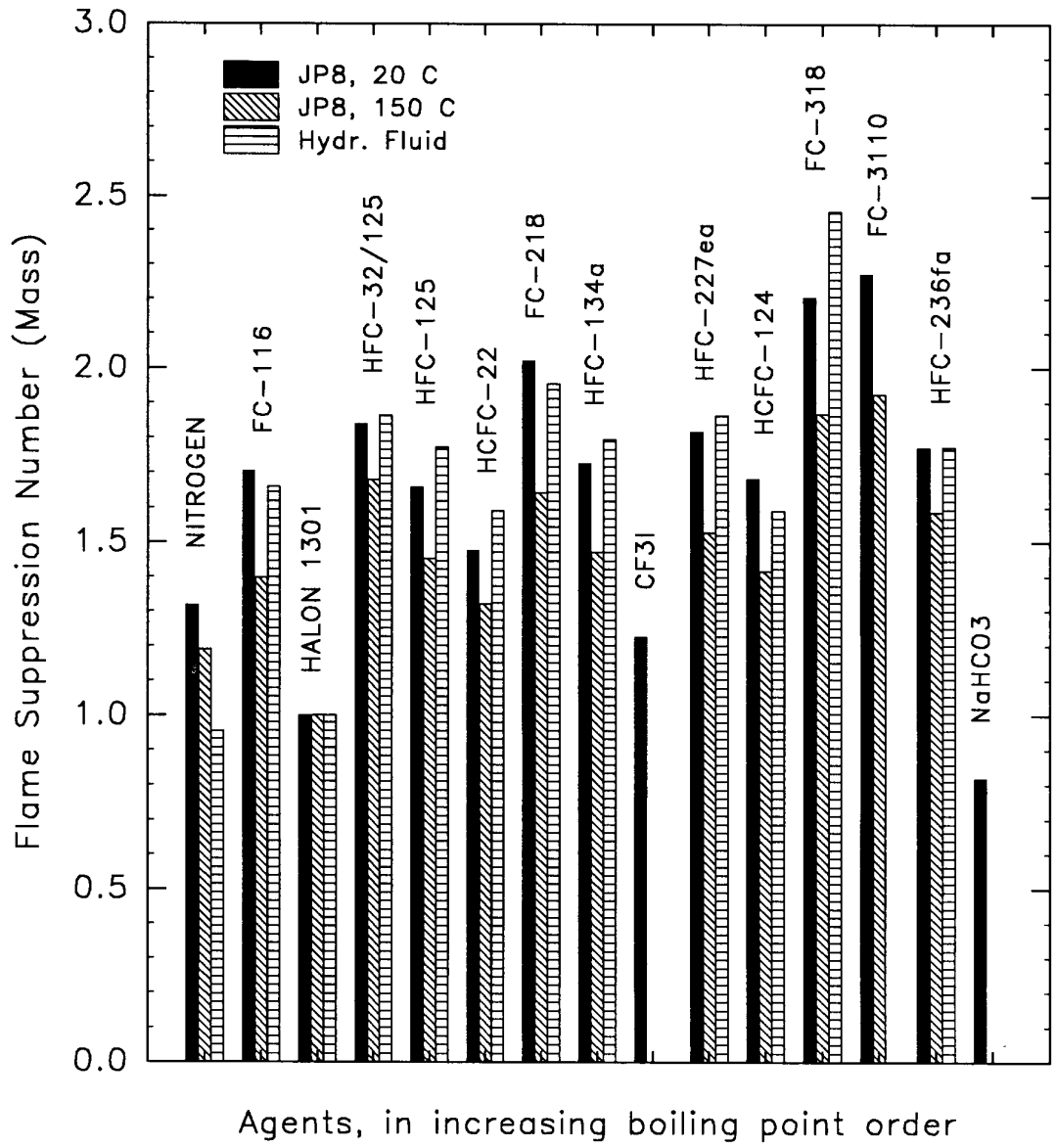

Figure 45. Flame suppression number (FSN) computed on a relative mass basis.

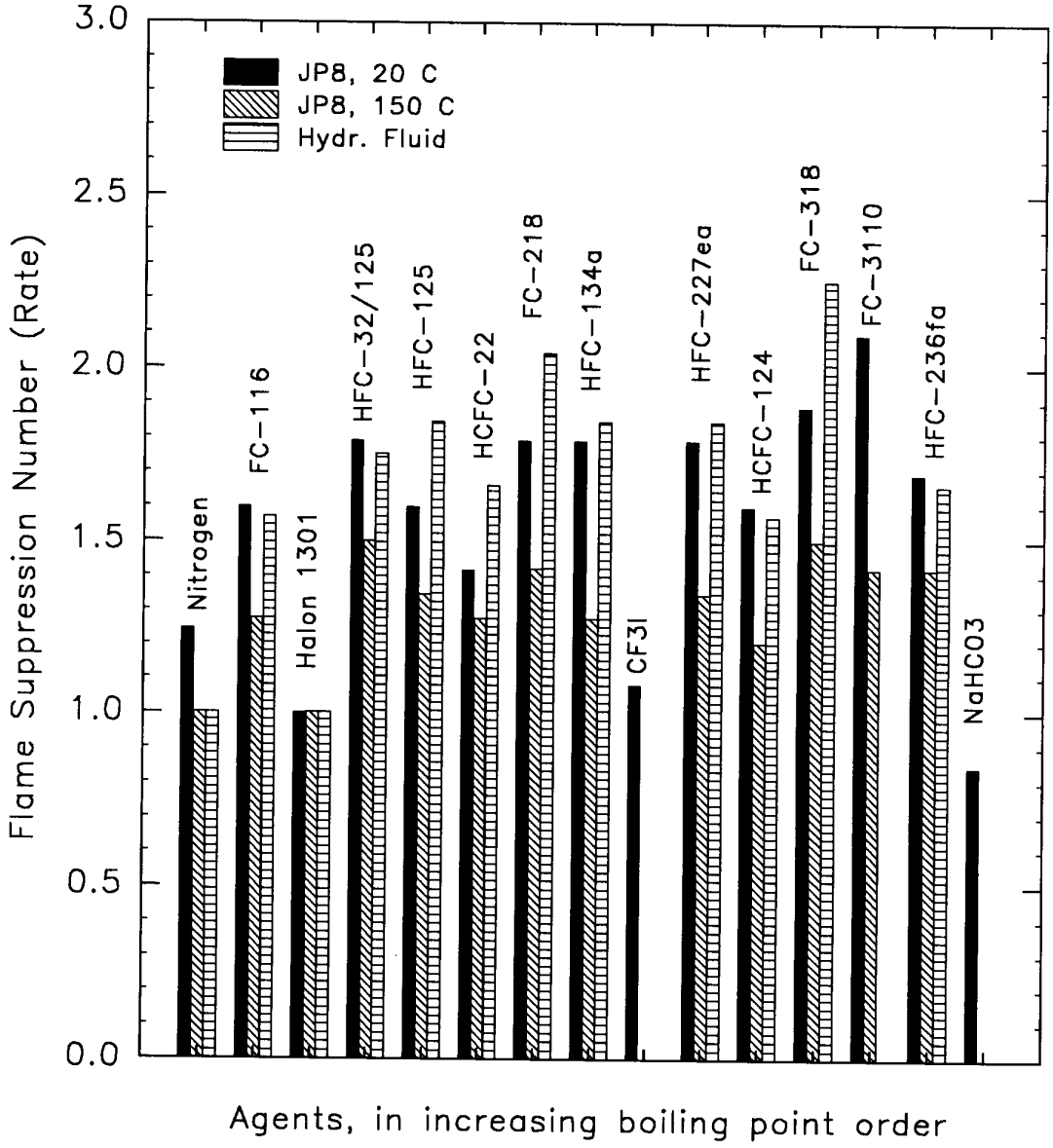

Figure 46. Agent flame suppression number (FSN) based upon relative rate of mass injected.

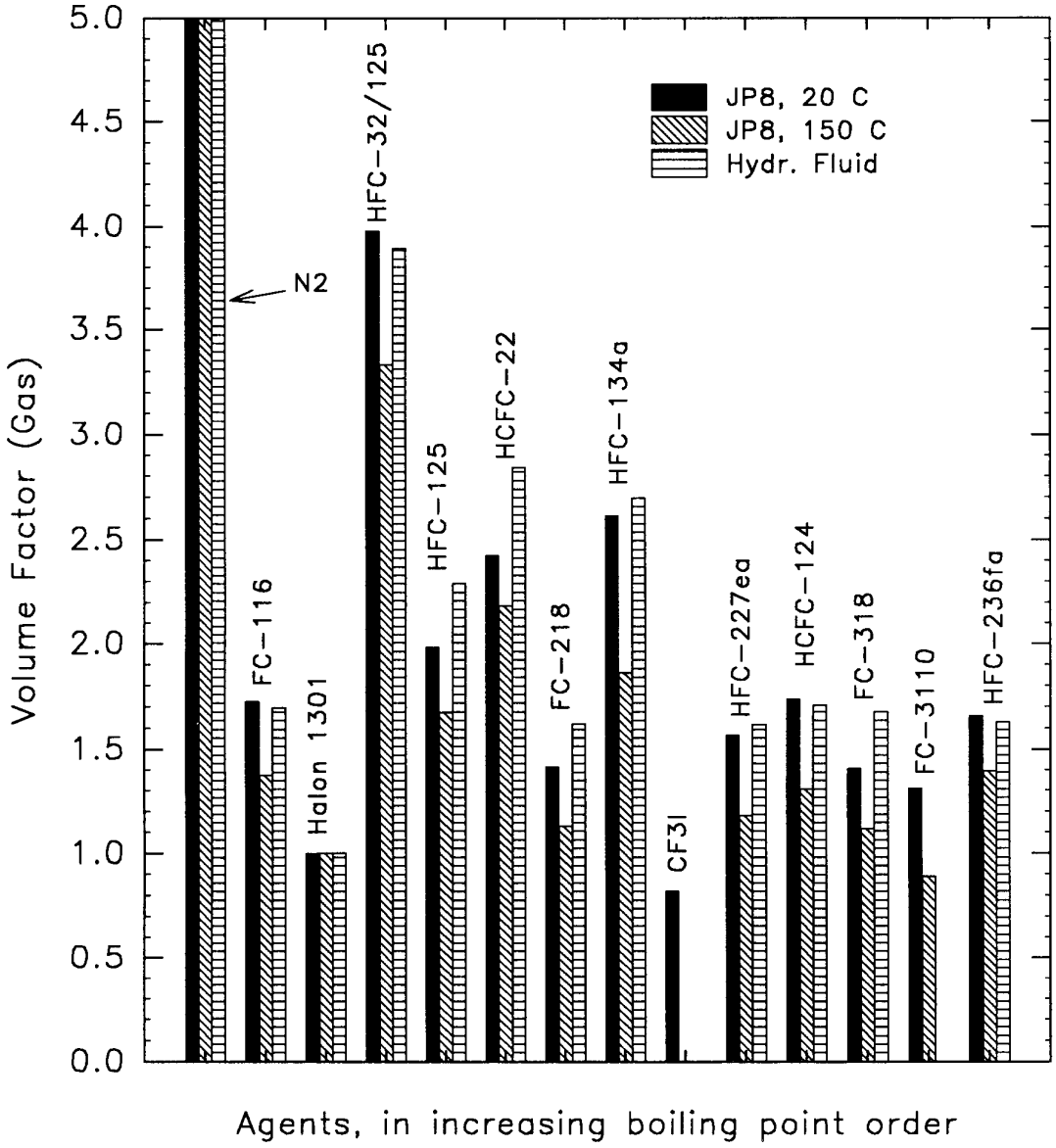

Figure 47. Dispersed gas volume factor (based upon 101 kPa and 22 °C air).

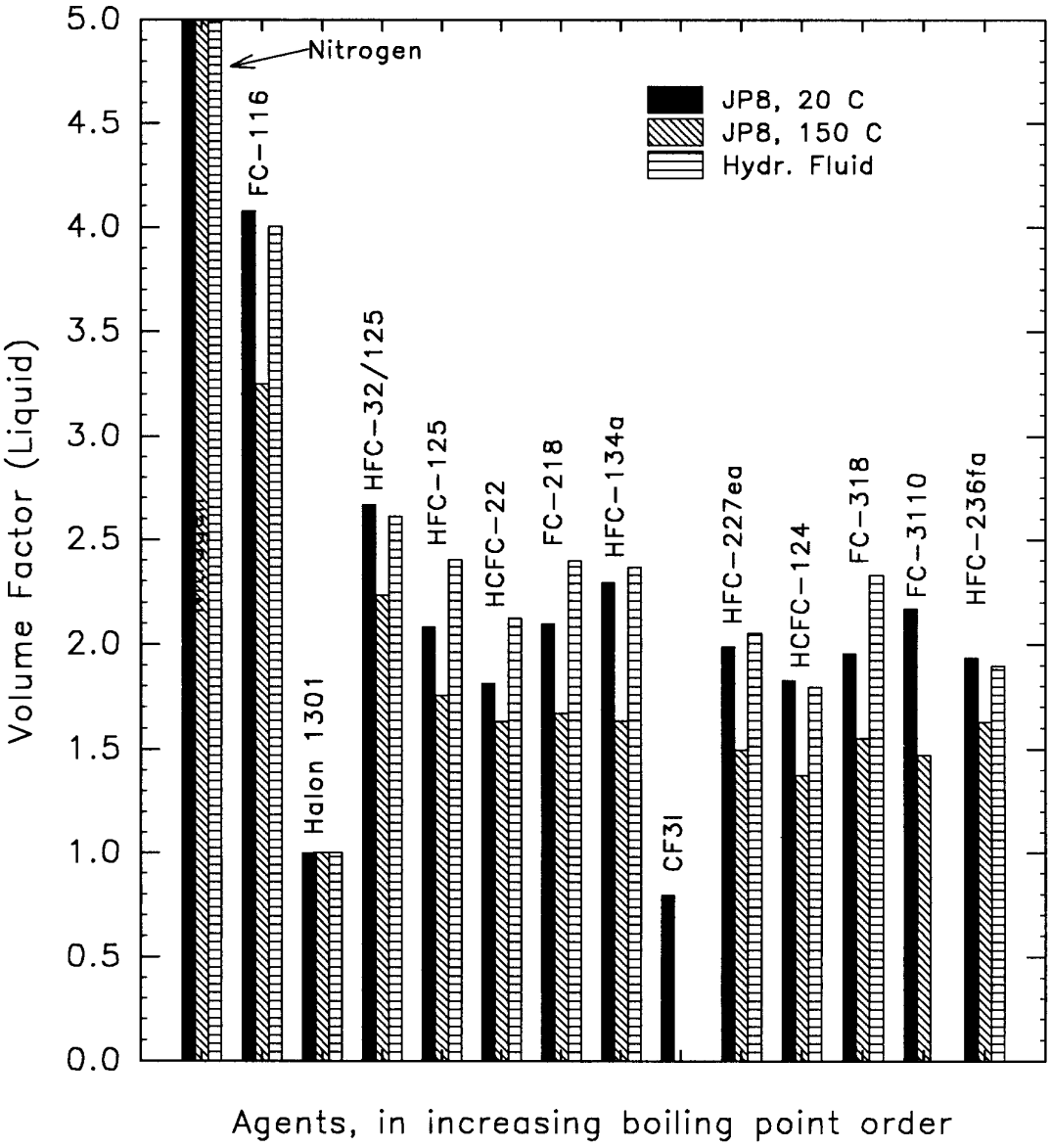

Figure 48. Storage volume factor of different agents based upon saturated liquid conditions at 20 °C.

6. The core gaseous agents all performed better in the turbulent spray burner relative to halon 1301 than was predicted from cup burner measurements. Generally speaking, about twice as much mass and volume were needed to suppress the spray flame using the core alternative agents when compared to halon 1301.

4.5 High Speed Premixed Flames and Quasi-detonations

4.5.1 Introduction. An anti-aircraft device entering a dry bay could lead to a situation in which a vaporizing fuel spray produces a combustible mixture which is then ignited by a glowing fragment. If the space were confined, the pressure would increase behind the reaction front, accelerating the flame. A transition to turbulence would likely occur as the flame encounters clutter in the dry bay. If the ventilation is insufficient to relieve the pressure build up, the possibility of a supersonic detonation would exist, leading to destructive over-pressures in the dry bay.

A supersonic flame is distinct from the flames simulated in the cup, OFDF and spray burners. As a result, the effectiveness of an agent in preventing a detonation depends upon different chemical and physical mechanisms. A shock wave precedes the supersonic flame. Obstructions in the flow promote intense mixing of the fresh reactants with the combustion products and cause the pressure waves to interact with the mixing region. Given enough distance, the flame can accelerate dramatically, increasing the temperature of the reaction zone behind the shock and further adding to the heat release rate. Depending upon the geometric details, the wave can approach its theoretical Chapman-Jouguet velocity and accompanying high pressure ratio. Even a slight variation in composition of the reactants near the limit of detonation can cause a dramatic change in the wave velocity and cause destructive pressures to be attained.

There exists an extensive literature describing the kinetics and dynamics of flame/shock wave systems formed within classical detonation tubes (*e.g.*, Lefebvre *et al.*, 1992; Nettleton, 1987; Lee, 1984; Baker *et al.*, 1983; Westbrook, 1982). Chapman and Wheeler (1926) were the first to note that a methane/air flame could be accelerated to a terminal velocity in a shorter distance within a circular tube by placing obstacles into the flow. Lee *et al.*, (1984) built on this observation to study quasi-detonations in hydrogen/air and hydrocarbon/air mixtures. A quasi-detonation propagates more slowly than a true detonation due to pressure losses in the flow, but its structure is more complex than a true detonation, and the mechanism of its propagation is not fully understood. Although an obstructed flow is more difficult to analyze than the flow in a smooth-walled tube, the complex arrangement was chosen for the current study because it more closely simulates a potentially damaging condition in the dry bay. The desire to rapidly suppress a flame and the associated pressure build up in such a situation is the primary motivation behind this study.

4.5.2 Experimental Facility. The effectiveness of a fire fighting agent in suppressing a high speed, premixed flame or quasi-detonation can be rated by the extent to which it decelerates the propagating wave and simultaneously attenuates the hazardous shock which is always ahead of the flame. Because the fire extinguishant is unlikely to be released prior to the establishment of a turbulent flame, the traditional experiment in which the flame inhibitor is premixed with the fuel and air prior to ignition (*e.g.*, Das, 1986) does not replicate the chemistry critical to the actual situation. Each dry bay on an aircraft has a different geometry, and the release of the agent once a fire is detected is highly variable. Heinonen *et al.*, (1991) injected suppressant into a chamber shortly following the ignition of a fuel spray in air, but had difficulty controlling the mixing and in duplicating the process. The

complexities and biases associated with the fluid dynamics of release can be avoided by premixing the agent with the fuel and air in a portion of the tube distinct from where the flame is initiated.

The two-section, deflagration/detonation tube shown in Figures 49 and 50 was designed to produce the desired environment for both the flame initiation and flame suppression regimes. A repeatable, uninhibited turbulent flame was fully established in the driver section, the design of which was based directly upon the work of Peraldi *et al.*, (1986). They found that a 50 mm inner diameter tube with a blockage ratio of 0.43 could be used to create repeatable, high-speed flames and quasi-detonations within the first several meters of an 18 m tube. By varying the equivalence ratio of ethene/air mixtures from 0.5 to 2.1, they were able to produce flame velocities between about 600 and 1300 m/s.

The driver section was 5 m long and was equipped at the closed end with a spark plug. This section was filled with the combustible mixture of ethene and air. The gas handling system consisted of a vacuum pumping network; pressurized gas cylinders for the fuel, oxidizer and agent; and a dual circulating pump. The ignition energy was delivered in a microexplosion of a tin droplet short-circuiting the tips of nichrome electrodes connected to an 80 V power supply. Spiral-shaped obstructions made of 6.4 mm stainless steel rods with a pitch equal to the inner diameter of the tube were inserted into the tube, to produce an area blockage ratio of 44%, close to the value shown by Lee *et al.* (1984) to promote a quasi-detonation in their facility. The second section of the deflagration/detonation tube contained the gaseous agent along with the same fuel/air mixture used in the driver section. The diameter was the same and its length was 2.5 m. An identical spiral insert was used to maintain a high level of mixing. The two sections were separated from each other by a 50 mm inner diameter, stainless steel, high vacuum gate valve, which remained closed until just before ignition.

Pressure transducers and photodiodes were located along the test section to monitor the strength and speed of the combustion wave. Their output was recorded on a multi-channel, digital storage oscilloscope. The pressure transducer mounting is depicted in Figure 51 and a schematic of the photodiode mounting is shown in Figure 52. A logic diagram of the photodiode sequencing system is shown in Figure 53.

4.5.3 Operating Procedure. The whole system was evacuated to 10^{-1} Pa before filling the two sections separately with the desired mixtures, which were attained through the method of static partial pressures. The fuel/air ratio and total pressures were held constant across the gate valve. The initial temperature was the ambient value, 22 $\pm$ 3 °C. The oxidizer used in all experiments was breathing grade air. Ethene (CP grade, 99.5% volume purity) was chosen as the fuel because it had been demonstrated (Lee *et al.*, 1984) that subsonic flames, quasi-detonations, and full detonations all could be obtained in a tube of this geometry simply by varying the stoichiometry. After filling, the gases were homogenized independently using a double, spark-free circulating pump, recirculating the entire tube volume a total of 20 times. The mixtures were left for five minutes to become quiescent. About ten seconds prior to ignition, the gate valve was opened manually.

After ignition, the flame propagated into the driver section and accelerated quickly due to the intense turbulence created by the interactions of the flow with the obstacles, generating a shock wave ahead of it. After passing through the open gate valve the flame/shock system encountered the same combustible mixture and a certain amount of agent in the test section. A rendering of the flame/shock system passing through the gate valve is shown in Figure 54. Depending on the concentration of the agent, the flame was or was not extinguished and the pressure wave attenuated.

Experiments using 5% ethene in air mixtures were run under a variety of conditions to assess the operation of the system. Figure 55 is an example of the pressure trace when the N_2 partial pressure is (a) insufficient to extinguish the flame radiation, and (b) sufficient for suppression of an air/ethene

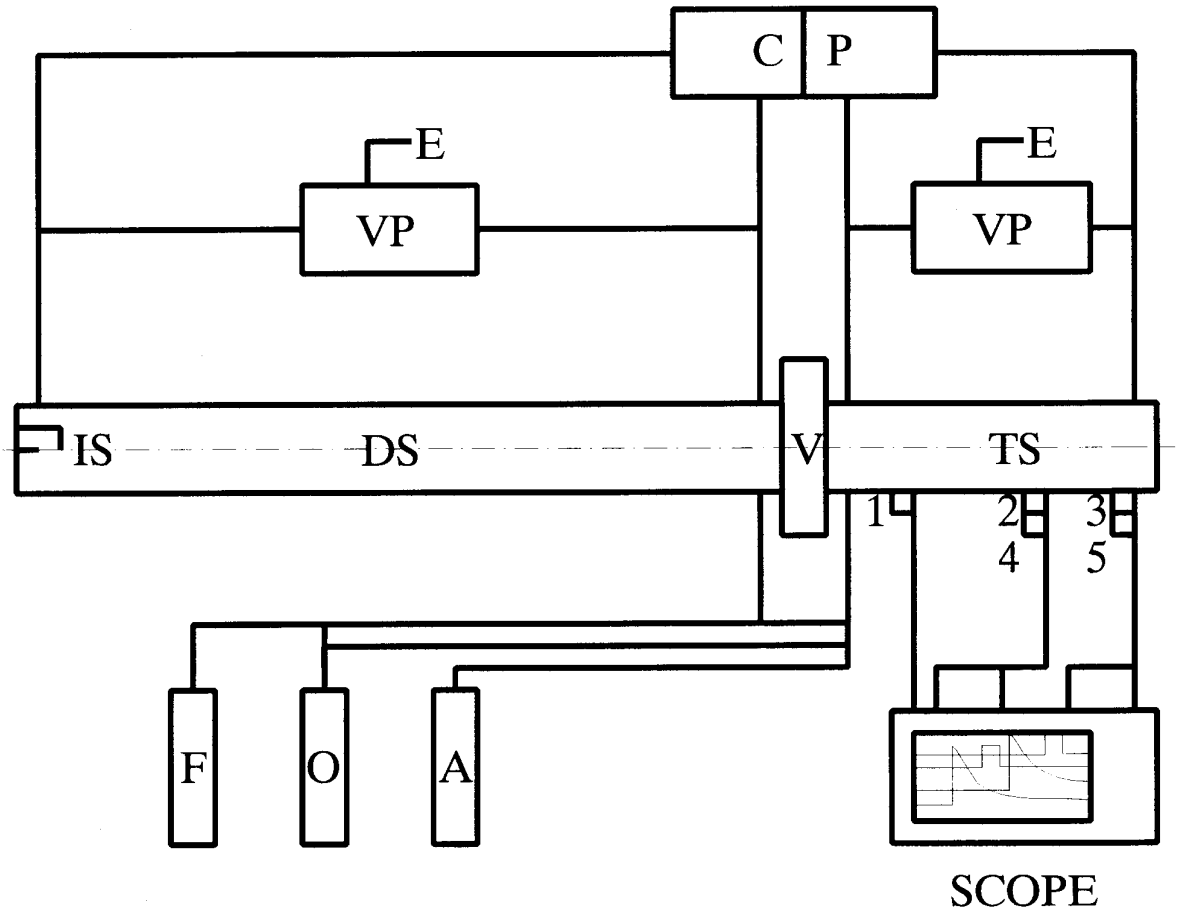

DS - Driver Section, TS - Test Section, V - High Vacuum Gate Valve, IS - Ignition Source, CP - Dual Circulating Pump, VP - Rotary Vacuum Pump, E - Exhaust, F - Fuel, O - Oxidizer, A - Agent, 1 - Triggering Transducer, 2,3 - Piezo-electric Pressure Transducers, 4,5 - Fast Photodiodes, SCOPE - Collects Four Pressure and Visible Radiation Signals

Figure 49. Schematic diagram of detonation/deflagration tube facility.

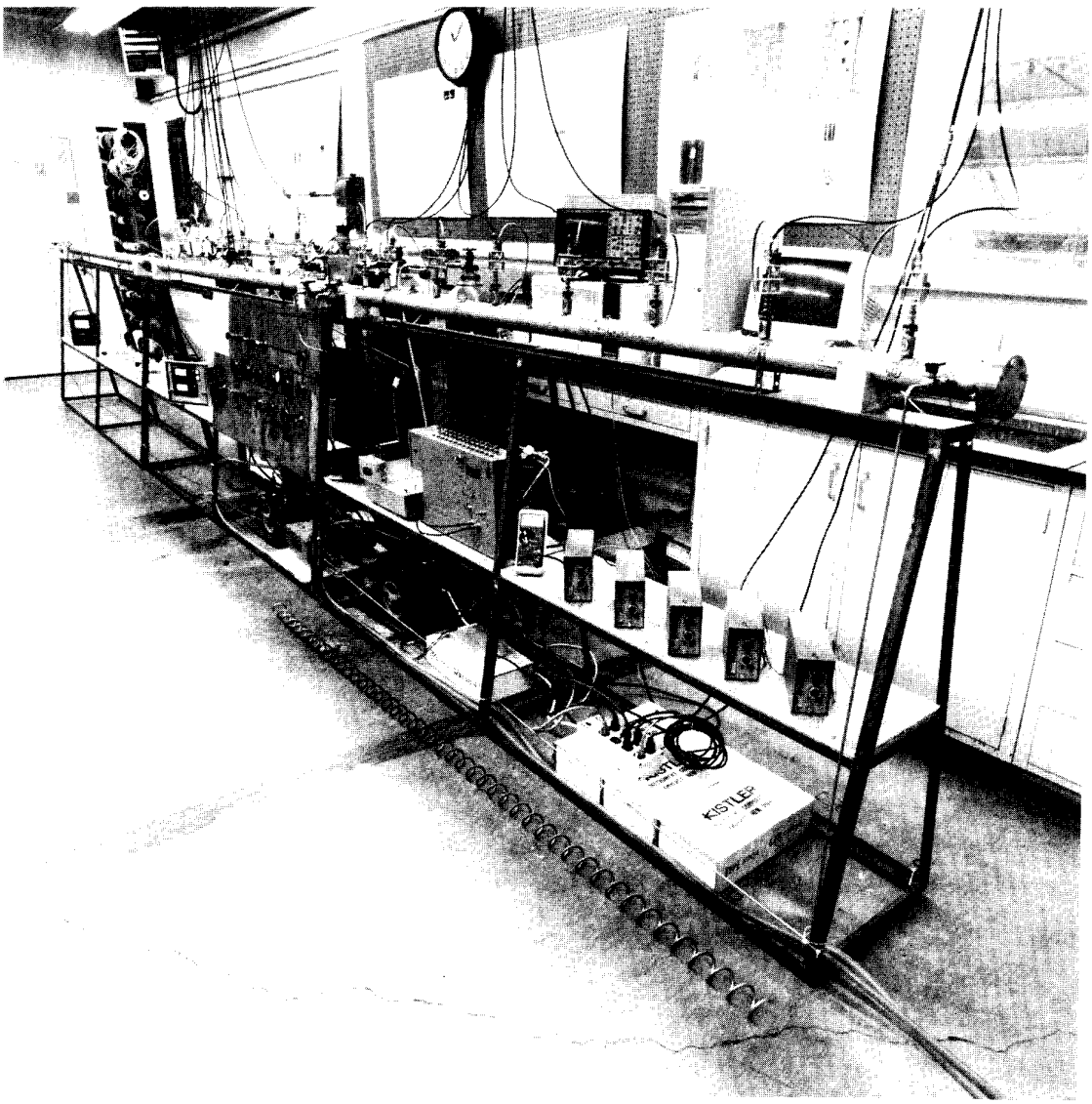

Figure 50. Photograph of detonation/deflagration tube facility.

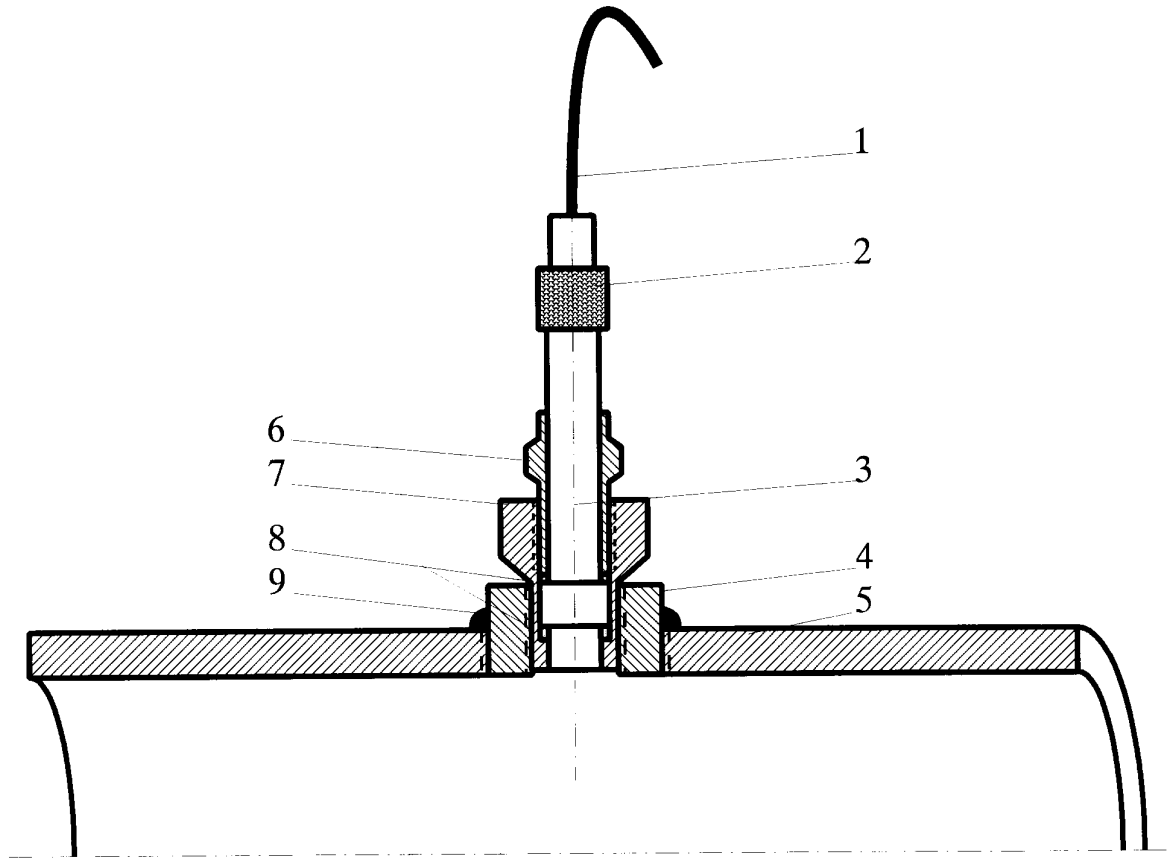

1 - Low-noise Cable, 2 - Cable Connector, 3 - Piezo-electric Pressure Transducer, 4 - Stub, 5 - Tube, 6 - Retaining Nut, 7 - Holder, 8 - Seals, 9 - Seal Weld

Figure 51. Pressure transducer mounting.

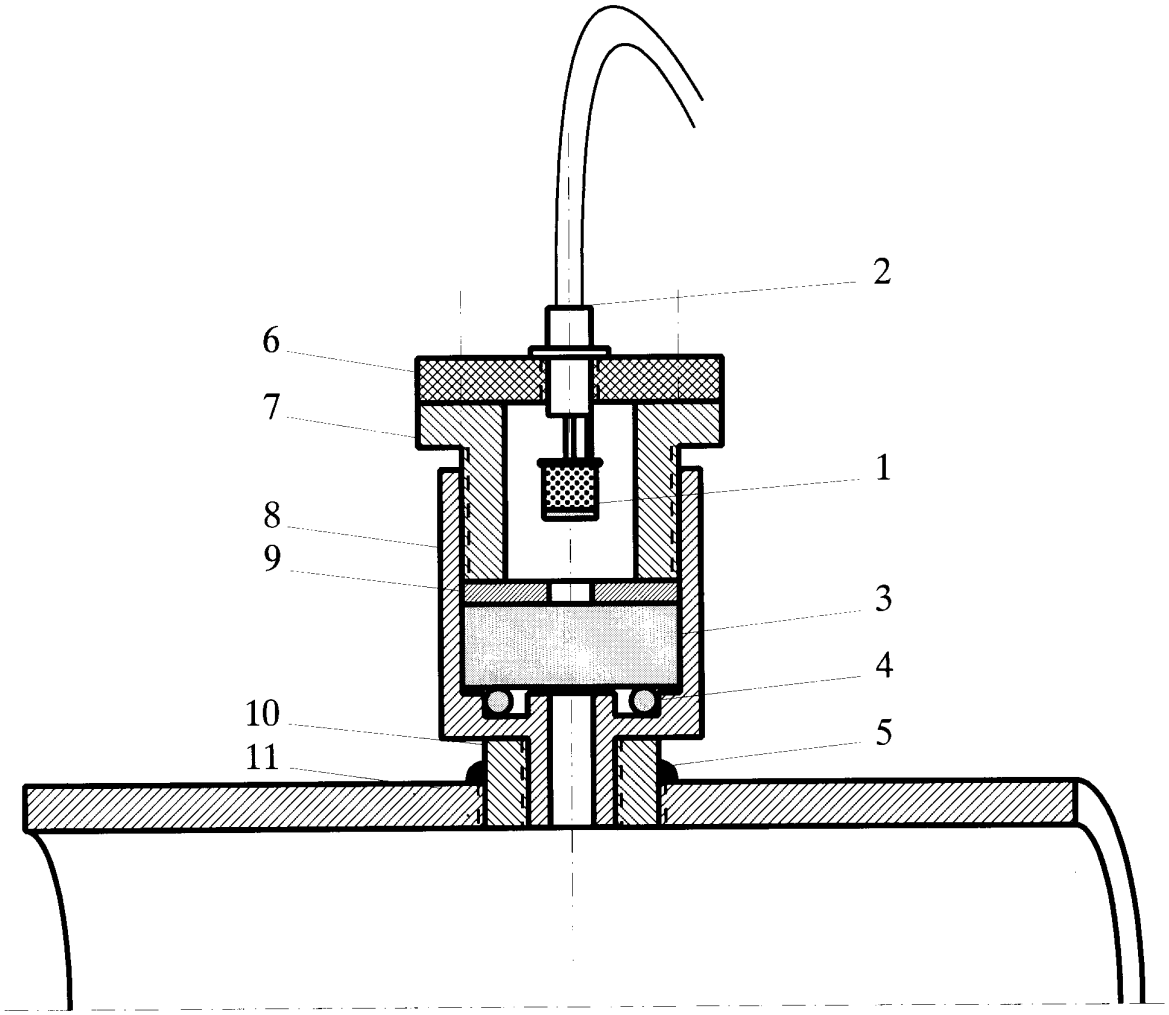

1 - Fast Photodiode, 2 - BNC Cable, 3 - Quartz Window,
4 - "O" Ring, 5 - Seal Weld, 6 - Plexiglas Cover, 7 - Barrel,
8 - Holder, 9 - Washer, 10 - Stub, 11 - Tube

Figure 52. Photodiode mounting.

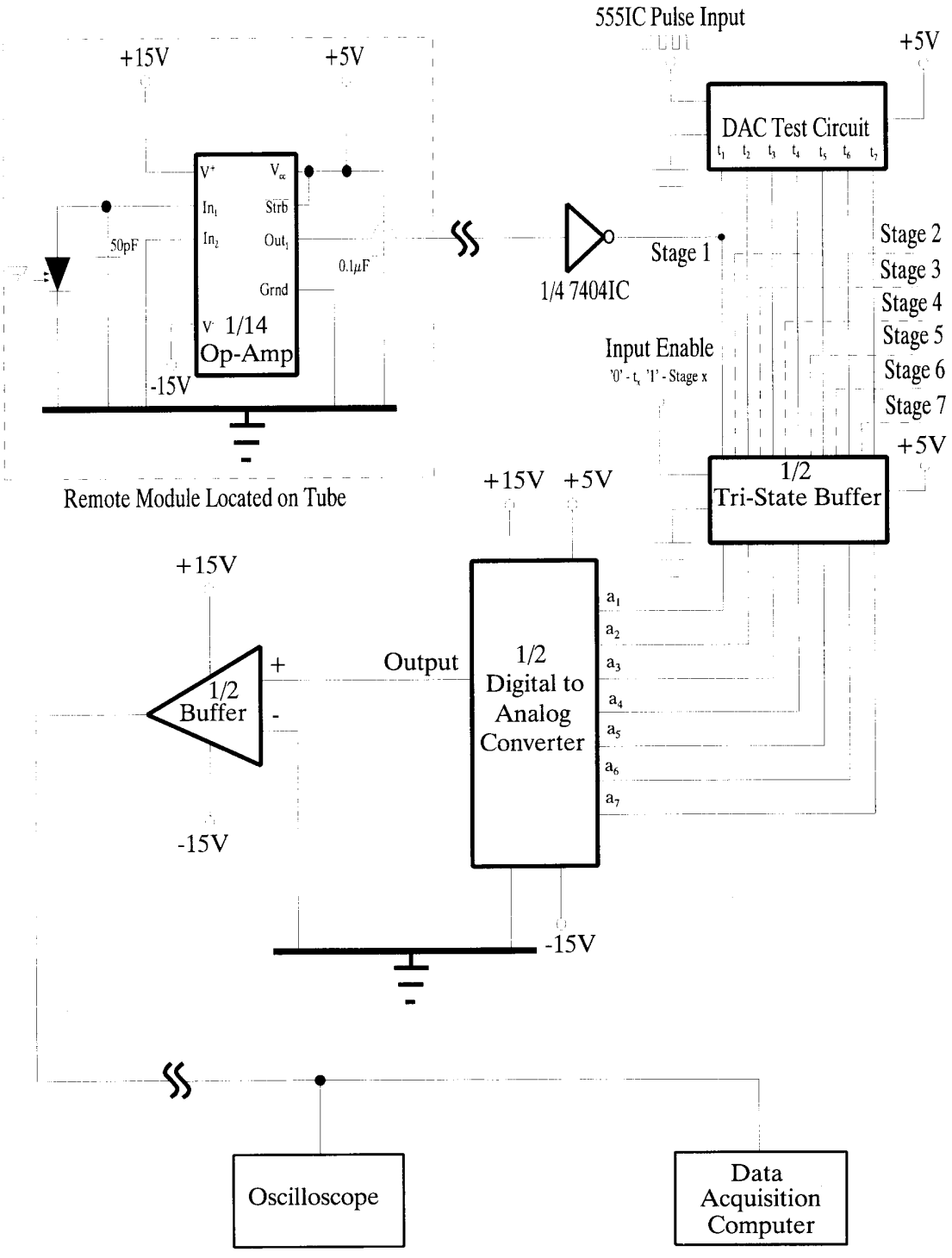

Figure 53. Logic diagram of photodiode sequencing system.

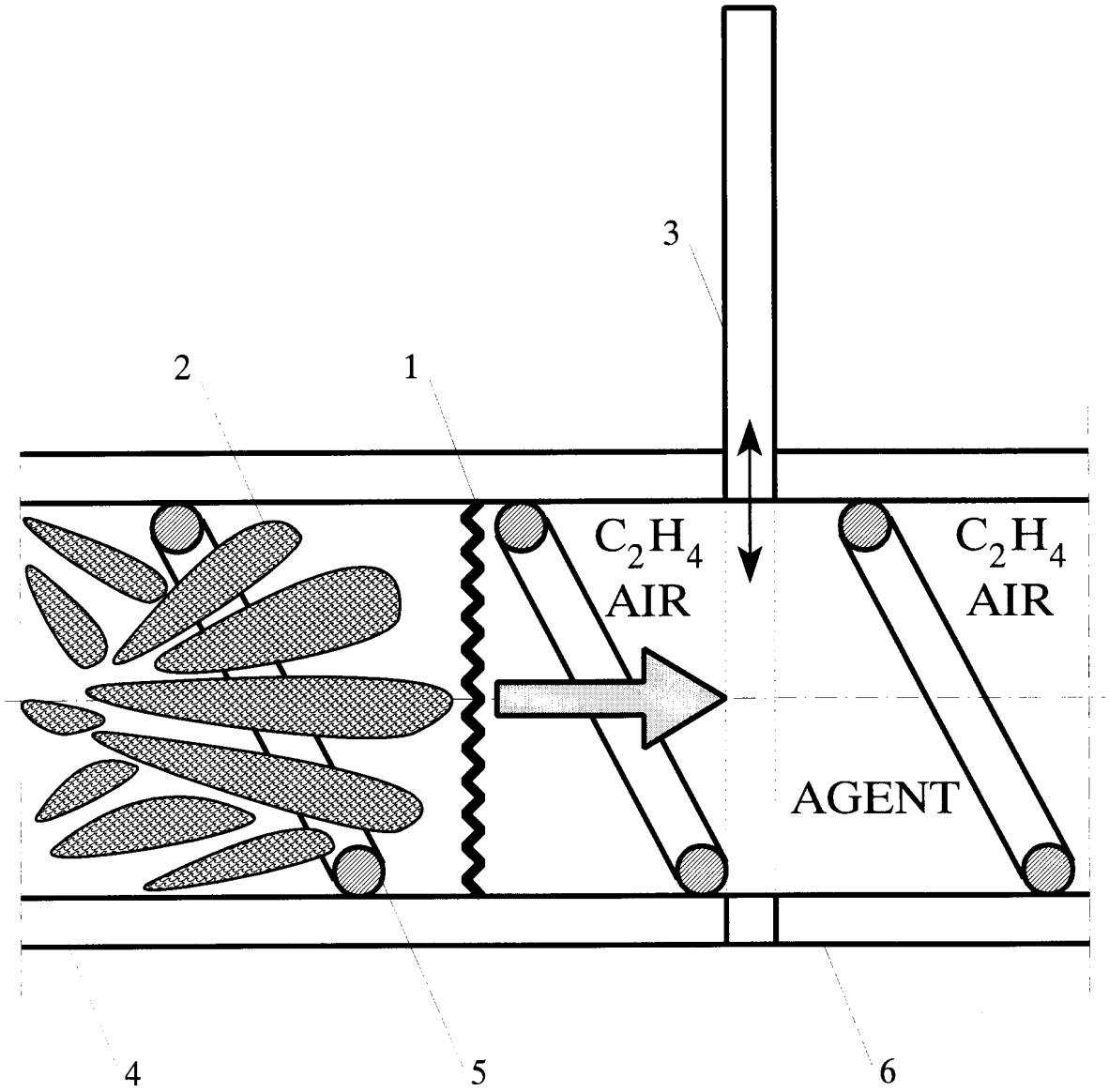

1 - Shock Wave, 2 - Turbulent Premixed Flame, 3 - Gate Valve,
4 - Driver Section, 5 - Spiral Obstruction, 6 - Test Section

Figure 54. Rendering of high-speed turbulent flame entering test section.

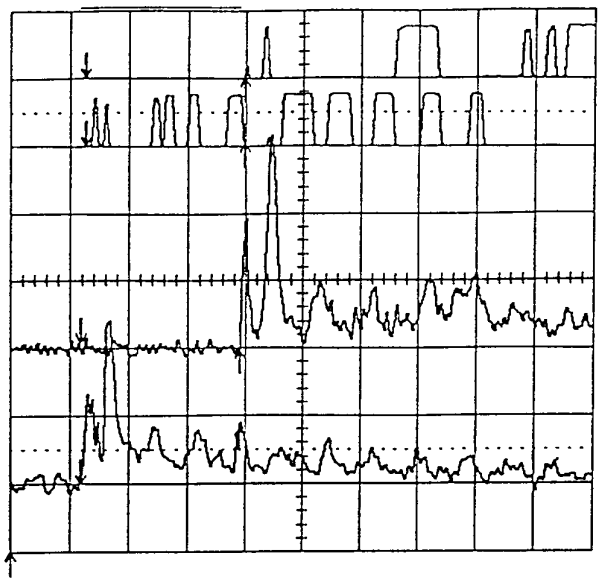

a)

1% vol. C_4F_{10}

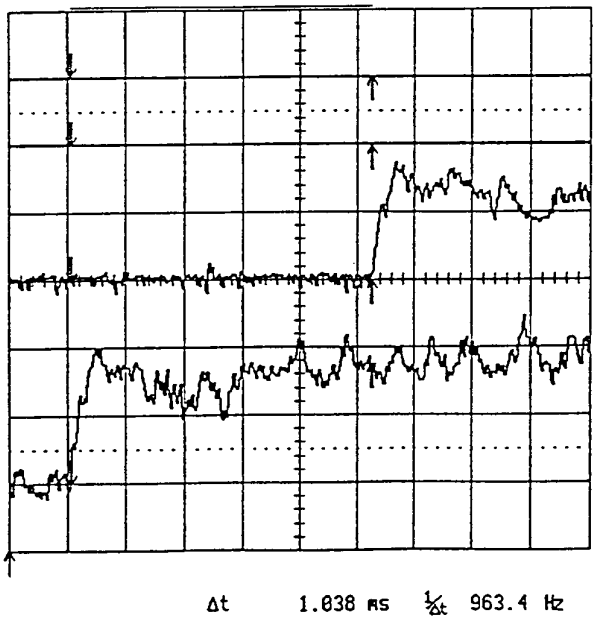

b)

10% vol. C_4F_{10}

Figure 55. Pressure traces comparing (a) non-suppressed and (b) suppressed flames using FC-31-10.

mixture at a total pressure of 100 kPa. Knowing the distance between the two pressure transducers, the shock speed was determined from the time lag between the pressure rises. The pressure ratio was tabulated from the initial pressure in the tube and either the first peak or the maximum pressure increase. The sensitivity of the flame speed and pressure ratio to the voltage of the ignition system, the mixing time of the components before ignition, the presence or absence of the gate valve, the speed of opening the gate valve, and cleaning the tube between runs were all investigated.

Experiments were conducted with 100% nitrogen in the test section, a 5% ethene in air mixture in the driver section, and the total pressure equal to 20, 50 and 100 kPa. The incident shock wave velocity measured 2.2 m beyond the gate valve and 0.3 m from the end of the tube was 420 $\pm$ 8 m/s at all three total pressures. The pressure ratio based upon the initial pressure rise was 2.5 $\pm$ 0.5, and about 3.0 $\pm$ 1.0 based upon the peak increase.

As can be seen in Figure 56, no significant changes in shock speed occurred for a partial pressure fraction (which is approximately equal to the mole fraction) of nitrogen in air greater than 40%. The region of no change was extended down to 30% for the 20 kPa case. When no suppressing nitrogen was added to the test section the shock velocities attained values of 780 and 1170 m/s, respectively, for the 20 kPa and 100 kPa experiments. The pressure ratio based upon the initial rise is plotted in Figure 57. P_1/P_0 increased dramatically at the same point as the velocity when the partial pressure of nitrogen was decreased, reaching maxima of 26 and 18, respectively, for the 20 kPa and 100 kPa initial conditions when no nitrogen was added to the ethene/air mixture. The peak pressure ratio, which normally did not correspond to the initial pressure pulse, exceeded 50:1 for the 20 kPa and 50 kPa experiments. The 100 kPa experiments generated peak pressure ratios around 30:1.

The results of the preliminary parameter assessment led to an experimental protocol which yielded flame speeds which were reproducible from run to run within about $\pm$ 2%. Pressures downstream of the shockwave had a higher variability ($\pm$ 20%) because of the complex shock structures created by interactions with the spiral rod inserts.

4.5.5 Results and Analysis. Mach number and pressure ratio were the two dependent parameters which were measured as a means to characterize the extent of flame suppression. The Mach number was based upon the time it took for the pressure wave to travel the distance between the two pressure transducers, normalized by the sonic velocity of the reactant gases in the test section. The pressure ratio was evaluated from the average amplitude of the first pressure pulse to be recorded by each transducer, normalized by the initial pressure. Consecutive pressure jumps occurred, as can be seen in Figure 55, indicating that localized explosions in the mixing region between the spirals were present. Individual runs were concluded before the shock wave reflected from the end plate arrived back at the pressure transducers. The distance between the leading shock wave and the flame front was measured in some of the experiments from the time lag between the photodiode and pressure transducer response at the same location. The primary independent variables were agent type and concentration. The fuel/air equivalence ratio and the system absolute pressure were also varied for a number of agent experiments.

Table 13 summarizes the results with no suppressant in the test section, and compares the Mach number, pressure ratio, and flame spacing to the situation in a "fully suppressed" flame, in which pure nitrogen was located in the test section. Note that neither the Mach number nor pressure ratio go to zero for the fully suppressed case because total dissipation of the shock wave would require a substantially longer tube. On the other hand, the flame radiation disappears entirely; hence, the infinite separation distance.

The bromine atom in CF_3Br is known to inhibit laminar flames by scavenging active radicals from the chain-branching reactions. Experiments using halon 1301 were run to compare to an

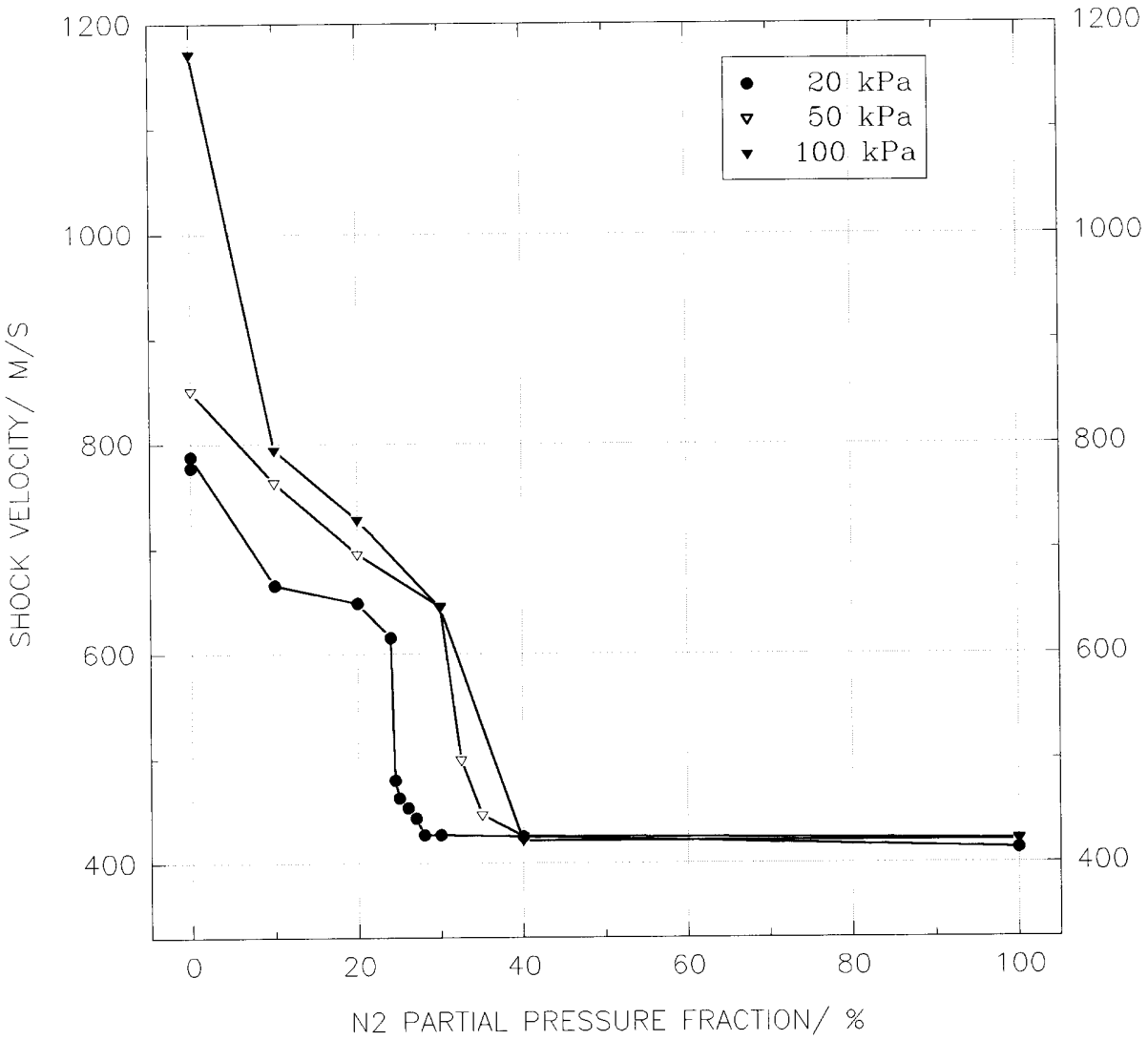

Figure 56. Effect of initial pressure on the reduction of shock wave velocity by nitrogen.

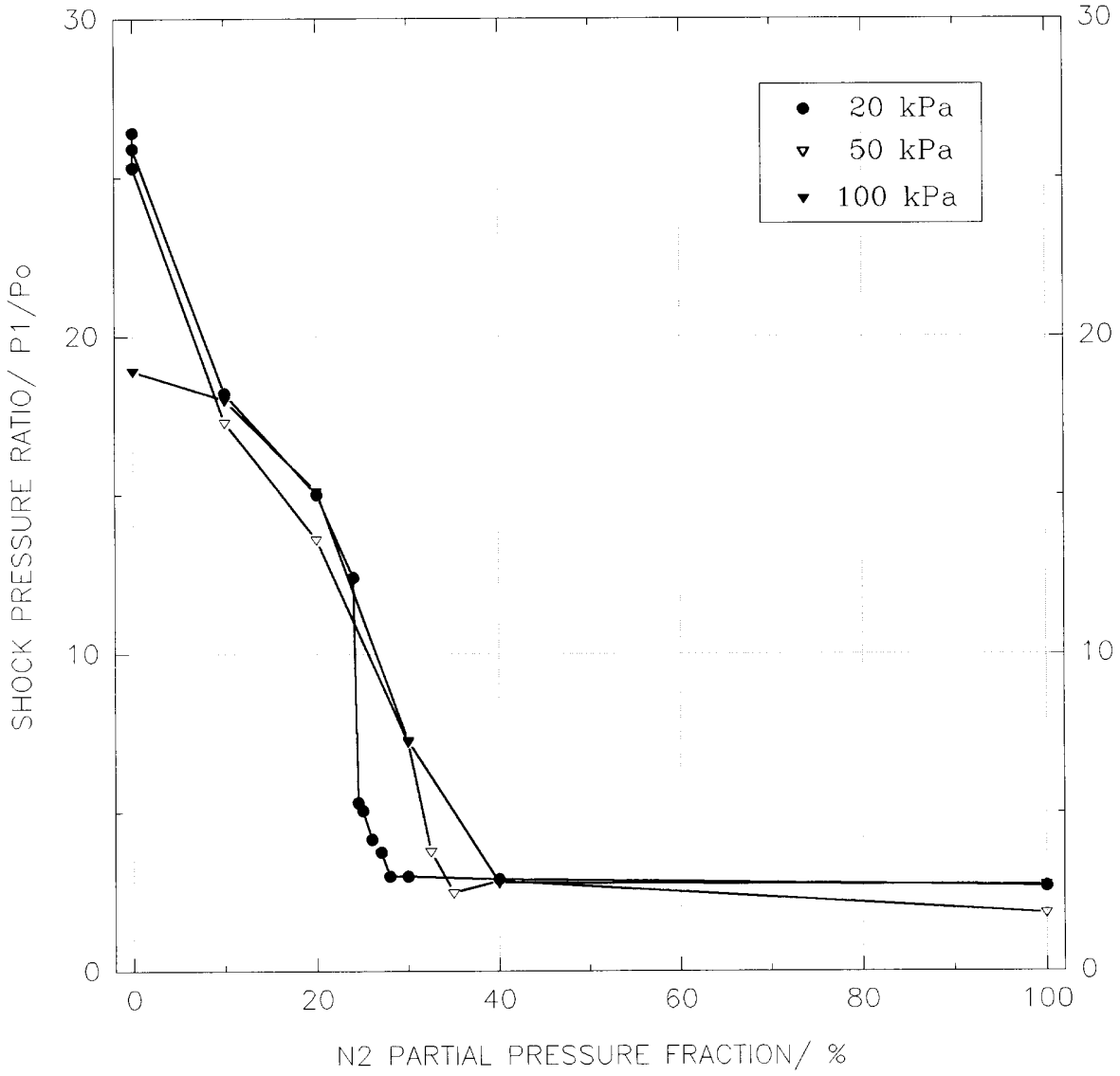

Figure 57. Effect of initial pressure on the reduction in pressure ratio by nitrogen.

Table 13. Summary of flame parameters for ethene/air mixtures under suppression extremes

Amount of N_2 added to Test Section	Initial Pressure	Equivalence Ratio	Mach Number	Pressure Ratio	Flame/Shock Separation Distance, mm
0%	20 kPa	0.75	2.4 ± 0.1	26 ± 1	[a]
	50 kPa	0.75	2.6 ± 0.1	26 ± 1	[a]
	100 kPa	0.75	3.4 ± 0.1	18 ± 2	3 ± 1
	100 kPa	1.00	4.1 ± 0.1	26 ± 2	2 ± 1
	100 kPa	1.25	4.5 ± 0.1	35 ± 3	[a]
100%	20 kPa	0.75	1.25 ± 0.05	2.5 ± 0.5	∞
	50 kPa	0.75	1.25 ± 0.05	2.0 ± 0.5	∞
	100 kPa	0.75	1.25 ± 0.05	2.5 ± 0.5	∞
	100 kPa	1.00	1.3 ± 0.1	3.5 ± 0.5	∞

[a] quantity not measured

inerting agent like N_2, and to determine the suitability of the facility for assessing the effectiveness of a wide range of agents for suppressing high speed turbulent flames and detonations. Figures 58 and 59 show the shock Mach numbers and the respective pressure ratios measured at three different total pressures as a function of the partial pressure fraction of CF_3Br in the test section. The largest effect of total pressure occurred between 50 and 100 kPa for halon, compared to between 20 and 50 kPa for N_2. Halon 1301 suppressed the flame at a partial pressure fraction of 10% to the same extent as if the test section had been completely filled with nitrogen. An unusual behavior occurred in the 100 kPa experiments when the concentration was between 2% and 3%. Both the Mach number and pressure ratio increased with the amount of CF_3Br, followed by the expected decrease for large concentrations. The reversal, while small, was greater than the uncertainty in the data.

Halocarbons, unlike nitrogen, are known to promote the production of soot. To determine the sensitivity of the shock velocity to soot contamination, a series of experiments with a 5% ethene/air mixture at a total pressure of 20 kPa was run for CF_3Br partial pressure fractions between 0 and 10% with and without cleaning the tube and spirals in the test section. The performance was similar, with the maximum deviation between the cleaned and uncleaned results amounting to less than 35 m/s.

4.5.5.1 Lean Mixtures at 100 kPa. Attenuation of the shock speed and pressure increase by the core agents and CF_3I was measured with the ethene/air equivalence ratio fixed at 0.75 (5.0% by volume C_2H_4), an initial absolute pressure of 100 kPa, and an initial temperature of 22 °C. It was found that the amplitude and speed of the pressure wave, and the speed of the trailing flame, were all strongly dependent on the agent type and concentration. The flame always followed the shock wave in such a way that both speeds were equal. However, when the amount of the agent in the mixture was increased, the distance between the shock and flame increased as well, up to around 100 mm as

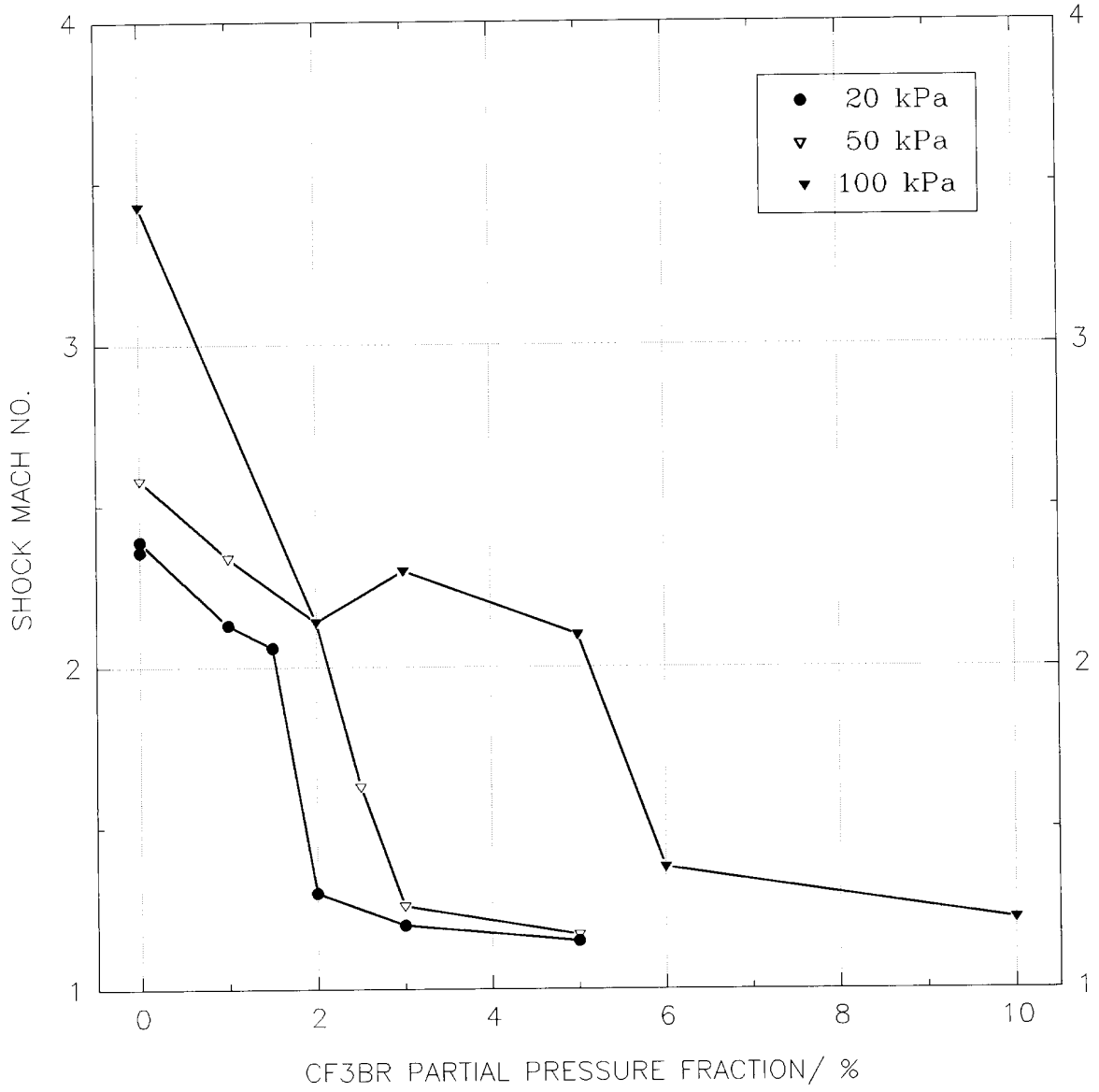

Figure 58. Effect of initial pressure on the reduction in shock wave Mach number by CF_3Br.

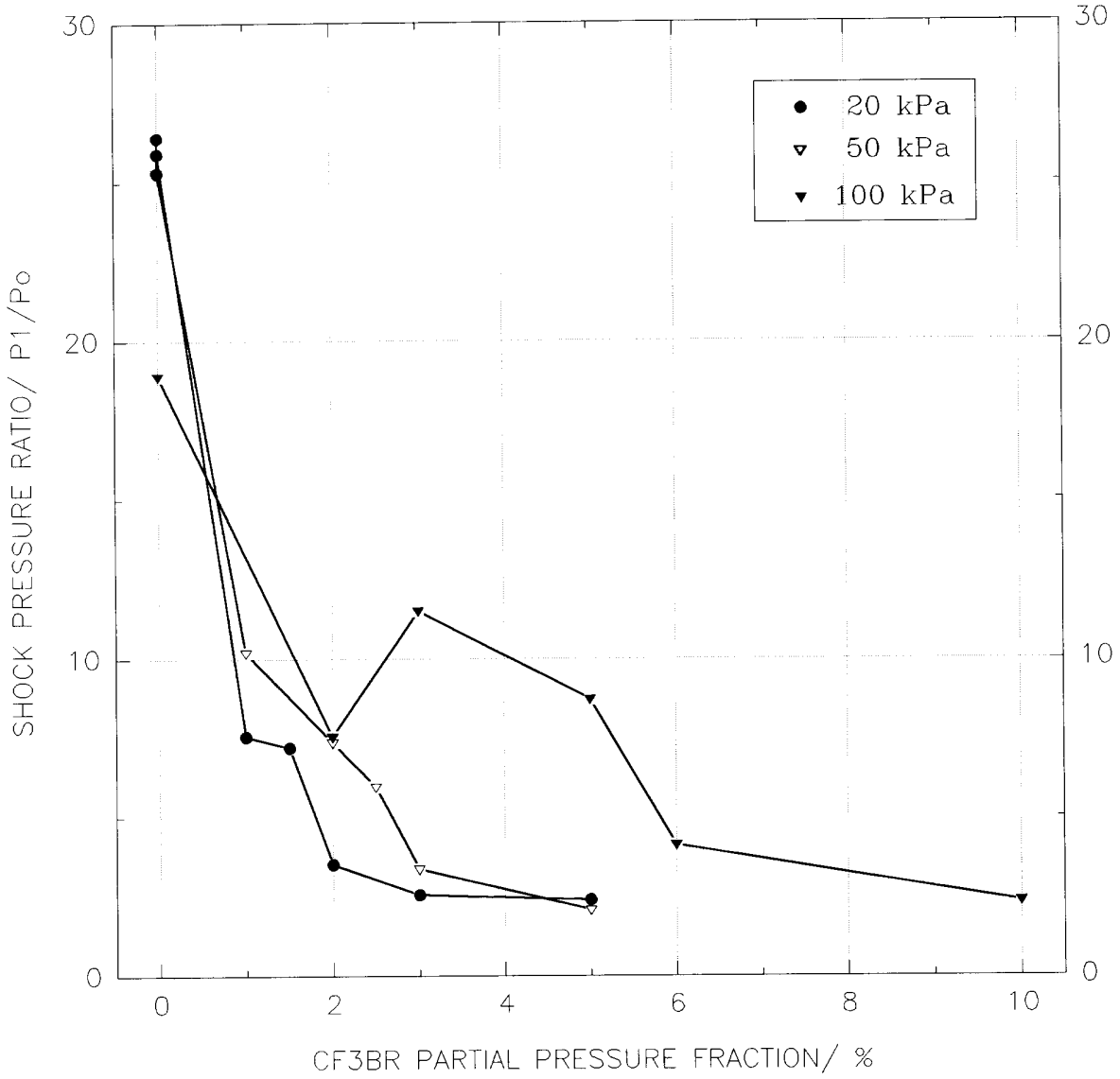

Figure 59. Effect of initial pressure on the reduction in pressure ratio by CF_3Br.

full suppression was approached. At the extinguishing concentration the radiation disappeared, which indicated the absence of the flame. In that situation the pressure wave amplitude was attenuated by a factor of eight and the wave speed by a factor of three, similar to the results for nitrogen (see Table 13).

The results for all the alternative agents are compared in Figures 60-63. The amount of agent is expressed both as a mass fraction and as a partial pressure fraction. The Mach numbers and pressure ratios at zero represent the pure combustible mixture with no flame suppressing agent present. One can see that the concentrations necessary for total extinguishment for all the compounds are between 40 and 50% by mass. However, at low concentrations the Mach numbers and pressure ratios are higher for some agents than even the value for the pure combustible mixture. Because of the sheer number of data, it is instructive to examine the results by the class of compound; *i.e.*, FCs, HFCs, HCFCs and the IFC (CF_3I).

The FCs, as a class, were generally the best performers on both a partial pressure and mass fraction basis. In fact, FC-116 was superior to CF_3Br, and FC-318 was about equivalent. FC-218 and FC-31-10 slightly enhanced the pressure ratio in low concentration. This can be seen in Figures 64 and 65. FC-218 reduced the pressure ratio to less than 5:1 at a mass fraction of 0.29, which was better than with CF_3Br.

Adding hydrogen to the molecule had a significant effect on the performance of the HFCs, shown in Figures 66 and 67. The HFC-32/125 mixture produced peak pressures more than double the value for no suppressant. The Mach number was increased to its highest value of 4.1 when the mass fraction was 11%. It wasn't until the mass fraction exceeded 38% that the HFC-32/125 mixture became as effective as nitrogen in reducing the speed and pressure build-up of the shock wave. The two fluoropropanes, HFC-227ea and HFC-236fa produced the lowest pressure build-up of the HFCs and did a good job of suppressing the shock speed.

The chlorine atom in the two HCFCs created an additional complexity because chlorine is a strong oxidizer. From Figure 68, one can see that HCFC-22 was the least effective on a mass basis of all of the agents in fully suppressing the combustion wave Mach number, requiring a mass fraction of over 50% in the test section. The maximum pressure ratio for HCFC-124 was 32:1 at a 23% mass fraction (see Figure 69), which was exceeded only by HFC-125 and the HFC-32/125 mixture (Figure 67).

The one IFC tested was CF_3I. The Mach number and pressure build-up, shown in Figure 70, were cut about in half with partial pressure fractions in the test section of only 15 to 20%. None of the other chemicals, including CF_3Br, was able to accomplish that. Unfortunately, when the mass fraction was increased to 30%, the Mach number shot back up and the pressure ratio attained a value of 21:1, which was greater than when no CF_3I was present. This reversal, which was slight in the bromine-containing halon 1301, changed what at first appeared to be the most effective suppressing agent into one of the least effective agents. It is known that iodine atoms can cause a catalytic effect in some reactions by lowering the overall activation energy. At intermediate concentrations the possibility also exists that the iodine (and bromine) recombined, reducing their impact on the combustion process. It is not out of the question that in the cases under consideration both of these effects became important.

4.5.5.2 Stoichiometric Mixtures. Changing the fuel/air mixture (*i.e.*, the equivalence ratio) changes the flame temperature and radical concentration significantly. Figure 71 demonstrates the impact of equivalence ratio on the shock Mach number and pressure ratio with no agent in the test section. To see if the relative performance of the agents was dependent upon the fuel/air ratio a number of experiments were run under stoichiometric conditions. The equivalence ratio was based upon the amount of ethene in the mixture and was not adjusted to account for the contribution of the

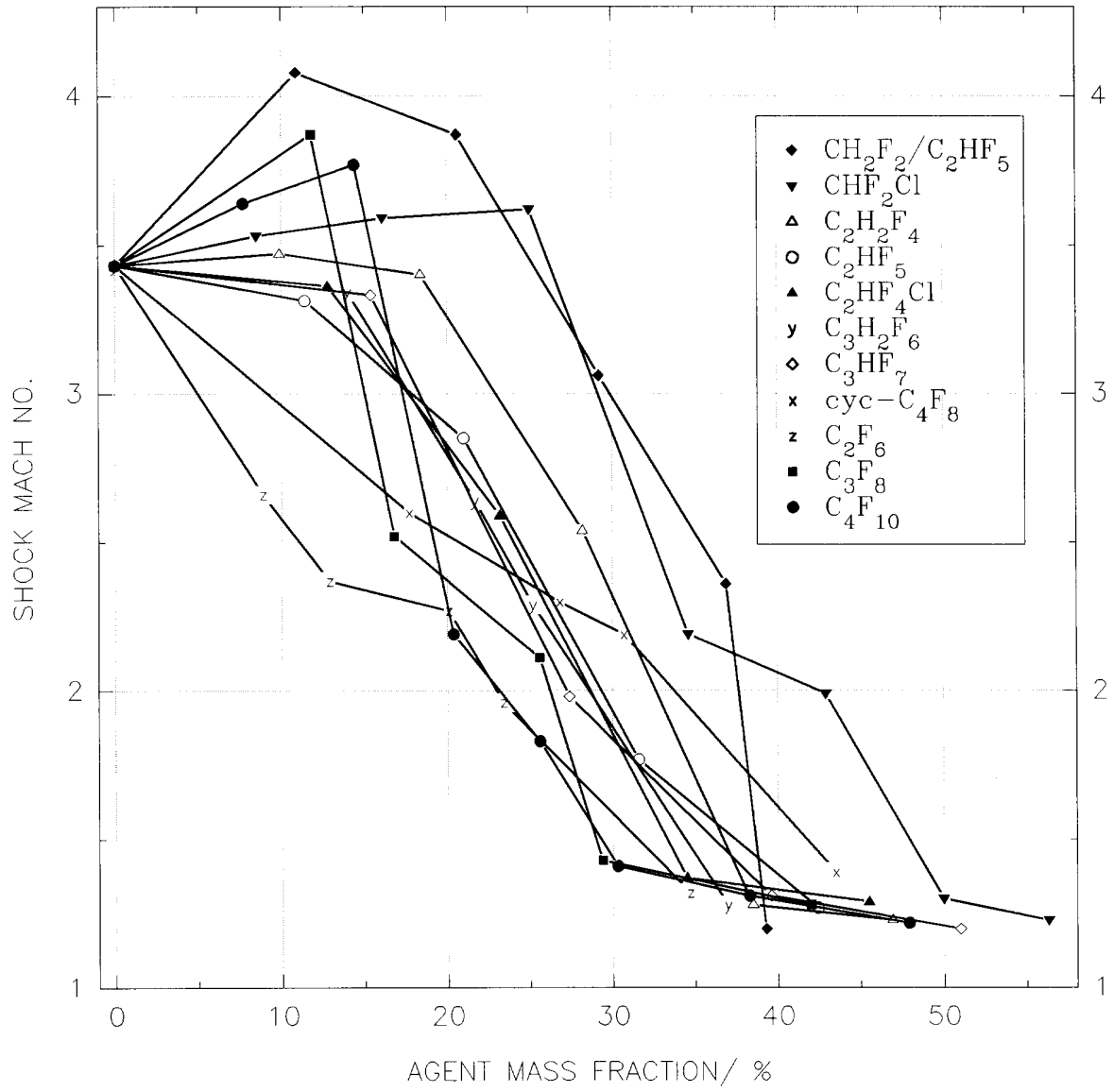

Figure 60. Reduction in shock Mach number as a function of mass fraction for all agents tested.

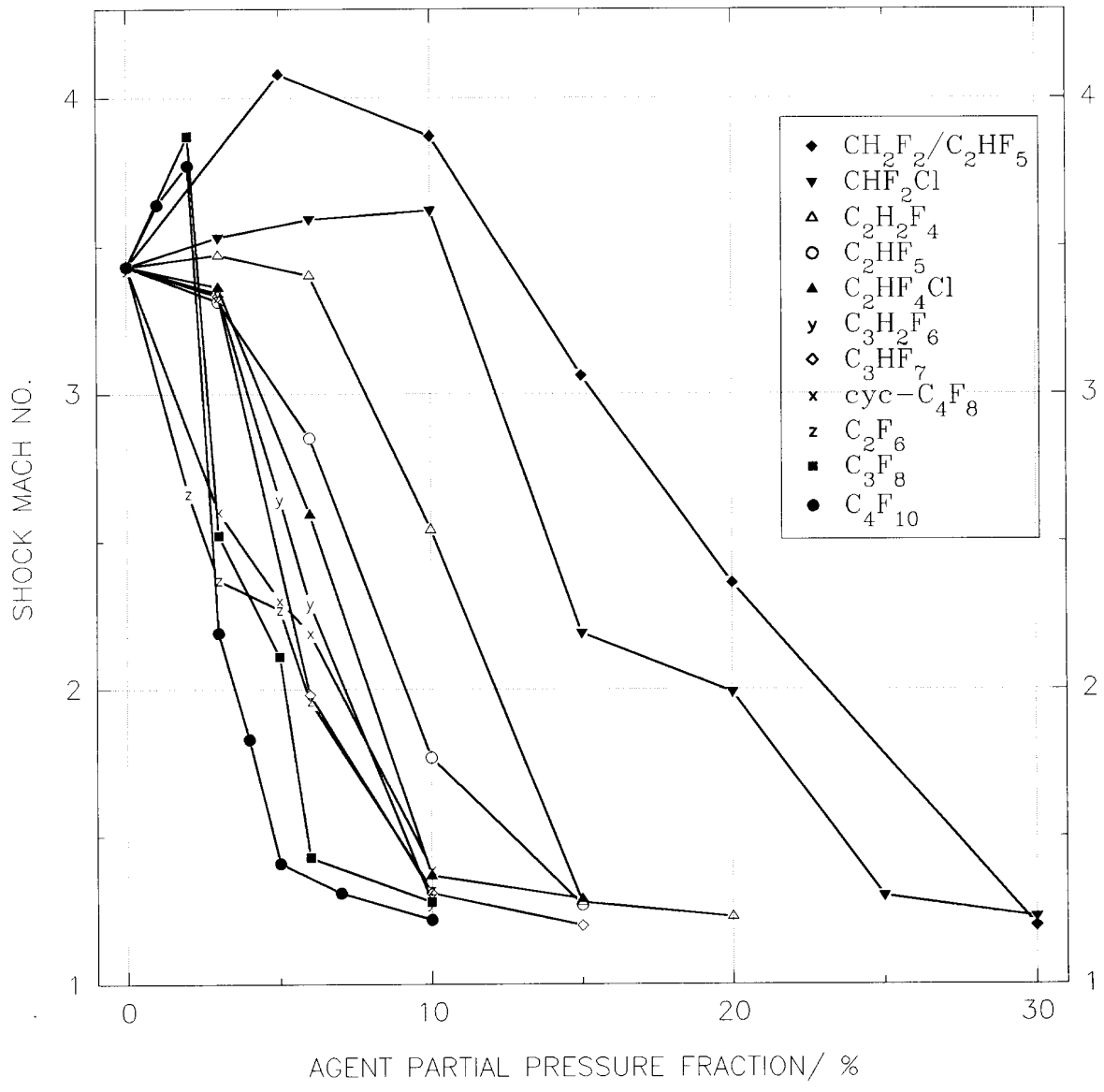

Figure 61. Reduction in shock Mach number as function of partial pressure for all agents tested.

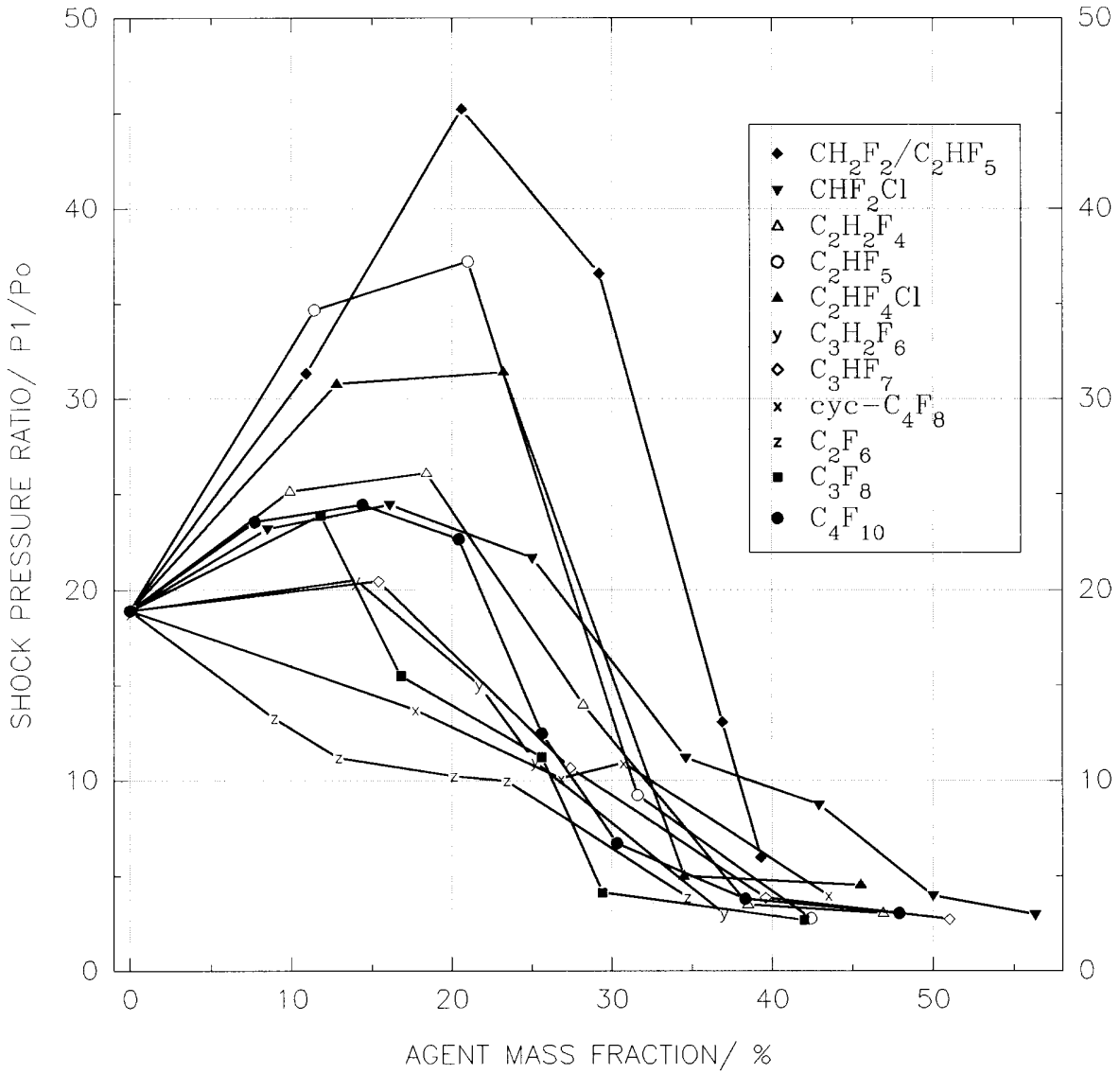

Figure 62. Reduction in pressure ratio as a function of mass fraction for all agents tested.

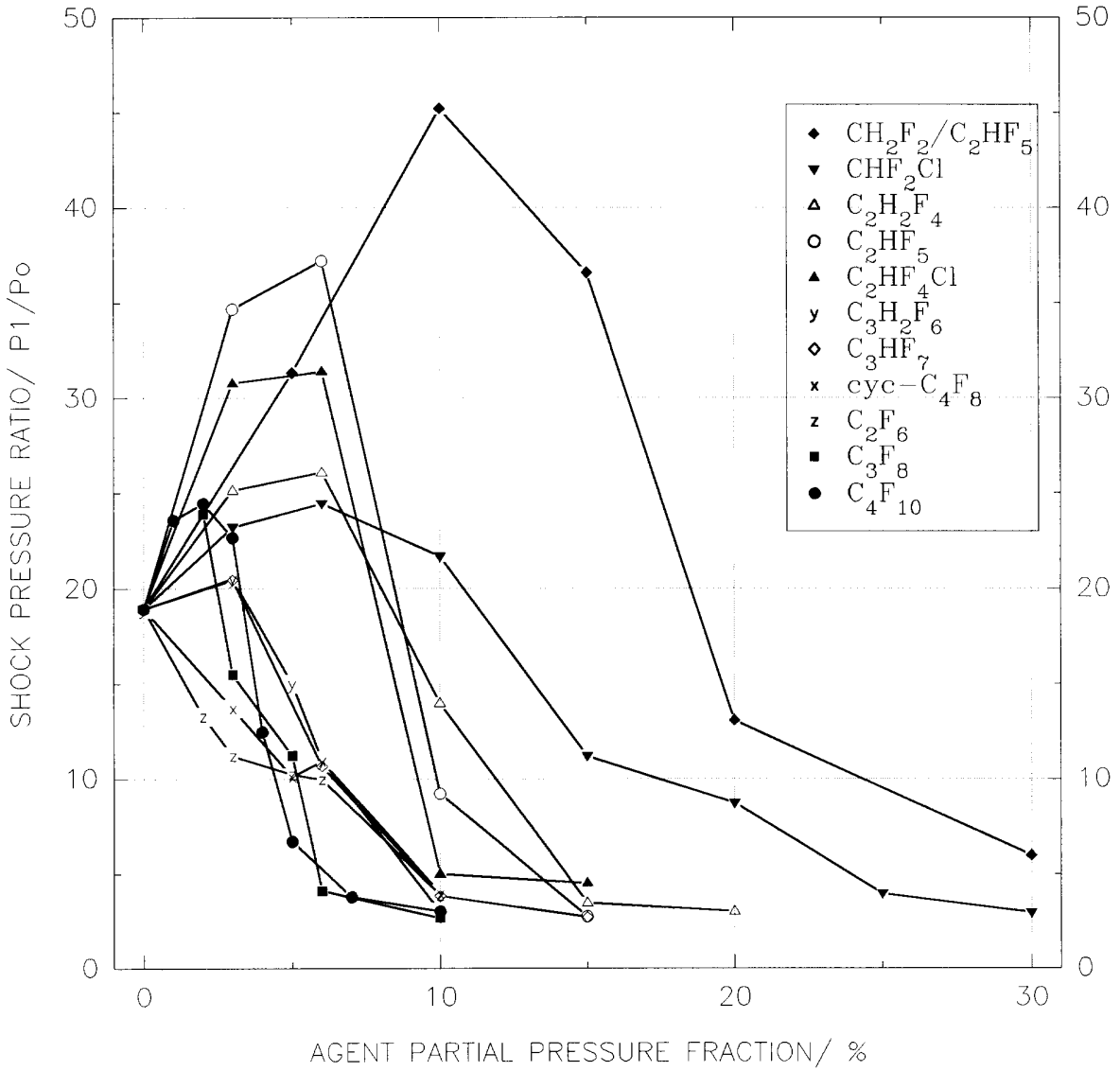

Figure 63. Reduction in pressure ratio as a function of partial pressure for all agents tested.

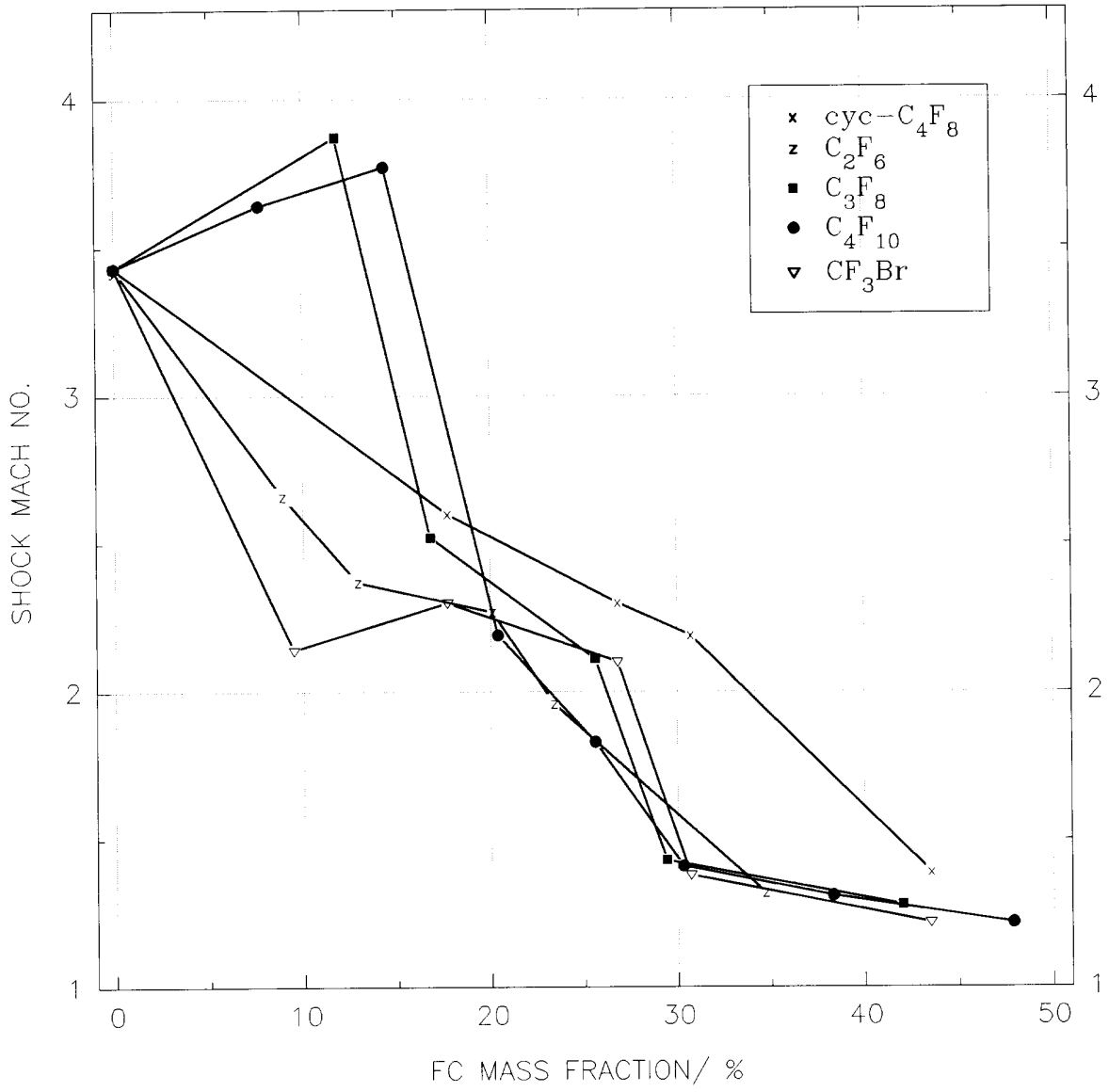

Figure 64. Reduction in shock Mach number vs mass fraction of FCs compared to CF_3Br.

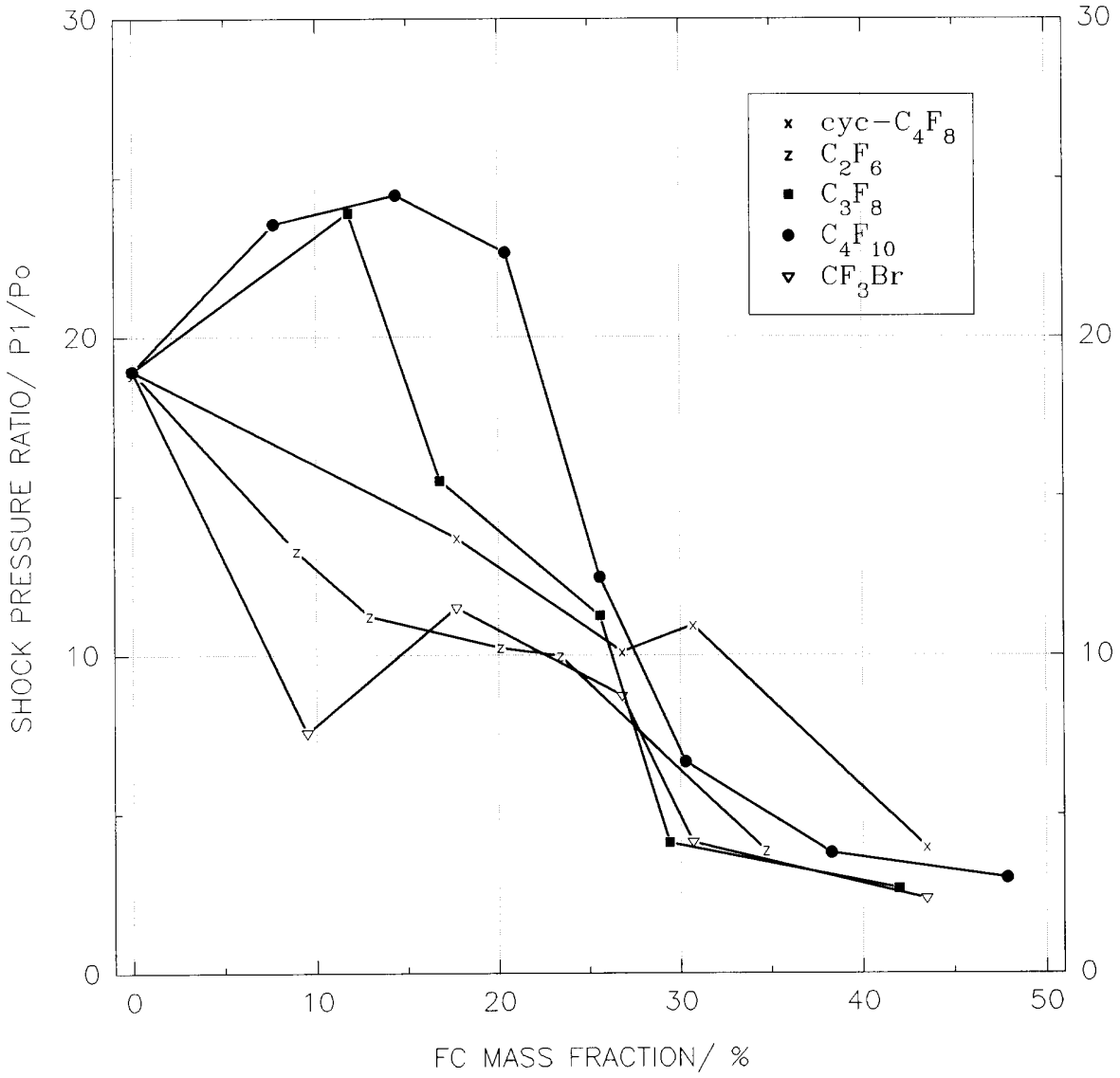

Figure 65. Reduction in pressure ratio as function of FC mass fraction compared to CF_3Br.

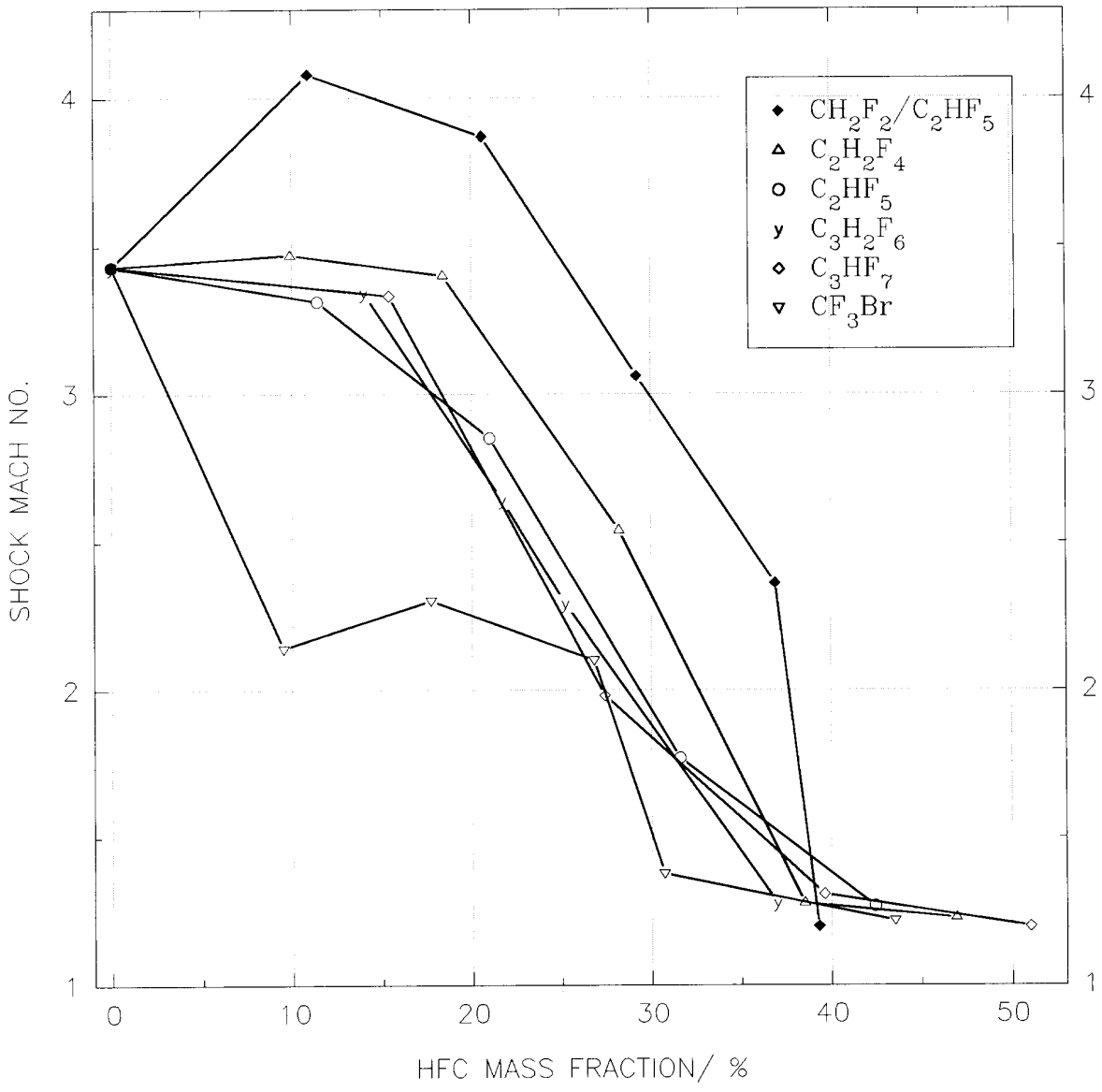

Figure 66. Reduction in shock Mach number as function of HFC mass fraction, compared to CF_3Br.

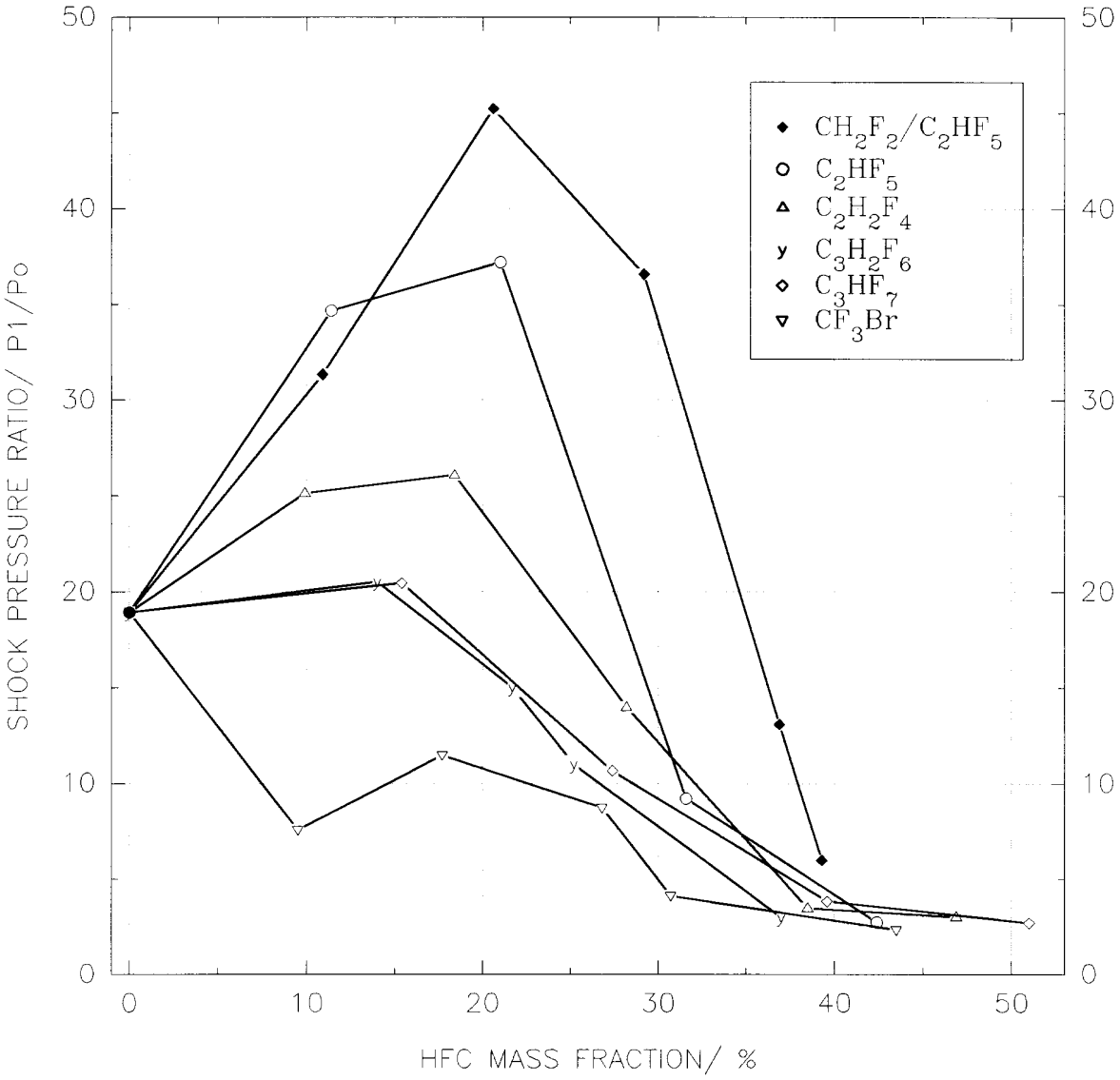

Figure 67. Reduction in pressure ratio as a function of hydrofluorocarbon mass fraction, compared to CF_3Br.

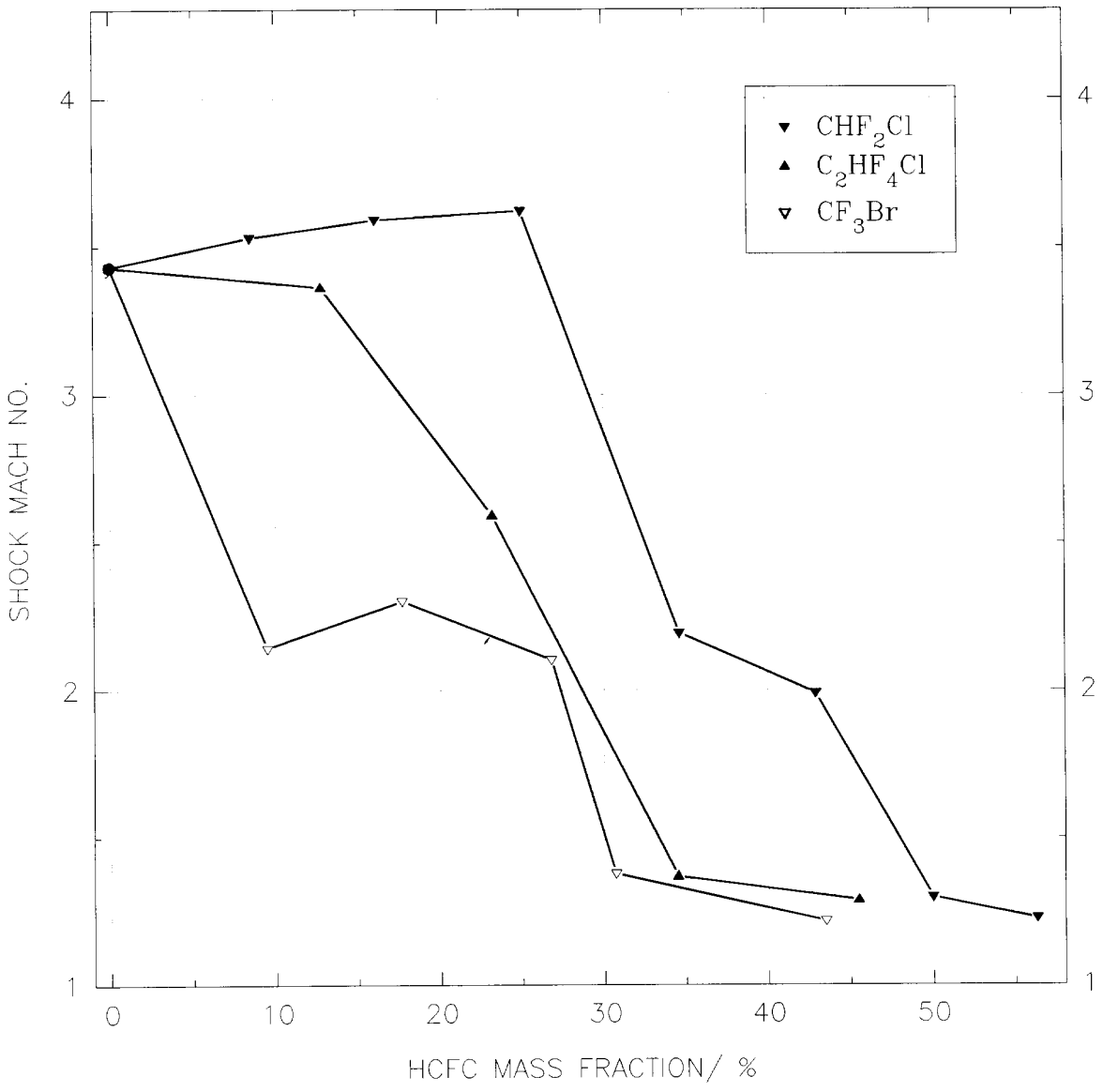

Figure 68. Reduction in shock Mach number as a function of hydrochlorofluorocarbon mass fraction, compared to CF_3Br.

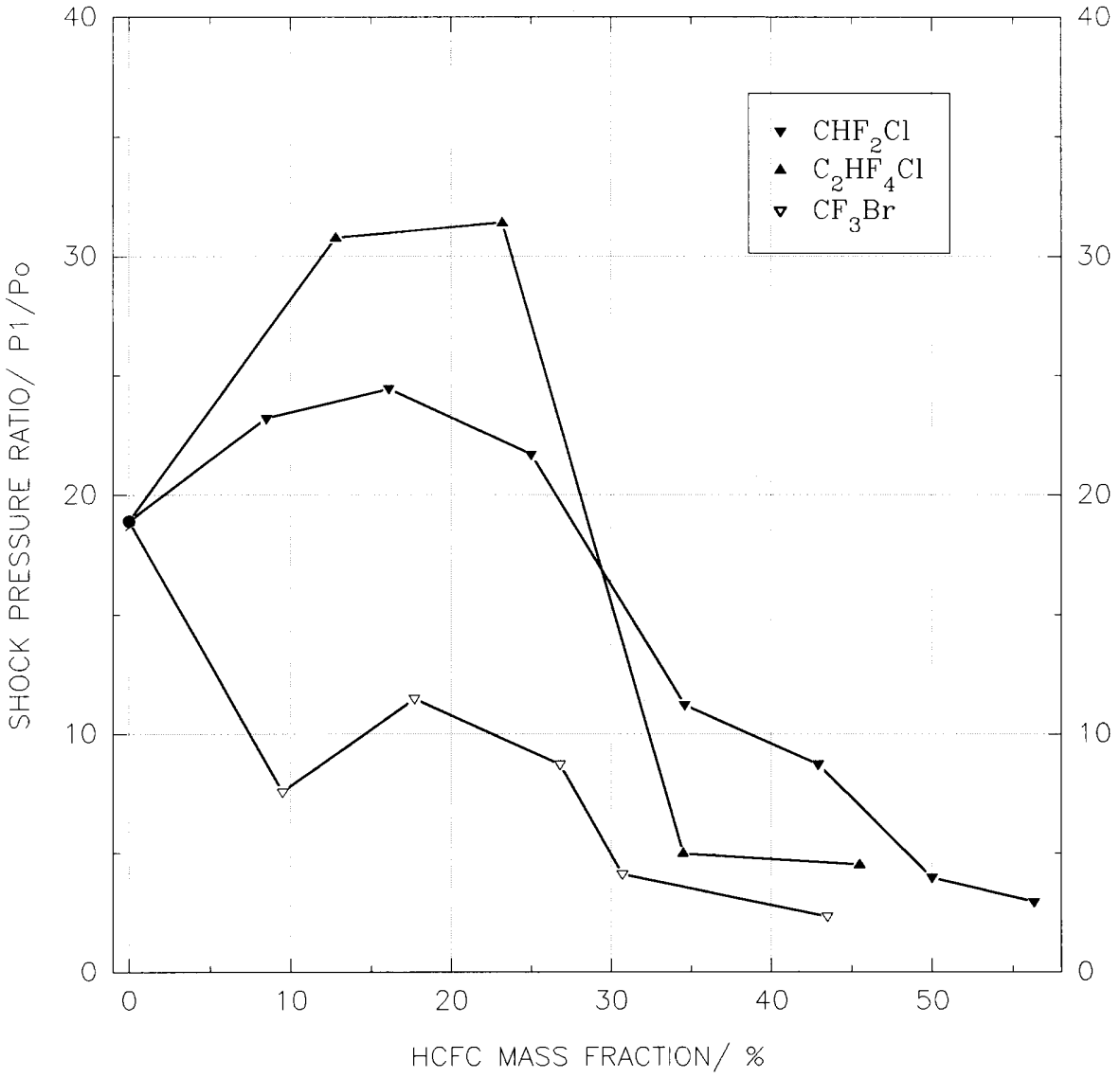

Figure 69. Reduction in pressure ratio as a function of hydrochlorofluorocarbon mass fraction, compared to CF_3Br.

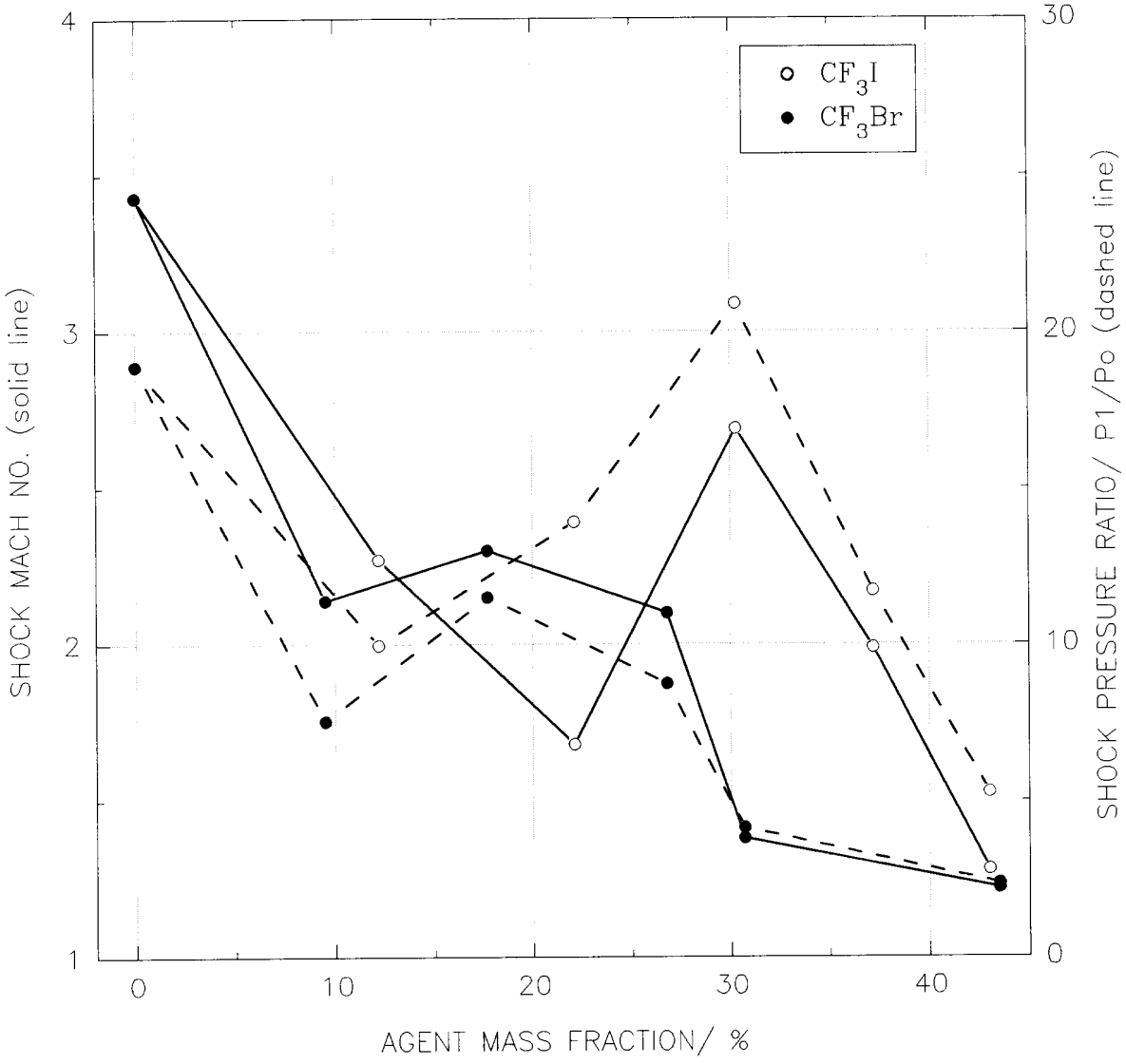

Figure 70. Reduction in shock wave Mach number and pressure ratio as a function of CF_3I mass fraction, compared to CF_3Br.

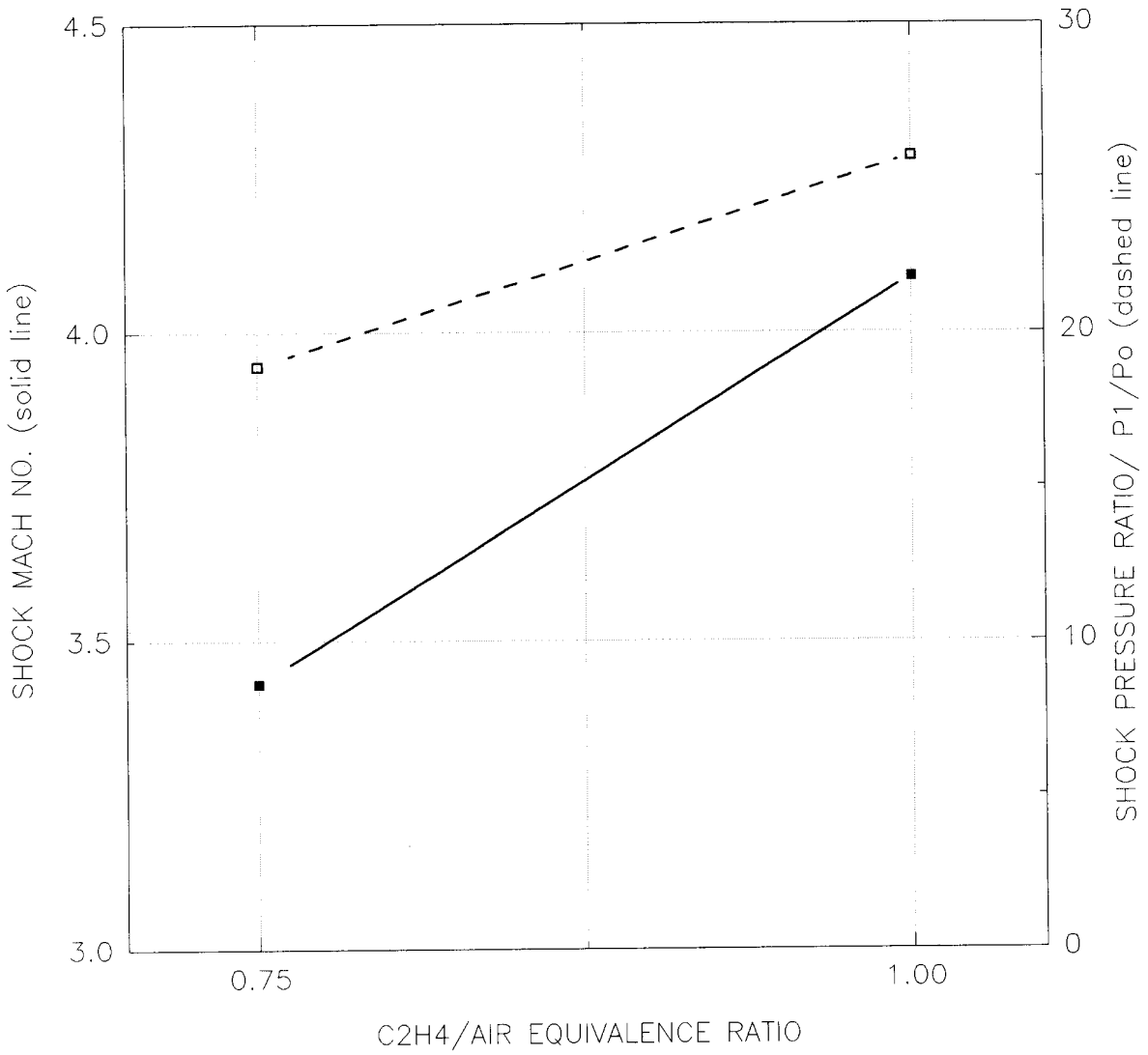

Figure 71. Effect of fuel/air equivalence ratio on shock wave Mach number and pressure ratio.

agent to the fuel or oxidizer pool. The initial pressure and temperature remained the same for the stoichiometric experiments: 100 kPa and 22 °C.

The results for the FCs are plotted in Figures 72-74. In all cases, the Mach number and pressure ratio increased as the fuel/air mixture was changed from lean to stoichiometric. The shapes of the curves, in the most part, were not significantly altered. The impact was greatest at low concentrations, decreasing as the partial pressure fraction reached 8%. For FC-116, the biggest difference occurred at a partial pressure fraction of 3%.

A distinctly different behavior occurred with the two HFCs shown in Figures 75 and 76. The hydrogen atoms attached to the agent molecules had less of an enhancing effect under stoichiometric conditions. The over-pressure was greatly reduced when the equivalence ratio was increased, leading to a cross-over condition where both the Mach number and pressure ratio became less for the stoichiometric condition. The implication of these data is that HFC-125 and the HFC-32/125 mixture increase in relative effectiveness under stoichiometric conditions.

Trifluoroiodomethane behaved no differently in suppressing the shock speed and pressure ratio under lean and stoichiometric conditions. From the data in Figure 77 it can be seen that the Mach number and pressure ratio increased uniformly over the range of partial pressure fractions investigated at an equivalence ratio of 1.0. The reversal of suppression effectiveness at partial pressure fractions between 3% and 6% observed at an equivalence ratio of 0.75 also occurred for stoichiometric combustion.

4.5.5.3 Ranking the Agents. The results which were gathered indicated the complexity of the suppression process in the deflagration/detonation tube. Because one does not know *a priori* the conditions in an actual dry bay fire zone, and because different initial conditions (*i.e.*, pressure, temperature and fuel/air ratio) affect the amount of agent required for suppression to varying degrees, a specific set of initial conditions was chosen at which all the agents were compared: 100 kPa, 22 °C, and 0.75 ethene/air equivalence ratio. The reduction in pressure ratio rather than the Mach number was chosen as the measure of suppression because of its direct impact on the structural integrity of the dry bay. The amount of halon 1301 required to reduce the pressure (a) to 10% and (b) to one-half the maximum increase was used to normalize the results.

Figure 78 displays three different performance parameters calculated under these conditions. The flame suppression number (FSN) is defined as the mass fraction of an agent required for suppression divided by the required mass fraction of halon 1301. The volume factor (VF) is defined as the storage volume of the alternative agent necessary for suppression divided by the storage volume of the CF_3Br. The saturated liquid density of the agents at 20 °C was used to convert mass to volume. Halon 1301 has a VF and FSN of unity by definition. For the other chemicals, the smaller these values the better is the agent.

While there were some reversals depending upon the basis of evaluation (*i.e.*, 90% reduction FSN, 50% reduction FSN, or VF), Figure 78 shows that FC-218 was clearly the best performer under the conditions tested, and that the HFC-32/125 mixture and HCFC-22 were the worst. The FSN of FC-116 based upon a 50% reduction in pressure build-up was the lowest of all agents, even performing better than halon 1301. However, because hexafluoroethane does not condense at room temperature its density is low, leading to a volume factor which is undesirably high. Nitrogen, which is also a gas at room temperature, had a VF of 32. On a mass basis nitrogen performed almost as well as 1301. The CF_3I had the third lowest volume factor of the alternative agents, although its FSN values were close to the highest.

4.5.6 Conclusions and Recommendations from the Premixed Deflagration/Detonation Study. It is necessary to emphasize that the experimental conditions in the deflagration/detonation tube differed

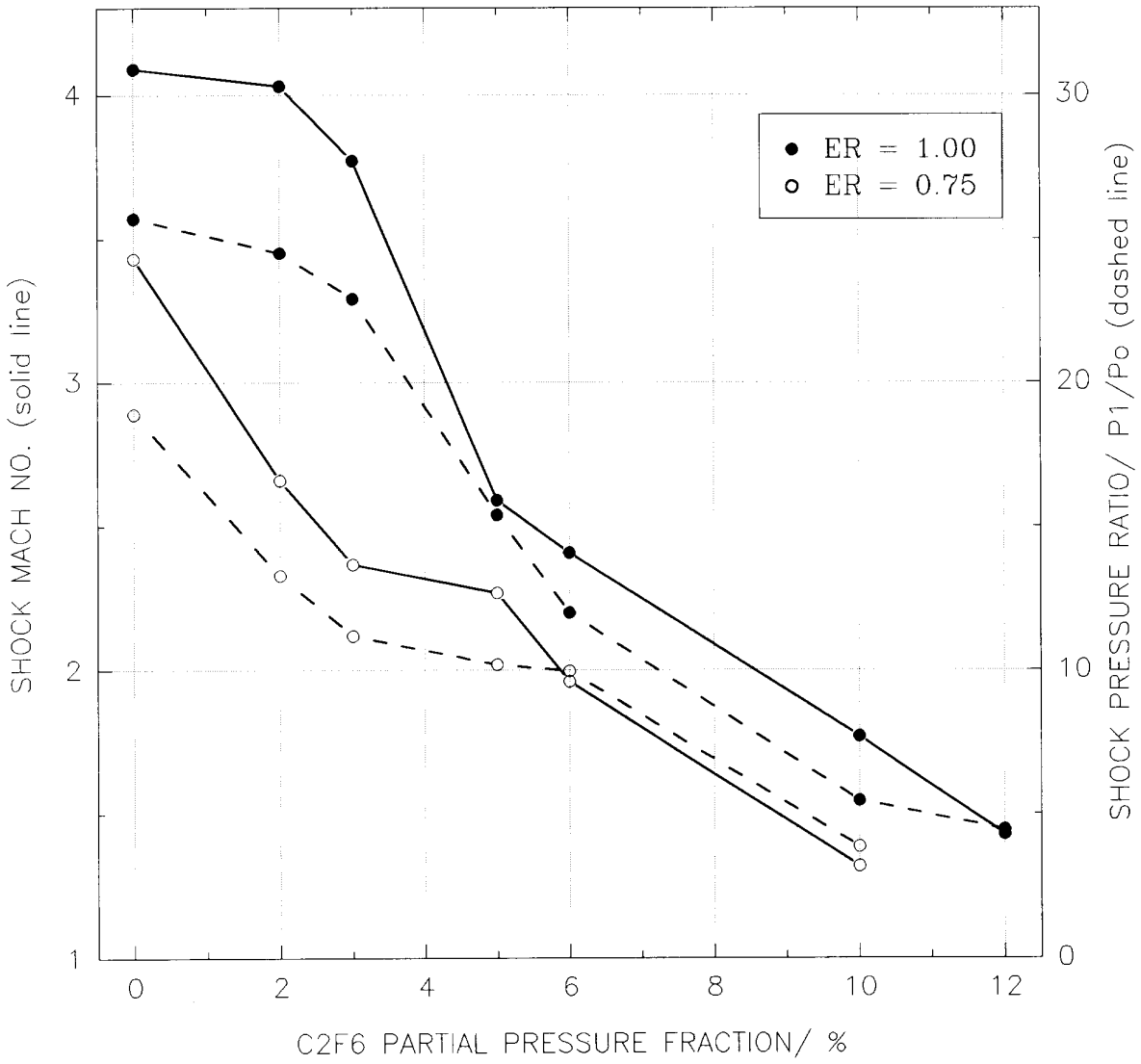

Figure 72. Effect of equivalence ratio on the reduction in Mach number by partial pressure of FC-116.

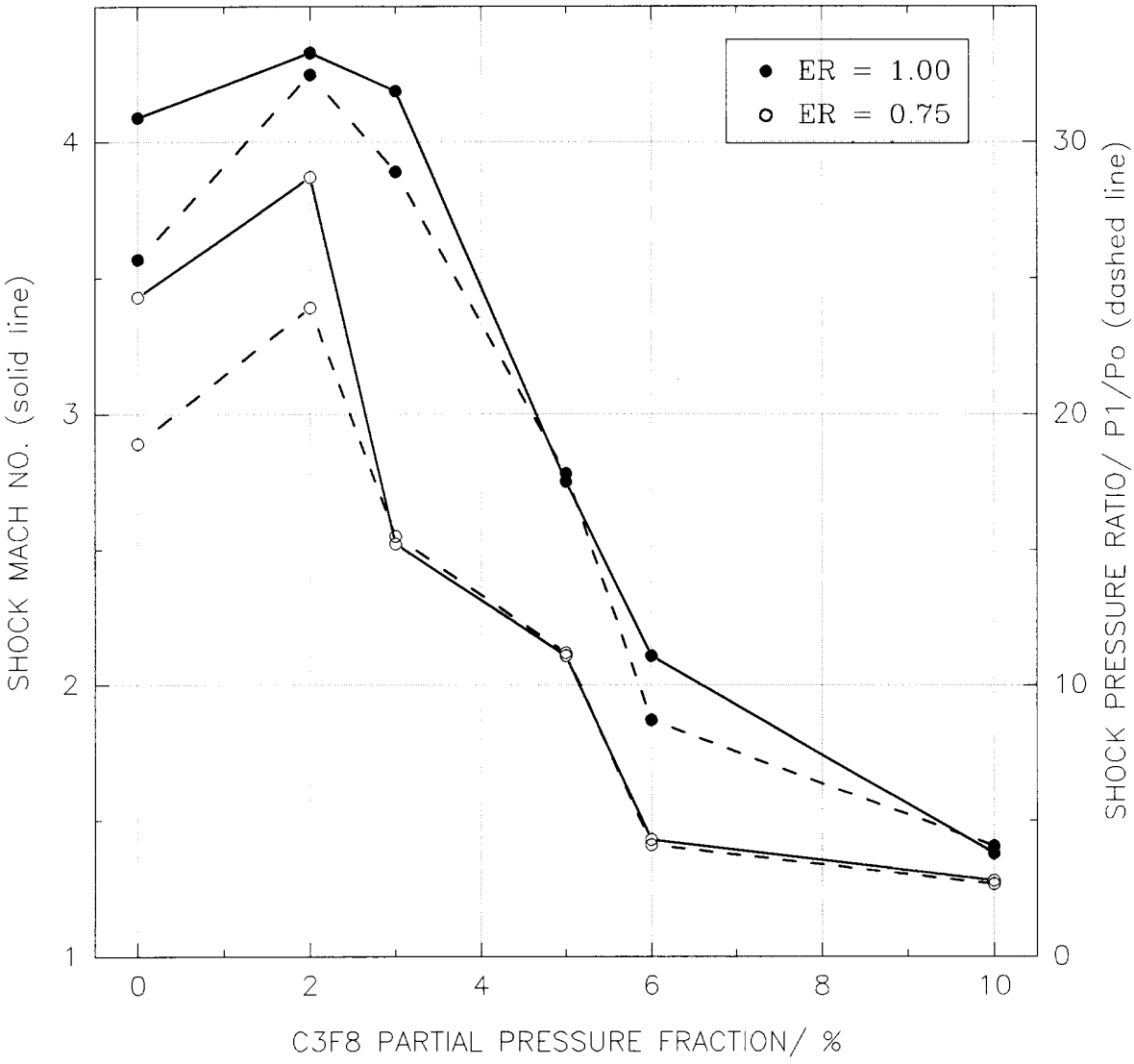

Figure 73. Effect of equivalence ratio on the reduction in shock Mach number and pressure ratio by partial pressure of FC-218.

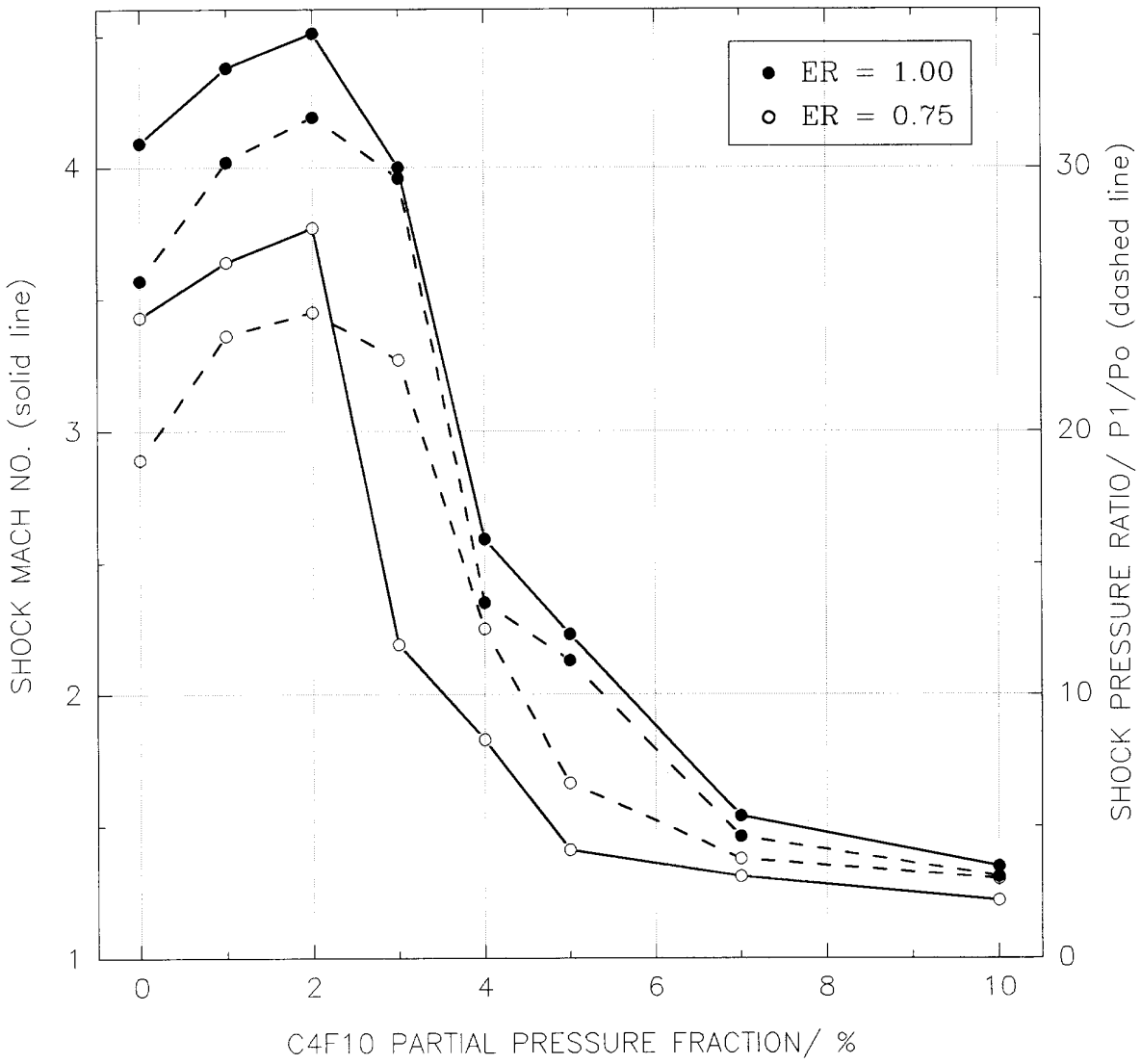

Figure 74. Effect of equivalence ratio on the reduction in shock Mach number and pressure ratio by partial pressure of FC-31-10.

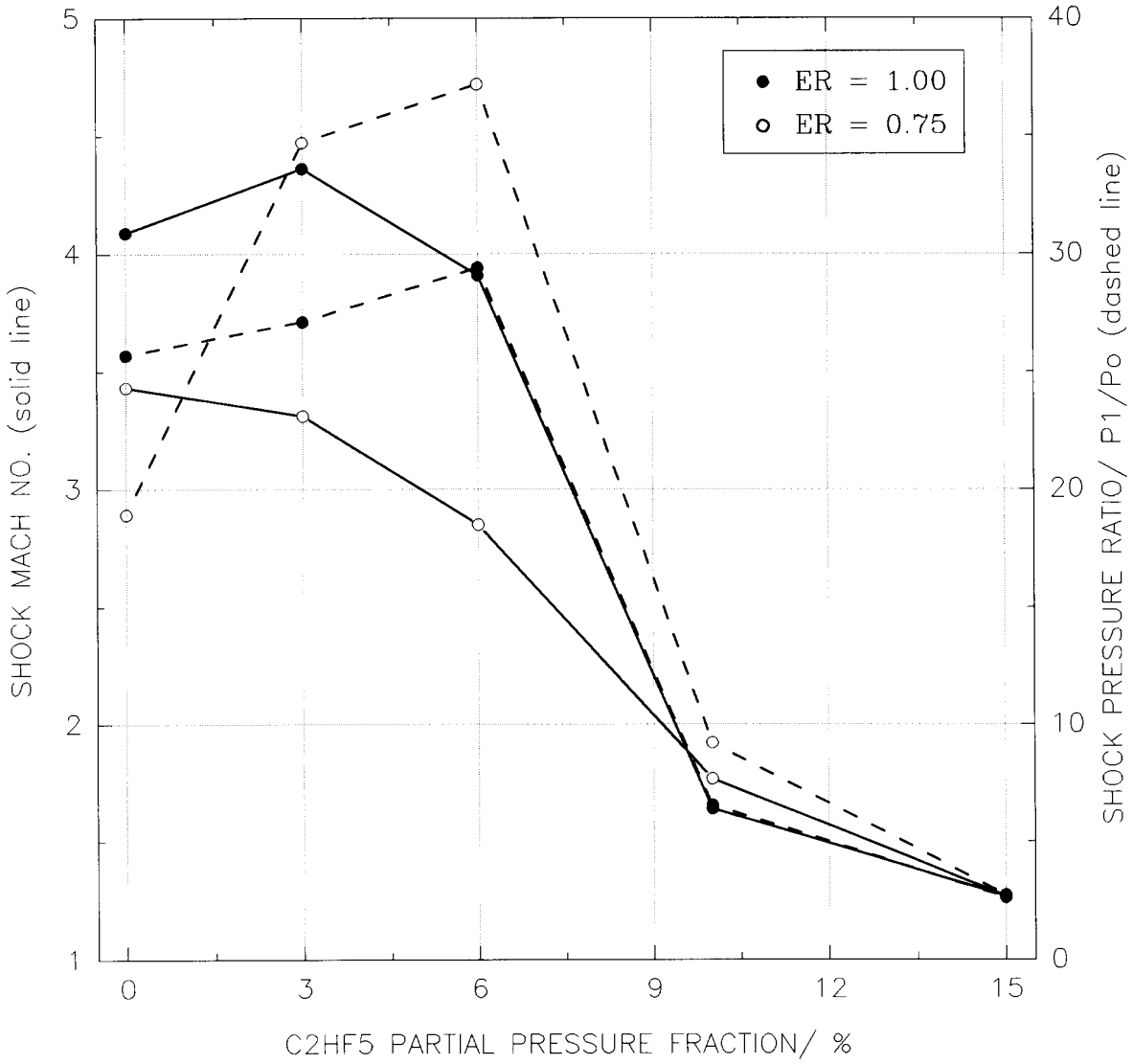

Figure 75. Effect of equivalence ratio on the reduction in shock wave Mach number and pressure ratio by partial pressure of HFC-125.

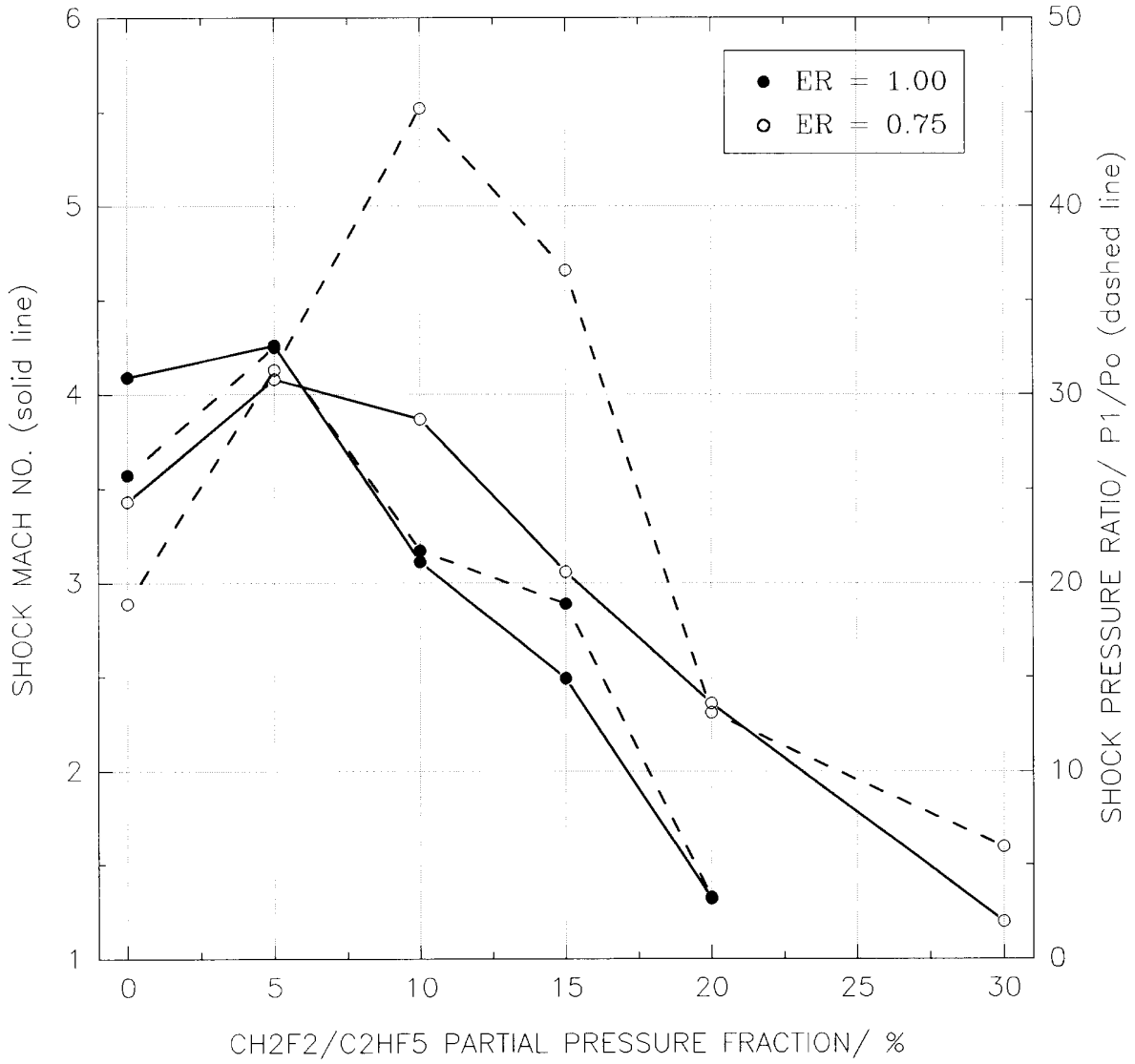

Figure 76. Effect of equivalence ratio on the reduction of shock wave Mach number and pressure ratio by partial pressure of HFC-32/125 mixture.

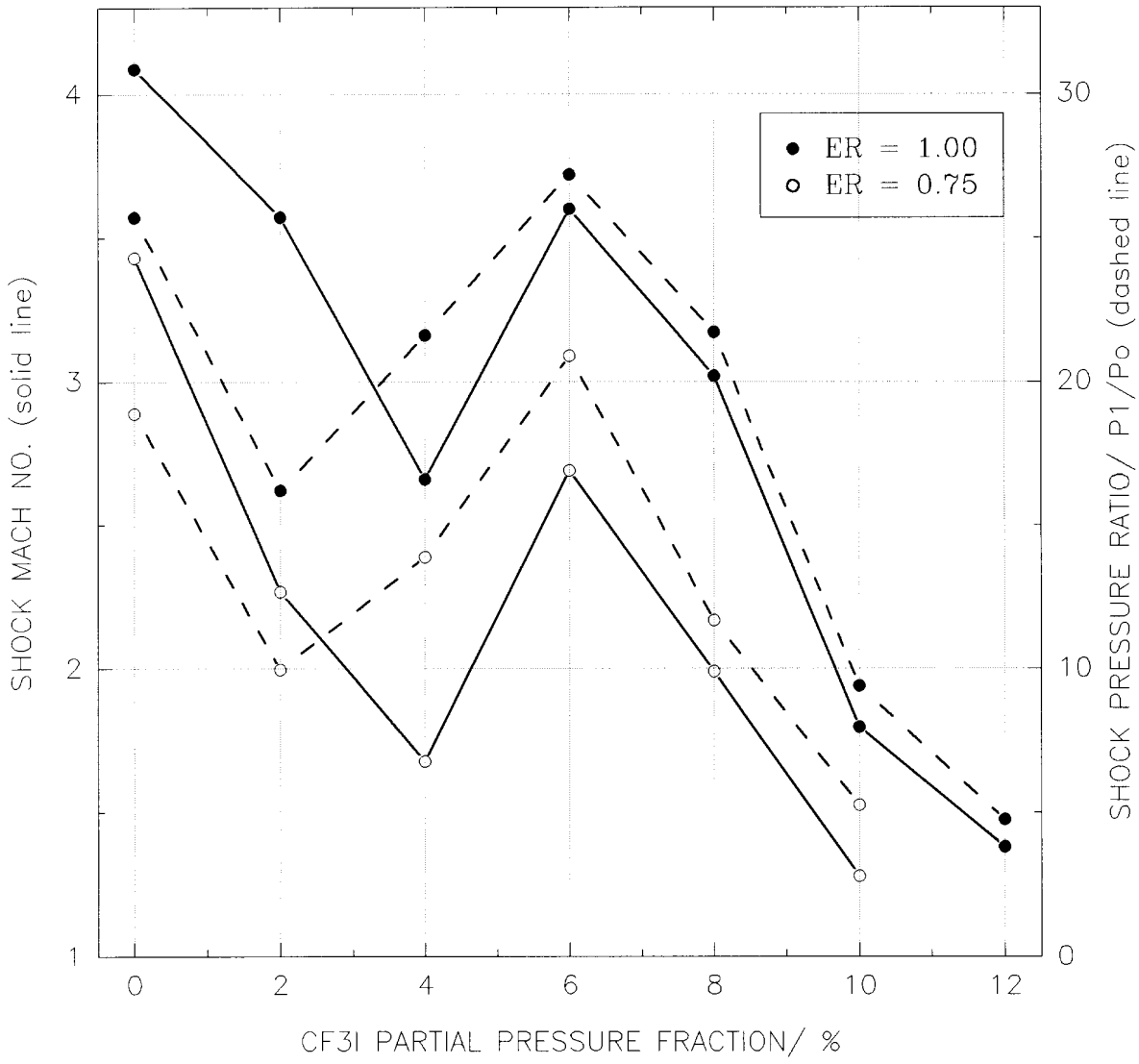

Figure 77. Effect of equivalence ratio on the reduction of shock wave Mach number and pressure ratio by partial pressure of CF_3I.

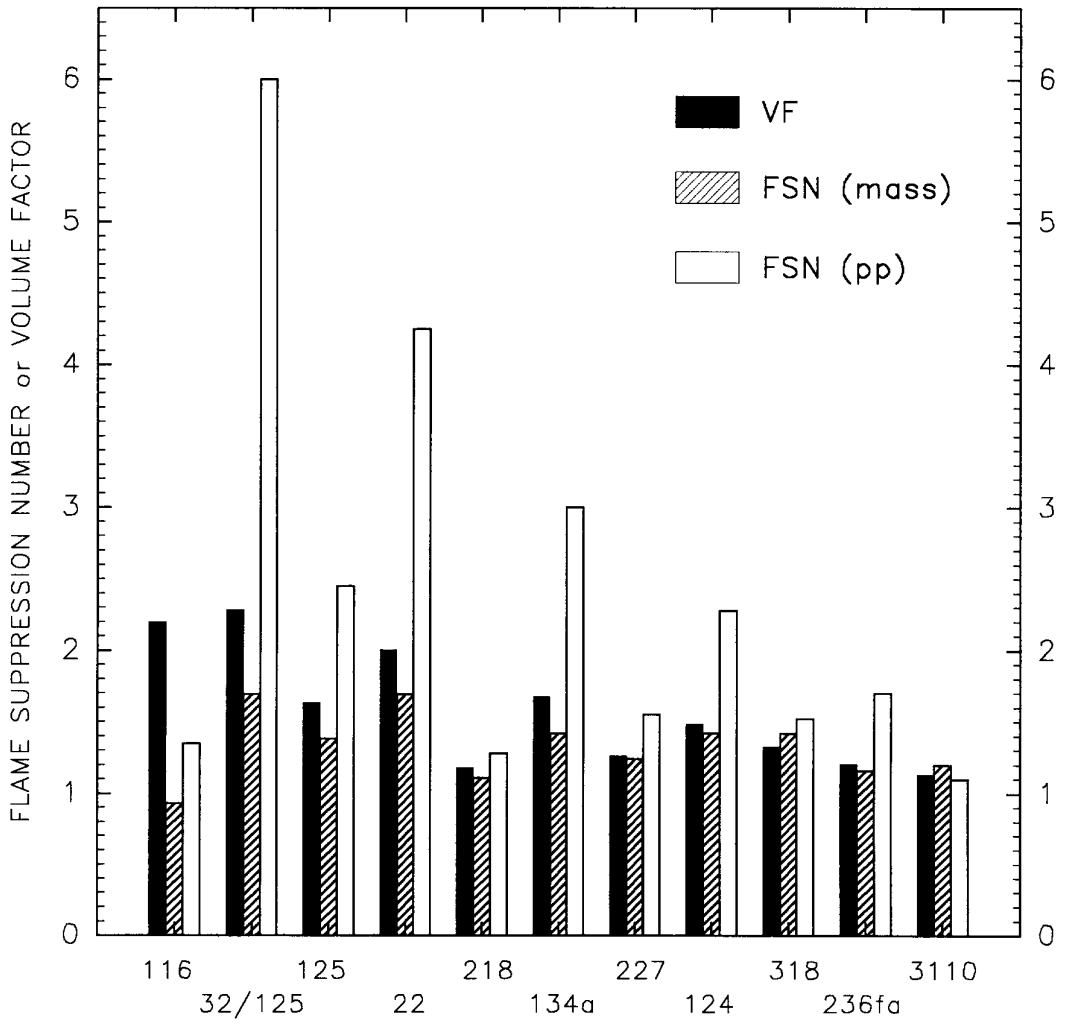

Figure 78. Flame suppression numbers and volume factors of the agents examined in the detonation/deflagration tube.

significantly from those used in the cup burner, opposed-flow diffusion flame burner and turbulent spray flame burner. The main qualitative difference was the occurrence of a strong shock wave ahead of the flame. That wave influenced the gasdynamic, thermodynamic and chemical state of the pure combustible mixture in the driver section and the mixture containing an agent in the test section. Another feature was a high level of turbulence within the flame due to its high speed and the interactions with the spiral obstruction. The quantitative difference was a supersonic regime (relative to the undisturbed mixture) of flame/shock propagation and strong pressure changes (due to confinement and shock) during the process. Thus the oxidizer, fuel and agent molecules underwent preliminary processes before entering the flame zone.

4.5.6.1 Conclusions. The following conclusions can be drawn based on the results obtained:

1. Suppression of highly dynamic flames can be effectively studied in the two-sectional tube, permitting clear discrimination of performance among various alternative extinguishing agents.

2. The high-speed turbulent flame and the flame in the quasi-detonation wave under suppression strictly follows the shock wave which is always ahead of it in such a way that its velocity is the same as the shock velocity. The distance between the flame and the shock increases with the amount of an extinguishing agent. At extinguishment the flame disappears while the residual shock still exists.

3. The suppression process of the lean ethene/air mixture is pressure dependent both for chemically inert nitrogen and chemically active halon 1301. That may be related to the fact that the oxidation mechanism of ethene is known to be pressure dependent.

4. The analysis of the suppression data for the lean ethene/air mixture leads to the division of the alternative compounds into four general categories. These are, in order of decreasing effectiveness: CF_3Br and CF_3I; perfluorocarbons; hydrofluorocarbons; and hydrochlorofluorocarbons. Within each of the categories the agents can be ordered (on a mole fraction basis) approximately inversely according to the molecular weight of the molecule.

5. The extinguishing concentrations of the more effective agents are around 10% by volume and 40% by weight, while less effective ones are 15-30% by volume and 40-50% by weight. The least effective agent is the HFC-32/125 mixture, giving unusually high pressure ratios. HCFC-22 requires the highest extinguishing concentration of all the alternatives.

6. The presence of a hydrogen-containing suppressant in the combustible mixture results in a significant increase in pressure ratio relative to that for the pure combustible mixture. The phenomenon occurs also for the compounds not containing hydrogen atoms at relatively lower concentrations but the impact is not so dramatic. The impact is generally weaker for stoichiometric relative to lean mixtures. That may be related to the fact that the agent acts as an extra fuel, causing the mixture to be richer. It is suspected that the effect may be associated with the release of hydrogen during the process which enhances the branching steps in the ethene oxidation mechanism. It is also not out of the question that a homogeneous autocatalysis occurs lowering the overall activation energy and enhancing the oxidation mechanism.

7. The behavior of CF_3I is different from the other agents. At lower concentrations (2-3% by volume) the performance is the best of all the alternatives. However, at intermediate concentrations (3-7% by volume) the performance is worsened significantly. Eventually at higher concentrations, up to the extinguishing value of 10%, the performance is comparable with the perfluorocarbons and CF_3Br. The phenomenon is independent of the equivalence ratio of the combustible mixture. The behavior at the intermediate concentrations may be attributed to the catalytic effect caused by the iodine atoms.

4.5.6.2 Recommendations. The relative ranking of the agents in Figure 78 can be used as a guide to choose a replacement for halon 1301 for suppressing high-speed turbulent flames and quasi-detonations. The influence of rich equivalence ratios up to 1.5, of other gaseous fuels, and of various tube geometries on the performance of the selected agents should be explored to determine the generality of the rankings. A more fully instrumented apparatus would allow the evolution of the flame and shock all along the length of the tube to be followed, and the key intermediate species and products of combustion to be ascertained.

The unusual behavior of CF_3I in lean and stoichiometric ethene/air mixtures indicates a critical need for further research into the kinetics of the compound. It is recommended that a shock tube be designed to investigate the dynamic and kinetic characteristics under high pressure and temperature conditions as well as various mixture compositions. The set-up should include a special dump chamber for collecting combustion products and optical access for spectroscopic measurements of important species.

In general, the application of this unique experimental apparatus for studying fire suppression processes under highly dynamic conditions should provide the information necessary to establish a physical/chemical model of the phenomena, contributing to the fire safety of facilities exposed to fast flames, explosions and detonations.

4.6 Summary of Conclusions on Flame Suppression Effectiveness

1. The relative ranking of the agents depends upon whether one uses a mass basis or a volume basis.

2. The relative ranking of the agents varies only slightly among the three non-premixed burners, but a substantially different ranking results from the premixed deflagration/detonation apparatus.

3. The relative ranking of the agents is not much affected by the fuel type or air temperature.

4. The quantity of agent required to suppress a flame varies with the type of burner generally in the following order:

   cup burner $\approx$ low strain OFDF > spray burner > high strain OFDF > deflagration tube

5. The quantity of agent required to suppress a non-premixed flame varies somewhat with the type of fuel in the following order:

   propane > heptane > JP-8 > JP-5 > HF-5606 > HF-83282

6. The quantity of agent required to suppress the turbulent spray flame increases with decreasing rate of agent injection.

7. The quantity of agent required to attenuate the shock wave speed and pressure ratio in the deflagration/detonation tube varies with equivalence ratio, sometimes increasing as one goes from lean to stoichiometric and sometimes decreasing.

8. Sodium bicarbonate was the most effective suppressant of the three non-premixed flames, requiring less mass than halon 1301. In general, the smaller size particles were more effective.

9. Iodotrifluoromethane was more effective than halon 1301 in suppressing the spray burner flame, had a similar effectiveness with the cup burner flames, and was less effective in attenuating the shock speed and pressure in the detonation/deflagration apparatus.

10. None of the core agents performed as well as halon 1301 in any of the four flame suppression studies, requiring from approximately one and a half to four times the storage volume as halon 1301 to suppress the different flames.

11. HCFC-124 was the generally the best performer of the core agents in suppressing the non-premixed flames, and FC-218 was judged the best for attenuating the shock speed and pressure in the detonation/deflagration tube.

12. FC-116 was the poorest performer (on a liquid storage volume basis) of all the core agents evaluated in the flame suppression tests; the HFC-32/125 mixture was the second poorest performer, and led to the highest over-pressures in the lean detonation/deflagration tube study.

4.7 References

Baker, W.E., Cox, P.A., Westine, P.S., Kulesz, J.J. and Strehlow, R.A., *Explosion Hazards and Evaluation,* Elsevier, 1983.

Bajpai, S.N., "An Investigation of the Extinction of Diffusion Flames by Halons," *Journal of Fire and Flammability 5*, 255 (1974a).

Bajpai, S.N., "Extinction of vapor fed diffusion flames by Halons 1301 and 1211-Part I," *ser No. 22430, Factory Mutual research Corporation*, Norwood, Massachusetts, November (1974b).

Bui, M. and Seshadri, K. "Comparisons between experimental measurements and numerical calculations of the structure of heptane-air diffusion flames," *Combust. Sci. Tech. 79*, No 4-6, 293 (1991).

Chapman, W.R. and Wheeler, R.N.V., "The Propagations of Flame in Mixtures of Methane and Air. Part IV. The Effect of Restrictions in the Path of the Flame," *Journal of the Chemical Society*, London, 1926.

Chelliah, H., Bui-Pham, M., Seshadri, K. and Law, C. K., "Numerical description of the structure of counterflow heptane-air flames using detailed and reduced chemistry with comparisons to experiments," *Twenty-Fourth Symposium (International) on Combustion*, The Combustion Institute, Pittsburgh, Pennsylvania, p. 851 (1992).

Creitz, E.C., "Inhibition of Diffusion Flames by Methyl Bromide and Trifluoromethyl Bromide Applied to the Fuel and Oxygen sides of the reaction zone," *Journal of Research of the National Bureau of Standards (U.S.) 65A*, 389, (1961).

Creitz, E.C., "Extinction of Fires by Halogenated Compounds - A Suggested Mechanism," *Fire Technology 8*, 131 1972.

Das, A., *Relationship Between Ignition Source Strength and Design Inerting Concentration of Halon 1301*, M.S. Thesis, Fire Protection Engineering Department, Worcester Polytechnic Institute, 1986.

Dodding, R.A., Simmons, R.F. and Stephens, A., "The Extinction of Methane - Air Diffusion Flames by Sodium Bicarbonate Powders," *Combustion and Flame 15*, 313 (1977).

Dow-Corning, Midlane, MI, Communication of Test Results, 1993.

Ewing, C.T., Faith, F.R., Hughes, J.T. and Carhart, H.W., "Flame Extinguishment Properties of Dry Chemicals: Extinction Concentrations for Small Diffusion Pan Fires," *Fire Technology 25*, 134 (1989).

Fendell, F. E., "Ignition and extinction in combustion of initially unmixed reactants," *J. Fluid Mechanics 21*, 281 (1965)

Galbraith Laboratories, Knoxville, TN, *Communication of Test Results*, 1993.

Gann, R.G., Barnes, J.D., Davis, S., Harris, J.S., Harris, R.H., Herron, J.T., Levin, B.C., Mopsik, F.I., Notarianni, K.A., Nyden, M.P., and Ricker, R.E., "Preliminary Screening Procedures and Criteria for Replacements for Halons 1211 and 1301," National Institute of Standards and Technology, NIST Technical Note 1278, U.S. Government Printing Office, Washington, DC (1990).

Gmurczyk, G., Grosshandler, W., Peltz, M. and Lowe, D., "A Facility for Assessing Suppression Effectiveness in High Speed Turbulent Flames," Eastern States Section Conference/The Combustion Institute, Princeton, 1993.

Gorden, S. and McBride, B.J., "Computer Program for the Calculation of Complex Chemical Equilibrium Compositions, Rocket Performance, Incident and Reflected Shocks, and Chapman-Jouget Detonations," NASA, NASA SP-273,(1976).

Goscoyne Laboratories, Baltimore, MD, *Communication of Test Results*, 1993.

Grosshandler, W.L., Lowe, D., Rinkinen, W., and Presser, C., "A Turbulent Spray Burner for Assessing Halon Alternative Fire Suppressants," ASME Winter Annual Meeting, December, 1993.

Hamins, A., *The Structure and Extinction of Diffusion Flames,* Ph.D. Thesis, University of California, San Diego, 1985.

Hamins, A., and Seshadri, K., "Prediction of overall chemical kinetic rate parameters for extinction of diffusion flames above multicomponent fuels," *Combust. Sci. Tech. 38*, 89 (1984a).

Hamins, A., and Seshadri, K., "Structure of counterflow diffusion flames burning multicomponent fuels," *Twentieth Symposium (International) on Combustion*, The Combustion Institute, Pittsburgh, Pennsylvania, p. 1905 (1984b).

Hamins, A., and Seshadri, K., "The influence of alcohols on the combustion of hydrocarbon fuels in diffusion flames," *Combust. Flame 64*, 43 (1986).

Hamins, A., and Seshadri, K., "The structure of diffusion flames burning pure binary, and ternary solutions of methanol, heptane, and toluene," *Combust. Flame 68*, 295 (1987).

Hamins, A., Thridandam, H., and Seshadri, K., "Structure and extinction of a partially premixed diffusion flame," *Chem. Eng. Sci. 40*, 2027 (1985).

Heinonen, E.W., Kirst, J.A. and Moussa, N.A., *Fire/Explosion Protection Characterization and Optimization: Alternative Dry Bay Fire Suppression Agent Screening, Medium-Scale Test Results*, Final Report, NUMERI OC 91/16, Report JTCG/AS-91-VR-005, 1991.

Hirst, R. and Booth, K., "Measurements of Flame-Extinguishing Concentrations," *Fire Technology 13*, No. 4, (1977).

Kent, J.H., and Williams, F.A., "Extinction of Laminar Diffusion Flames for Liquid Fuels," *Fifteenth Symposium (International) on Combustion*, pp. 315-325, The Combustion Institute, Pittsburgh, 1974.

Krishnamurthy, L., Williams, F.A., and Seshadri, K., "Asymptotic Theory of Diffusion Flame Extinction in the Stagnation-Point Boundary Layer," *Combust. Flame 26*, 363 (1976).

Lee, J.H.S., "Fast Flames and Detonations," *Chemistry of Combustion Processes*, The American Chemical Society, 1984.

Lee, J.H., Knystautas, R. and Chan, C.K., "Turbulent Flame Propagation in Obstacle-filled Tubes," *Twentieth Symposium (International) on Combustion*, The Combustion Institute, 1984.

Lefebvre, M.H., Nzeyimana, E., Van Tiggelen, P.J., *Progress in Astronautics and Aeronautics*, AIAA, 1992.

Liñan, A., "The Asymptotic Structure of Counterflow Diffusion Flames for Large Activation Energies," *Acta Astronautica 1*, 1007 (1974).

Lum, L., National Institute of Standards and Technology, Gaithersburg, MD, Personal Communication, 1993.

Miller, E. and McMillion, L.G., "The Suppression of Opposed-Jet Methane-Air Flames by Methyl Bromide," *Combustion and Flame 84*, 37 (1992).

Milne, T.A., Green, C.L., and Benson, D.K.,"The Use of the Counterflow Diffusion Flame in Studies of Inhibition Effectiveness of Gaseous and Powder Agents," *Combustion and Flame 15*, 255 (1970).

Mitani, T., "Flame Retardant Effects of CF3Br and NaHCO3," *Combustion and Flame 50*, 177 (1983).

Nettleton, M.A., *Gaseous Detonations, Their Nature, Effects and Control,* Chapman and Hall, 1987.

Peraldi, O., Knystautas, R. and Lee, J.H., "Criteria for Transition to Detonation in Tubes," *Twenty-first Symposium (International) on Combustion*, The Combustion Institute, p. 1629, 1986.

Peters, N., "Local premixing due to flame stretch and nonpremixed turbulent combustion," *Combust. Sci. Tech. 30*, 1 (1982).

Peters, N., "Laminar diffusion flamelets in nonpremixed turbulent combustion," *Prog. Energy Combust. Sci. 10*, 319 (1984).

Pitts, W.M., Nyden, M.R., Gann, R.G., Mallard, W.G. and Tsang, W., "Construction of an Exploratory List of Chemicals to Initiate the Search for Halon Alternatives," *NIST Technical Note 1279*, U.S. Government Printing Office, Washington, DC, 1990.

Reid, R.C., Prausnitz, J.M., and Sherwood, T.K., *The Properties of Gases and Liquids*, Third Edition, pp. 404-411, McGraw/Hill, New York, 1977.

Seshadri, K., Mauss, F., Peters, N. and Warnatz, J., " A flamelet calculation of benzene formation in coflowing laminar diffusion flames," *The Twenty-Third Symposium (International) on Combustion*, The Combustion Institute, Pittsburgh, Pennsylvania, 463 (1990).

Seshadri, K., and Williams, F.A., "Effect of CF_3Br on counterflow combustion of liquid fuel with diluted oxygen," *ACS Symposium Series, No. 16, Halogenated Fire Suppressants*, R.G. Gann (Ed.), American Chemical Society, Washington, DC, p. 149 (1975).

Seshadri, K., and Williams, F.A., "Structure and extinction of counterflow diffusion flames above condensed fuels: comparison between poly(methylmethacrylate) and its liquid monomer, both burning in nitrogen-air mixtures," *J. Polymer Sci. 16*, 1755 (1978a).

Seshadri, K., and Williams , F. A., "Laminar flows between parallel plates with injection of a reactant at high Reynolds number," *Int. J. Heat Mass Transfer 21*, 251 (1978b)

Sheinson, R.S., Penner-Hahn, J.E., and Indritz, D., "The Physical and Chemical Action of Fire Suppressants," *Fire Safety Journal 15*, 43 (1989).

Simmons, R.F., and Wolfhard, H.G., *Transactions of the Faraday Society, 52*:53-59 (1956).

Smooke, M.D., Puri, I.K., and Seshadri, K., "A comparison between numerical calculations and experimental measurements of the structure of a counterflow diffusion flame burning diluted methane in diluted air," *Twenty-First Symposium (International) on Combustion*, The Combustion Institute, Pittsburgh, Pennsylvania, p. 1783 (1986).

Strasser, A., Liebman, I., and Kuchta, J.M., "Methane Flame Extinguishment with Layered Halon or Carbon Dioxide," *Fire Technology 10*, 25 (1974).

Tucker, D.M., Drysdale, D.D. and Rasbash, D.J., "The Extinction of Diffusion Flames Burning in Various Oxygen Concentrations by Inert Gases and Bromotrifluormethane," *Combustion and Flame 41*, 293 (1981).

Van Wylen, G.J., and Sonntag, R.E., *Fundamentals of Classical Thermodynamics*, Second Edition, John Wiley and Sons, p. 400, 1978.

Vazquez, I., Grosshandler, W., Rinkinen, W., Glover, M., and Presser, C., "Suppression of Elevated Temperature Hydraulic Fluid and JP-8 Spray Flames," *Fourth International Symposium on Fire Safety Science*, Ottawa, June, 1994.

Westbrook, C.K., *Nineteenth Symposium (International) on Combustion*, The Combustion Institute, p. 127, 1982.

Westbrook, C.K., "Chemical Kinetics of Hydrocarbon Oxidation in Gaseous Detonations," *Combustion and Flame 46*, 191, 1982.

Williams, F.A., "A Unified View of Fire Suppression," *Journal of Fire and Flammability 5*, 54 (1974).

Williams, F.A., *Combustion Theory*, Second Edition, Addison Wesley, 2nd Edition, (1985).

Williams, F.A. and Peters, J.W., "Studies of Dry Powder Extinguishment of Diffusion Flames for Condensed Fuels," *Final Technical Report, National Bureau of Standards*, NBS Grant No. NB81NADA, June 15, 1982.